Spring 5-16-2011

Distinct Neuromuscular Patterns from a Single Motor Network

Rachel S. White
School of Medicine, whiters@mail.med.upenn.edu

Distinct Neuromuscular Patterns from a Single Motor Network

Abstract
My thesis aimed to elucidate several aspects of motor circuit regulation and its impact on movement. It is well established that a single motor network can produce different output patterns in response to different inputs. However, in most model systems it remains challenging to identify the neurons comprising these networks and determine their role(s) in network operation, including whether each network neuron retains its role(s) when the network generates different output patterns. Also, most work on these circuits has occurred in the isolated nervous system, so little is known about how muscles respond to distinct neural outputs. I therefore aimed to address the cellular and synaptic mechanisms underlying these unresolved issues using the decapod crustacean stomatogastric nervous system. My work focused on a rhythmically active, network-driven motor circuit (central pattern generator [CPG] circuit) called the gastric mill (chewing) CPG in the crab stomatogastric ganglion. This circuit generates the gastric mill rhythm when activated by modulatory projection neurons (e.g. MCN1, CPN2) located in the commissural ganglia, and it is regulated by identified sensory feedback. I addressed and confirmed the hypothesis that, in the isolated nervous system, different extrinsic inputs can drive different gastric mill motor patterns. This enabled me to determine, for the first time in a network-driven motor circuit, that different motor patterns generated by the same motor circuit are paced by the same set of rhythm generator neurons. I further hypothesized and confirmed that these distinct motor patterns are retained at the level of at least some target muscles, and hence likely underlie different behavioral patterns. Lastly, I obtained data supporting the hypothesis that different extrinsic inputs distinctly modify the influence of a sensory feedback pathway on the relevant projection neurons (MCN1, CPN2), enabling the same sensory system to have different effects on different gastric mill rhythms. These results provide among the most detailed comparisons of how motor patterns generated by a single sensorimotor system are selected and regulated. The results thereby provide evidence for several novel cellular and synaptic mechanisms that expand our appreciation of the number of degrees of freedom available to even small sensorimotor systems.

Degree Type
Dissertation

Degree Name
Doctor of Philosophy (PhD)

Graduate Group
Neuroscience

First Advisor
Michael P. Nusbaum

Keywords
Central pattern generator, stomatogastric, intercircuit regulation, excitatory junction potentials, projection neurons

DISTINCT NEUROMUSCULAR PATTERNS FROM A SINGLE MOTOR NETWORK

Rachel Sarah White

A DISSERTATION

in

Neuroscience

Presented to the Faculties of the University of Pennsylvania

in

Partial Fulfillment of the Requirements for the

Degree of Doctor of Philosophy

2011

Supervisor of Dissertation

_____

Michael Nusbaum, Ph.D., Professor of Neuroscience

Graduate Group Chair

_____

Rita Balice-Gordon, Ph.D., Professor of Neuroscience

Dissertation Committee:

Minghong Ma, Ph.D., Associate Professor of Neuroscience and Thesis Committee Chair

Diego Contreras, Ph.D., Associate Professor of Neuroscience

Marc Schmidt, Ph.D., Associate Professor of Biology

Farzan Nadim, Ph.D., Professor of Biology & Mathematics, Rutgers University, New Jersey Institute of Technology

ABSTRACT

DISTINCT NEUROMUSCULAR PATTERNS FROM A SINGLE MOTOR NETWORK

Rachel S. White

Thesis Advisor: Michael P. Nusbaum

My thesis aimed to elucidate several aspects of motor circuit regulation and its impact on movement. It is well established that a single motor network can produce different output patterns in response to different inputs. However, in most model systems it remains challenging to identify the neurons comprising these networks and determine their role(s) in network operation, including whether each network neuron retains its role(s) when the network generates different output patterns. Also, most work on these circuits has occurred in the isolated nervous system, so little is known about how muscles respond to distinct neural outputs. I therefore aimed to address the cellular and synaptic mechanisms underlying these unresolved issues using the decapod crustacean stomatogastric nervous system. My work focused on a rhythmically active, network-driven motor circuit (central pattern generator [CPG] circuit) called the gastric mill (chewing) CPG in the crab stomatogastric ganglion. This circuit generates the gastric mill rhythm when activated by modulatory projection neurons (e.g. MCN1, CPN2) located in the commissural ganglia, and it is regulated by identified sensory feedback. I addressed and confirmed the hypothesis that, in the isolated nervous system, different extrinsic inputs can drive different gastric mill motor patterns. This enabled me to determine, for the first time in a network-driven motor circuit, that different motor patterns generated by the same motor circuit are paced by the same set of rhythm generator neurons. I further hypothesized and confirmed that these distinct motor patterns are retained at the level of at least some target muscles, and hence likely underlie different behavioral patterns. Lastly, I obtained data supporting the hypothesis that different

extrinsic inputs distinctly modify the influence of a sensory feedback pathway on the relevant projection neurons (MCN1, CPN2), enabling the same sensory system to have different effects on different gastric mill rhythms. These results provide among the most detailed comparisons of how motor patterns generated by a single sensorimotor system are selected and regulated. The results thereby provide evidence for several novel cellular and synaptic mechanisms that expand our appreciation of the number of degrees of freedom available to even small sensorimotor systems.

TABLE OF CONTENTS

LIST OF ILLUSTRATIONS

FIGURE **PAGE**

CHAPTER 1: Introduction

CHAPTER 2: A Newly Identified Extrinsic Input Triggers a Distinct Gastric Mill Rhythm via Activation of Modulatory Projection Neurons

CHAPTER 5: State-dependent Proprioceptor Feedback During Different Gastric Mill Rhythms

LIST OF ABBREVIATIONS

AB	anterior burster
ACO	anterior commissural organ
AGR	anterior gastric receptor
AM	anterior median
CabPK	*Cancer borealis* pyrokinin
CabTRP Ia	*Cancer borealis* tachykinin-related peptide Ia
CabTRP Ia-IR	*Cancer borealis* tachykinin-related peptide Ia immunoreactivity
coc	circumoesophageal connective
coc_B	circumoesophageal connective projecting from the CoG to the brain
coc_{TG}	circumoesophageal connective projecting from the CoG to the TG
CNS	central nervous system
CoG	commissural ganglion
CPG	central pattern generator
CPN2	commissural projection neuron 2
DG	dorsal gastric neuron
dpon	dorsal posterior oesophageal nerve
dvn	dorsal ventricular nerve
EJP	excitatory junction potential
EPSP	excitatory postsynaptic potential
GM	gastric mill neuron
GMR	gastric mill rhythm
gpn	gastro-pyloric nerve

GPR	gastro-pyloric nerve
IC	inferior cardiac
Int1	interneuron 1
ion	inferior oesophageal nerve
IPSP	inhibitory postsynaptic potential
LG	lateral gastric
lgn	lateral gastric nerve
LP	Lateral Pyloric
LPG	lateral posterior gastric
lvn	lateral ventricular nerve
MCN1	modulatory commissural neuron 1
MCN5	modulatory commissural neuron 5
MG	medial gastric neuron
MPN	modulatory proctolin neuron
mvn	medial ventricular nerve
OG	oesophageal ganglion
on	oesophageal nerve
PD	pyloric dilator neuron
pdn	pyloric dilator nerve
poc/POC	post-oesophageal commissure
PRO	protraction
PY	pyloric
RET	retraction
son	superior oesophageal nerve
STG	stomatogastric ganglion

stn	stomatogastric nerve
STNS	stomatogastric nervous system
TG	thoracic ganglion
vcn	ventral cardiac nerve
VCNs	ventral cardiac neurons
VD	ventricular dilator neuron

CHAPTER 1

INTRODUCTION

Rhythmically active motor circuits: central pattern generators

Rhythmic motor patterns underlie many behaviors, including breathing, walking, and chewing. Central pattern generators (CPGs) are the neuronal circuits that generate the basic neuronal pattern underlying these behaviors (Marder and Calabrese, 1996; Marder and Bucher, 2001; Selverston 2010). Hence, CPG output, via its synaptic actions onto motor neurons, drives coordinated, rhythmic muscle contractions (Marder et al., 2005; Doi and Ramirez, 2008; Briggman and Kristan, 2008; Rauscent et al., 2009; Klein et al., 2010). These neuronal circuits must also integrate both internal and external sensory and CNS information to make their output environmentally- and behaviorally appropriate.

Studies in many vertebrate and invertebrate model systems indicate that the general principles by which CPGs operate are the same in all animals (Marder & Calabrese 1996; Stein et al. 1997; Marder & Bucher 2001; Marder et al. 2005; Guertin 2009; Selverston 2010). One shared principle of CPG operation across animals and behaviors is that they all generate rhythmic motor output in response to a non-rhythmic input, which they then impose onto motor neurons that drive muscles to generate the appropriate coordinated movement. A second shared principle is that, in the isolated CNS, CPGs can still generate at least a basic version of the rhythmic motor pattern that they generate *in vivo*. This latter feature makes these networks particularly attractive for elucidating the cellular and synaptic mechanisms by which CPGs in particular, and neuronal networks in general, generate behaviorally-relevant activity patterns.

The source of the rhythmicity in CPG systems generally derives from intrinsically

bursting neurons (pacemaker-driven CPG) or synaptically interacting sets of neurons (network-driven CPG) (Marder and Bucher 2001). Pacemaker-driven CPGs, such as those for vertebrate respiration, heartbeat control in the leech and food filtering in decapod crustaceans, tend to be continuously active in vivo and in the isolated nervous system (Kristan et al. 2005; Marder and Bucher 2007; Garcia et al. 2011). Network-driven CPGs, such as that for locomotion in both vertebrates and invertebrates and for chewing in decapod crustaceans, are episodically active and are driven by sets of projection and sensory neurons (Marder et al. 2005; Marder and Bucher 2007; Ryczko et al. 2010; Selverston 2010).

CPGs are also multifunctional constructs (Marder and Bucher 2001; Marder et al. 2005; Dickinson 2006; Grillner 2006; Garcia et al. 2011). That is, each CPG can be configured, often by different metabotropic inputs, to generate distinct activity patterns. This property results from the ability of distinct inputs to alter, in different ways, the intrinsic and synaptic properties of network neurons (Marder & Bucher 2007; Dubuc et al. 2008; El Manira et al. 2010; Garcia et al. 2011; Harris-Warrick 2010).

Although CPGs continue to operate in the isolated CNS, their output *in vivo* is continually influenced by various descending (higher-order) and ascending (sensory) inputs (Stein et al. 1997; Nusbaum et al. 2001; Rossignol et al. 2006; Buschges et al. 2008; Pearson 2008; Stein 2009; Gossard et al. 2011; Le Ray et al. 2011). However, in most systems the projection neurons relevant to a particular motor pattern are relatively inaccessible and represent a large number of neurons. As a result, the functional organization of the projection neurons that drive particular motor patterns is poorly understood in most systems. For example, the hypothesis that different motor patterns result from the activation of distinct but overlapping sets of projection neurons has received support from several motor systems, but has yet to be established at the level

of identified neurons in any system (Georgopoulos et al. 1995; Kristan and Shaw 1997; Liu and Fetcho 1999; Morgan et al. 2002; Briggman and Kristan 2008). Additionally, there are only a few systems in which information is available regarding the extent to which different CPG output patterns, which are primarily studied in vitro in isolated nervous system experiments, are retained at the level of muscle contractions (Morris et al. 2000; Thuma et al. 2003; Stein et al. 2006; Zhurov and Brezina 2006; Fort et al. 2007).

Sensorimotor integration is pivotal to enabling CPGs to generate environmentally- and behaviorally appropriate motor patterns (Lund and Kolta 2006; Rossignol et al. 2006; Buschges et al. 2008; Pearson 2008; Blitz and Nusbaum 2011). Sensory feedback, for example, regulates many aspects of rhythmic motor patterns including its cycle period, phase durations, and the CPG- and motor neuron firing patterns and rates. Furthermore, sensory input to CPGs has both phase-specific actions and longer-lasting influences, such as the ability to activate or terminate CPG activity. Sensory input to motor systems is also extensively regulated, both pre- and postsynaptically, enabling it to have context-specific actions. There remain, however, many unresolved issues pertaining to sensorimotor integration. For example, the synaptic- and circuit-level consequences of context-specific sensory actions remain to be determined in most systems.

The decapod crustacean stomatogastric nervous system

The decapod crustacean foregut is a 4-compartment structure composed of the oesophageous (swallowing) and a 3-compartment stomach that includes, from rostral to caudal, the cardiac sac (food storage), gastric mill (chewing) and pylorus (filtering of chewed food) (Fig. 1A) (Johnson and Hooper 1992). The pylorus communicates directly

with the midgut, through which nutrients are absorbed.

Chewing movements in the gastric mill, which is controlled by a CPG on which this thesis is focused, involve a coordinated rhythmic alternation of protraction and retraction by a single medial tooth and paired lateral teeth (Turrigiano and Heinzel, 1992; Heinzel et al. 1993). This behavior results, indirectly, from rhythmic alternating contraction of protractor- and retractor-specific striated muscles. This relationship is indirect because the muscles attach to, and hence move ossicles (cartilaginous skeletal structures) that in turn connect to the teeth. Thus, tooth protraction and retraction are pivot movements resulting from these ossicles acting like fulcrums.

For my experiments I used the isolated STNS from the crab *Cancer borealis*. The STNS is an extension of the CNS that contains 4 ganglia plus their connecting and peripheral nerves (Fig. 1B). The four ganglia include the paired commissural ganglia (CoG: ~500 neurons each), the oesophageal ganglion (OG: 14 neurons) and the stomatogastric ganglion (STG: 26 neurons) (Kilman and Marder 1996). The STG contains the gastric mill and pyloric CPGs (Marder and Bucher 2007; Stein 2009). There is only a single nerve, the stomatogastric nerve (*stn*), that connects the STG with the rest of the CNS, including the CoGs and OG (Fig. 1B). Each CoG connects with the *stn* via two nerves, the superior- (*son*) and inferior oesophageal nerve (*ion*) (Fig. 1B). There are no more than 20 different projection neurons that innervate the STG, nearly all of which originate as bilaterally symmetric pairs in the CoGs (Coleman et al. 1992). All but two of the CoG projection neurons extend their axons through the *sons* (Coleman et al. 1992). The two projection neurons that instead extend through the *ions* are MCN1 and MCN5 (modulatory commissural neurons 1/5: Coleman and Nusbaum 1994; Norris et al. 1996). The ability to selectively identify MCN1 activity in the *ion* nerve, based on its spike amplitude, firing pattern and response pattern to stimulating identified pathways, is

a pivotal aspect of my studies. There is also one interneuron each from the gastric mill (interneuron 1: Int1) and pyloric (anterior burster: AB) CPGs that project to the CoGs and regulate the activity of the projection neurons that drive these CPGs (Fig. 2). The peripheral nerves that branch laterally and posteriorly from the STG contain the axons of the gastric mill and pyloric motor neurons that innervate the gastric mill and pyloric muscles (Fig. 1B).

Nearly all (22 of 26) of the STG neurons contribute to the gastric mill and/or pyloric motor circuits (Hooper et al., 1986; Weimann et al. 1991; Weimann and Marder, 1994; Kilman and Marder 1996). The STG somata are located around the perimeter of the central neuropil (Fig. 3). All STG neurons are monopolar and project their primary neurite into the neuropil, where it branches extensively before projecting from the STG to innervate muscles or more central ganglia (Bucher et al. 2007; Marder and Bucher 2007). These somata are electrically inexcitable, and their spike initiation zones tend to be located near the edge of the ganglion (Raper 1979).

The relatively large diameter (25-120 μm) of the STG somata, and the ability to remove the connective tissue sheath encasing this ganglion, enables routine and long-lasting (e.g., hours) simultaneous intracellular recordings. This fact, along with the small number of STG neurons and the fact that most of them occur as single copies, has made their physiological identification and characterization routine across preparations (Marder and Bucher 2007; Stein 2009). All gastric mill neurons are present as single copies except the GM motor neuron (4 copies), while all pyloric motor neurons occur as single copies except for the PD and LPG neurons (2 copies each), and PY neurons (5 copies) (Kilman and Marder 1996) (Fig. 2). All but two of these neurons (Int1, AB) are motor neurons that innervate the striated muscles of the foregut (Weimann et al. 1991). Despite functioning as motor neurons, many of these neurons also make functionally-

important synapses within the STG and some of them are core CPG components. Additionally, all of these motor neurons are routinely recorded extracellularly from the peripheral nerves (e.g. Fig. 4). The activity of each neuron is readily identified in these nerve recordings because (a) each nerve contains few axons, (b) the extracellularly-recorded spike amplitude of each neuron is distinct, and (c) during the gastric mill and pyloric rhythms, the different motor neurons are sequentially active (e.g. Fig. 4). This level of accessibility makes this system ideal for examining the cellular and synaptic mechanisms underlying motor pattern generation (Nusbaum and Beenhakker 2002; Marder and Bucher 2007; Stein 2009).

All STG neurons are also readily recorded intracellularly (e.g. Fig. 4), due to their relatively large diameter and their laminar distribution around the central neuropil (Fig. 3). Due to their accessibility, all STG neurons have been extensively characterized in terms of their voltage-dependent properties, synaptic connections, neurotransmitters and responses to many applied neuromodulators (Harris-Warrick et al. 1992; Marder and Bucher 2007; Stein 2009). Additionally, their cellular and synaptic properties are state dependent, as they are modulated extensively by projection- and sensory neurons and circulating hormones (Harris-Warrick et al. 1998; Marder and Bucher 2007; Stein 2009).

The stomatogastric system is also advantageous for studying the CPG output at the level of the target muscles, because subsets of gastric mill and/or pyloric muscles can be left innervated and removed with the otherwise isolated STNS (Figs. 1B, 5). As a result, simultaneous recordings are possible from the STG motor neurons and their muscle targets (Hooper et al., 1986; Weimann et al. 1991; Jorge-Rivera and Marder 1996, 1997; Stein et al., 2006). In particular, gastric mill muscle contraction is driven by gastric mill protractor (LG, MG, IC, GM neurons) and retractor (DG, VD, AM neurons) motor neurons (Weimann et al. 1991).

Among the ~20 projection neurons that innervate the STG, 6 are identified and their actions on the STG characterized in *C. borealis*. Four of them, including MCN1, MCN5 and MCN7 plus commissural projection neuron 2 (CPN2), have their somata in the CoG (Fig. 1B) (Coleman and Nusbaum 1994; Norris et al. 1994, 1996; Blitz et al. 1999). MCN1 and CPN2 are pivotal for driving the gastric mill rhythm (Fig. 2; see below) (Norris et al. 1994; Coleman et al. 1995; Bartos et al. 1999; Beenhakker and Nusbaum 2004; Blitz et al. 2004).

With respect to CPG types, the STG contains both a pacemaker-driven CPG (pyloric circuit) and a network-driven CPG (gastric mill circuit) (Marder and Bucher 2007). The pyloric CPG generates a persistent pyloric rhythm in vivo and in the isolated STNS. The gastric mill (chewing) CPG is not spontaneously active either in vivo or in vitro. Instead, its activity is regulated by projection neuron inputs that also tend to not be spontaneously active (see below).

Gastric mill rhythm generation

The general organization of the crab gastric mill system is comparable to the vertebrate locomotor system (Kiehn 2010; Kiehn et al. 2010; Gossard et al. 2011; Le Ray et al. 2011; Jordan and Slawinska 2011). For example, both systems utilize network-driven CPGs that are regulated by descending projections. Reciprocal inhibition between functional antagonists underlies the gastric mill CPG and appears to be central to the locomotor CPG. Also, in both systems one phase duration is relatively constant (powerstroke phase: walking, stance phase; gastric mill, protraction) while the other phase duration (return stroke phase: walking, swing; gastric mill, retraction) exhibits most of the change that occurs with a change in cycle period. Lastly, in both systems, among others, the projection neurons receive rhythmic synaptic feedback from the CPG

they activate and thus, once the rhythm is activated, the projection neuron firing pattern changes from tonic to rhythmic (Coleman and Nusbaum 1994; Norris et al. 1994; Ezure and Tanaka 1997; Blitz and Nusbaum 2008; Grillner and Wallen 2002; Antri et al. 2009).

The crab gastric mill CPG is a small, well-characterized model system for network-driven CPGs (Marder and Bucher 2007; Stein 2009). The complete gastric mill motor circuit includes 4 protraction phase motor neurons, 3 retraction phase motor neurons plus 1 retraction phase interneuron (Fig. 2). However, during the two versions of the gastric mill rhythm that were characterized prior to my thesis research, the core CPG for rhythm generation includes only the reciprocally-inhibitory gastric mill neurons LG (lateral gastric, protraction phase motor neuron) and Int1 (retraction phase interneuron 1) (Coleman et al. 1995; Bartos et al. 1999; Saldeman et al. 2007; DeLong et al. 2009a). These two gastric mill rhythms are driven by tonically stimulating the projection neuron MCN1 or bath-applying the peptide CabPK (*Cancer borealis* pyrokinin). Gastric mill rhythm generation by CabPK also requires participation of the pyloric pacemaker interneuron AB, so really this version of the CPG is a hybrid between a network-driven and pacemaker-driven circuit (Saideman et al. 2007). Interestingly, despite configuring the same gastric mill neurons into distinct circuits, MCN1 and CabPK elicited the same gastric mill motor pattern (Saideman et al. 2007). In both cases, activity in the other 6 gastric mill motor neurons is not necessary for rhythm generation but is necessary to generate the appropriately coordinated chewing movements.

Gastric mill motor patterns can also be driven by activating sensory or CNS pathways (Fig. 2) (Beenhakker et al. 2004; Blitz et al. 2004, 2008). For each of the three input pathways thus far studied, the stimulated pathway elicits the gastric mill rhythm by triggering lasting activation of the same two identified projection neurons (MCN1, CPN2) (Fig. 2) (Beenhakker and Nusbaum 2004; Blitz et al. 2004, 2008; Wood et al. 2004).

The mechanisms underlying gastric mill rhythm generation are most extensively characterized for the rhythm driven by tonic stimulation of MCN1 (Coleman et al. 1995; Bartos et al. 1999; Beenhakker et al. 2005; Saideman et al. 2007; DeLong et al. 2009a). The core CPG for this rhythm includes the aforementioned neurons LG and Int1, plus the STG axon terminals of MCN1 ($MCN1_{STG}$). The pivotal aspects of rhythm generation during tonic MCN1 stimulation include (a) MCN1 causes a slow excitation of LG via its peptide cotransmitter CabTRP Ia (*Cancer borealis* tachykinin-related peptide Ia), (b) MCN1 causes a fast excitation of Int1 via its small molecule transmitter GABA, (c) both of these MCN1 synaptic actions occur only during retraction because during protraction the LG neuron synaptically inhibits $MCN1_{STG}$, and (d) during protraction, when MCN1 transmitter release is inhibited, its electrical coupling with LG is strengthened.

Motor pattern selection

Two identified pathways that activate distinct gastric mill rhythms include the mechanosensory ventral cardiac neurons (VCNs) and the proprioceptor gastro-pyloric receptor neurons (GPRs). These two sensory systems each trigger gastric mill rhythms by co-activating MCN1 and CPN2 (Beenhakker and Nusbaum 2004; Blitz et al. 2004). Despite their convergent actions on the same two projection neurons, the VCNs and GPRs elicit quantitatively distinct rhythms, although the overall motor pattern was qualitatively comparable. These studies supported the hypothesis that distinct inputs can elicit different motor outputs despite activating the same projection neurons. Recently, another gastric mill rhythm was identified in *C. borealis* in which the protractor phase neuron LG exhibits pyloric-timed activity instead of the tonic burst it generates during the VCN- and GPR-gastric mill rhythms (Wood et al. 2004). In the work by Wood et al. (2004), this novel rhythm occurred spontaneously and was largely mimicked by

selectively stimulating MCN1 with the distinct pyloric rhythm-timed activity pattern that it exhibited during this rhythm. The aspects of this rhythm not mimicked by MCN1 stimulation were likely to result from CPN2 activity, based on the known CPN2 synaptic actions (Norris et al. 1994). If this novel gastric mill rhythm was in fact also driven by MCN1 and CPN2, this would lend further support the hypothesis that the same projection neurons can generate different rhythms from the same motor circuit.

As reported in Chapter 2 of my thesis, I participated in a collaboration that determined that the novel gastric mill rhythm characterized by Wood et al. (2004) is triggered by stimulating a newly identified input pathway called the post-oesophageal commissure (POC) neurons (Blitz et al. 2008). The POC neurons are a bilateral population of peptidergic neurons (~100 neurons per side) that innervate the CoGs and, among other actions, trigger a long-lasting activation of MCN1 and CPN2 via its peptide transmitter CabTRP Ia. This activation of MCN1 and CPN2 is sufficiently strong to drive a relatively long-lasting (minutes to tens of minutes) gastric mill motor pattern.

As shown qualitatively in Thesis Chapter 2, and quantitatively in Chapter 3, the POC-triggered gastric mill motor pattern is distinct from the VCN-triggered gastric mill motor pattern (and hence, also the GPR-elicited motor pattern). One obvious distinction is that the protractor motor neuron LG burst is pyloric-timed, as in Wood et al. (2004), instead of tonic as occurs during the VCN- and GPR-triggered motor patterns.

In Thesis Chapter 3, I also establish that the core rhythm underlying the distinct VCN- and POC-triggered gastric mill motor patterns is generated by the same two neurons (LG and Int1). Little is known in most systems regarding the identity of the neurons responsible for rhythm generation, and even less is known regarding whether the core rhythm generator is preserved or changed when a CPG generates different motor patterns.

In Thesis Chapter 4, I determined that the different LG activity patterns that occur during the POC- and VCN-gastric mill rhythms in the isolated STNS are preserved at the level of the LG-innervated muscles (Fig. 5). Previous studies using the crustacean pyloric rhythm (Morris et al. 2000; Thuma et al. 2003), and the *Aplysia* feeding system (Zhurov and Brezina 2006), also showed that contractions of individual muscles can reflect the different centrally-generated motor neuron inputs they receive. It was not a foregone conclusion that these contraction patterns would be distinct because, despite being striated muscles, these muscle fibers exhibit slow contraction and relaxation dynamics (Jorge-Rivera and Marder 1996, 1997; Morris and Hooper 1997, 1998). Additionally, in general these muscle fibers do not generate action potentials but only excitatory junction potentials (EJPs) in response to their motor neuron input (Hooper et al. 1986; Weimann et al. 1991). In fact, previous work showed that some pyloric muscles effectively contract and relax with each pyloric cycle while, due to slow relaxation dynamics, others integrate their rhythmic neuronal input and exhibit a relatively smooth contraction across multiple cycles (Morris et al., 2000; Thuma et al. 2003).

In Thesis Chapter 5, I address whether sensory input to a motor circuit is regulated in a state-dependent manner. Specifically, I determined whether the GPR proprioceptor neuron has the same influence on the POC- and VCN-gastric mill rhythms. As indicated above, although these two pathways trigger different gastric mill motor patterns, they do so via the same projection neurons (MCN1, CPN2) and rhythm generator neurons (LG, Int1). A previous study had established that GPR selectively prolonged the retractor phase during the VCN-triggered gastric mill rhythm (Beenhakker et al. 2007). This influence resulted from GPR inhibition of $MCN1_{STG}$ (Beenhakker et al. 2005) and a gating-out by the VCN pathway of the GPR excitatory actions on MCN1 and CPN2 in the CoGs (Beenhakker et al. 2007). If the latter actions had not been gated-out,

then GPR would have altered the gastric mill motor pattern in additional ways. In Chapter 5, I found that the GPR actions in the CoGs are not gated-out during the POC-gastric mill motor pattern, and consequently its influence on this motor pattern was distinct from its influence on the VCN-motor pattern.

During my thesis research, I used the accessibility of the crab STNS to address a set of issues pertaining to the activation and regulation of CPG output to determine whether (1) distinct input pathways can trigger different versions of a motor pattern by activating the same projection neurons to drive the same rhythm generator neurons, (2) different CPG output patterns are retained at the level of the muscles that underlie the resulting behaviors, and (3) a sensory feedback pathway has state-dependent actions on a rhythmic motor system. In the following 4 chapters, I elaborate my findings regarding each of these issues and provide novel insights into flexibility available within rhythmic motor systems such as those within the crab STNS.

REFERENCES

Antri M, Fenelon K, Dubuc R (2009) The contribution of synaptic inputs to sustained depolarizations in reticulospinal neurons. J Neurosci 29:1140-1151.

Bartos M, Manor Y, Nadim F, Marder E, Nusbaum MP (1999) Coordination of fast and slow rhythmic neuronal circuits. J Neurosci 19:6650-6660.

Beenhakker MP, Nusbaum, MP (2004) Mechanosensory activation of a motor circuit by coactivation of two projection neurons. J Neurosci 24:6741-6750.

Beenhakker MP, Kirby MS, Nusbaum MP (2007) Mechanosensory gating of proprioceptor input to modulatory projection neurons. J Neurosci 27:14308-14316.

Beenhakker MP, DeLong ND, Saideman ST, Nadim F, Nusbaum MP (2005) Proprioceptor regulation of motor circuit activity by presynaptic inhibition of a modulatory projection neuron. J Neurosci 25:8794-8806.

Blitz DM, Nusbaum MP (2011) Sensorimotor integration in the stomatogastric nervous system. Curr Opin Neurobiol, In Press.

Blitz DM, Nusbaum MP (2008) State dependent presynaptic inhibition regulates central pattern generator feedback to descending inputs. J Neurosci 28:9564-9574.

Blitz DM, Beenhakker MP, Nusbaum MP (2004) Different sensory systems share projection neurons but elicit distinct motor patterns. J Neurosci 24:11381-11390.

Blitz DM, Christie AE, Coleman MJ, Norris BJ, Marder E, Nusbaum MP (1999) Different proctolin neurons elicit distinct motor patterns from a multifunctional neuronal network. J Neurosci 19:5449-5463.

Briggman KL, Kristan WB (2008) Multifunctional pattern-generating circuits. Annu Rev Neurosci 31:271-294.

Bucher D, Johnson CD, Marder E (2007) Neuronal morphology and neuropil structure in the stomatogastric ganglion of the lobster, Homarus americanus. J Comp Neurol 501:185-205.

Buschges A, Akay T, Gabriel JP, Schmidt J (2008) Organizing network action for locomotion: insights from studying insect walking. Brain Res Rev 57:162-171.

Coleman, MJ, Nusbaum MP, Cournil I, Claiborne B J (1992) Distribution of modulatory inputs to the stomatogastric ganglion of the crab, *Cancer borealis*. J Comp Neurol 325:581-594.

Coleman MJ, Meyrand P, Nusbaum MP (1995) A switch between two modes of synaptic transmission mediated by presynaptic inhibition. Nature 378:502-505.

Coleman MJ, Nusbaum MP (1994) Functional consequences of compartmentalization of synaptic input. J Neurosci 14:6544-6552.

DeLong ND, Beenhakker MP, Nusbaum MP (2009) Presynaptic inhibition selectively weakens peptidergic cotransmission in a small motor system. J Neurophysiol 102:3492-3504.

Dickinson PS (2006) Neuromodulation of central pattern generators in invertebrates and vertebrates. Curr Opin Neurobiol 16:604-614.

Doi A, Ramirez JM (2008) Neuromodulation and the orchestration of the respiratory rhythm. Respir Physiol Neurobiol 164:96-104.

Dubuc R, Brocard F, Antri M, Fénelon K, Gariépy F, Smetana R, Ménard A, Le Ray D, Di Prisco GV, Pearlstein E, Sirota MG, Derjean D, St-Pierre M, Zielinski B, Auclair F, Veilleux D (2008) Initiation of locomotion in lampreys. Brain Res Rev 57:172-182.

El Manira A, Kyriakatos A, Nanou E (2010) Beyond connectivity of locomotor circuitry – Ionic and modulatory mechanisims. Prog Brain Res 187:99-110.

Ezure K, Tanaka I (1997) Convergence of central respiratory and locomotor rhythms onto single neurons of the lateral reticular nucleus. Exp Brain Res 113:230-242.

Fort TJ, Brezina V, Miller MW (2007) Regulation of the crab heartbeat by FMRFamide-like peptides: multiple interacting effects on center and periphery. J Neurophysiol 98:2887-2902.

Garcia AJ, Zanella S, Koch H, Doi A, Ramirez J-M (2011) Networks within networks: The neuronal control of breathing. Prog Brain Res 188:31-50.

Georgopoulos AP (1995) Current issues in directional motor control. Trends Neurosci 18:506-510.

Gossard JP, Sirois J, Noue P, Cote MP, Menard A, Leblond H, Frigon A (2011) The spinal generation of phases and cycle duration. Prog Brain Res 188:15-29.

Grillner S, Wallen P (2002) Cellular bases of a vertebrate locomotor system-steering, intersegmental and segmental co-ordination and sensory control. Brain Res Rev 40:92-106.

Grillner S (2006) Biological pattern generation: the cellular and computational logic of networks in motion. Neuron 52:751-766.

Guertin PA (2009) The mammalian central pattern generator for locomotion. Brain Res Rev 62:45-56.

Harris-Warrick R (2010) General principles of rhythmogenesis in central pattern generator networks. Prog Brain Res 187:213-222.

Harris-Warrick RM, Johnson BR, Peck JH, Kloppenburg P, Ayali A, Skarbinski J (1998) Distributed effects of dopamine modulation in the crustacean pyloric network. Annu NY Acad Sci 860:155-167.

Harris-Warrick, RM, Marder E, Selverston AI, Moulins M, Eds. (1992) Dynamic Biological Networks: The Stomatogastric Nervous System. MIT Press:Cambridge, MA.

Heinzel HG, Weimann JM, Marder E (1993) The behavioral repertoire of the gastric mill in the crab, *Cancer pagurus*: an in situ endoscopic and electrophysiological examination. J Neurosci 13:1793-1803.

Hooper SL, O'Neil MB, Wagner R, Ewer J, Golowasch J, Marder E (1986) The innervation of the pyloric region of the crab, *Cancer borealis*: homologous muscles in decapod species are differently innervated. J Comp Physiol 159:227-240.

Johnson and Hooper (1992) Overview of the stomatogastric nervous system. In: Dynamic Biological Networks: The Stomatogastric Nervous System (Harris-Warrick et al., eds). MIT Press:Cambridge, MA, pp. 1-30.

Jordan LM, Slawinska U (2011) Modulation of rhythmic movement: control of coordination. Prog Brain Res 188:181-195.

Jorge-Rivera JC, Marder E (1997) Allatostatin decreases stomatogastric neuromuscular transmission in the crab, *Cancer borealis*. J Exp Biol 200:2937-2946.

Jorge-Rivera JC, Marder E (1996) TNRNFLRFamide and SDRNFLRFamide modulate muscles of the stomatogastric system of the crab *Cancer borealis*. J Comp Physiol 179:741-751.

Kiehn O (2010) Development and functional organization of spinal locomotor circuits. Current Opin Neurobiol 21:1-10.

Kiehn O, Dougherty KJ, Hagglund M, Morgius, Talpalar A, Restrepo CE (2010) Probing spinal circuits controlling walking in mammals. Biochem Biophys Res Commun 396:11-18.

Kilman VL, Marder E (1996) Ultrastructure of the stomatogastric ganglion neuropil of the crab, *Cancer borealis*. J Comp Neurol 374:362-375.

Kristan and Shaw (1997) Population coding and behavioral choice. Curr Opin Neurobiol 7:826-831.

Kristan WB, Calabrese RL, Friesen WO (2005) Neuronal control of leech behavior. Prog Neurobiol 76:279-327.

Le Ray D, Juvin L, Ryczko D, Dubuc R (2011) Supraspinal control of locomotion: the mesencephalic locomotor region. Prog Brain Res 188:51-70.

Liu KS, Fetcho JR (1999) Laser ablations reveal functional relationships of segmental hindbrain neurons in zebrafish. Neuron 23:325-335.

Lund JP, Kolta A (2006) Generation of the central masticatory pattern and its modification by sensory feedback. Dysphagia 21:167-174.

Marder E, Bucher D (2001) Central pattern generators and the control of rhythmic movements. Curr Biol 11:R986-r996.

Marder E, Bucher D (2007) Understanding circuit dynamics using the stomatogastric nervous system of lobsters and crabs. Annu Rev Physiol. 69:291-316.

Marder E, Bucher D, Schulz DJ, Taylor AL (2005) Invertebrate central pattern generation moves along. Curr Biol 15:R685-699.

Marder E, Calabrese RL (1996) Principles of rhythmic motor pattern generation. Physiol Rev 76:687-717.

Morgan PT, Jing J, Vilim FS, Weiss KR (2002) Interneuronal and peptidergic control of motor pattern switching in *Aplysia*. J Neurophysiol. 87:49-61.

Morris LG, Hooper SL (1997) Muscle response to changing neuronal input in the lobster (*Panulirus interruptus*) stomatogastric system: spike number- versus spike frequency-dependent domains. J Neurosci 17:5956-5971.

Morris LG, Hooper SL (1998) Muscle response to changing neuronal input in the lobster (*Panulirus interruptus*) stomatogastric system: slow muscle properties can transform rhythmic input into tonic output. J Neurosci 18:3433-3442.

Morris LG, Thuma JB, Hooper SL (2000) Muscles express motor pattern of non-innervating neural networks by filtering broad-band input. Nat Neurosci 3:245-250.

Norris BJ, Coleman MJ, Nusbaum MP (1996) Pyloric motor pattern modification by a newly identified projection neuron in the crab stomatogastric nervous system. J. Neurophysiol 75:97-108.

Norris BJ, Coleman MJ, Nusbaum, MP (1994) Recruitment of a projection neuron determines gastric mill motor pattern selection in the stomatogastric nervous system of the crab, *Cancer borealis.* J. Neurophysiol. 72:1451-1463.

Nusbaum MP, Beenhakker MP (2002) A small-systems approach to motor pattern generation. Nature 417:343-350.

Nusbaum MP, Blitz DM, Swensen AM, Wood D, Marder E (2001) The roles of co-transmission in neural network modulation. Trends Neurosci 24:146-154.

Pearson KG (2008) Role of sensory feedback in the control of stance duration in walking cats. Brain Res Rev 57:222-227.

Rauscent A, Einum J, Le Ray D, Simmers J, Combes D (2009) Opposing aminergic modulation of distinct spinal locomotor circuits and their functional coupling during amphibian metamorphosis. J Neurosci 29:11163-11174.

Ryczko D, Dubuc R, Cabelguen J (2010) Rhythmogenesis in axial locomotor networks: an interspecies comparison. Prog Brain Res 187:189-211.

Raper JA (1979) Nonimpulse-mediated synaptic transmission during the generation of a cyclic motor program. Science 205:304-306.

Rossignol S, Dubuc R, Gossard JP (2006) Dynamic sensorimotor interactions in locomotion. Physiol Rev 86:89-154.

Saideman SR, Blitz DM, Nusbaum MP (2007b) Convergent motor patterns from divergent circuits. J Neurosci 27:6664-6674.

Selverston AI (2010) Invertebrate central pattern generator circuits. Philos Trans R Soc Lond B 365:2329-2345.

Stein PSG, Grillner S, Selverston A, Stuart DG (1997) Neurons, Networks, and Motor Behavior. MIT Press:Cambridge, MA.

Stein W, Smarandache CR, Nickmann M, Hedrich UBS (2006) Fuctional consequences of activity-dependent synaptic enhancement at a crustacean neuromuscular junction. J Exp Biol 209:1285-1300.

Stein W (2009) Modulation of stomatogastric rhythms. J Comp Physiol A 195:989-1009.

Thuma JB, Morris LG, Weaver AL, Hooper SL (2003) Lobster (*Panulirus interruptus*) pyloric muscles express the motor patterns of three neural networks, only one of which innervates the muscles. J Neurosci 23:8911-8920.

Turrigiano GG, Heinzel H.-G. (1992) Behavioral correlates of stomatogastric network function. In: Dynamic Biological Networks, The Stomatogastric Nervous System (Harris-Warrick RM, Marder E, Selverston AI, Moulins M, eds), pp. 197-220, MIT Press: Cambridge, MA.

Weimann JM, Marder E (1994) Switching neurons are integral members of multiple oscillatory networks. Curr Biol 4:896-902.

Weimann JM, Meyrand P, Marder E (1991) Neurons that form multiple pattern generators: identification and multiple activity patterns of gastric/pyloric neurons in the crab stomatogastric system. J Neurophysiol 65:111-122.

Wood DE, Manor Y, Nadim F, Nusbaum MP (2004) Intercircuit control via rhythmic regulation of projection neuron activity. J Neurosci 24:7455-7463.

Zhurov and Brezina (2006) Variability of motor neuron spike timing maintains and shapes contractions of the accessory radula closer muscle of *Aplysia.* J Neurosci 26:7056-7070.

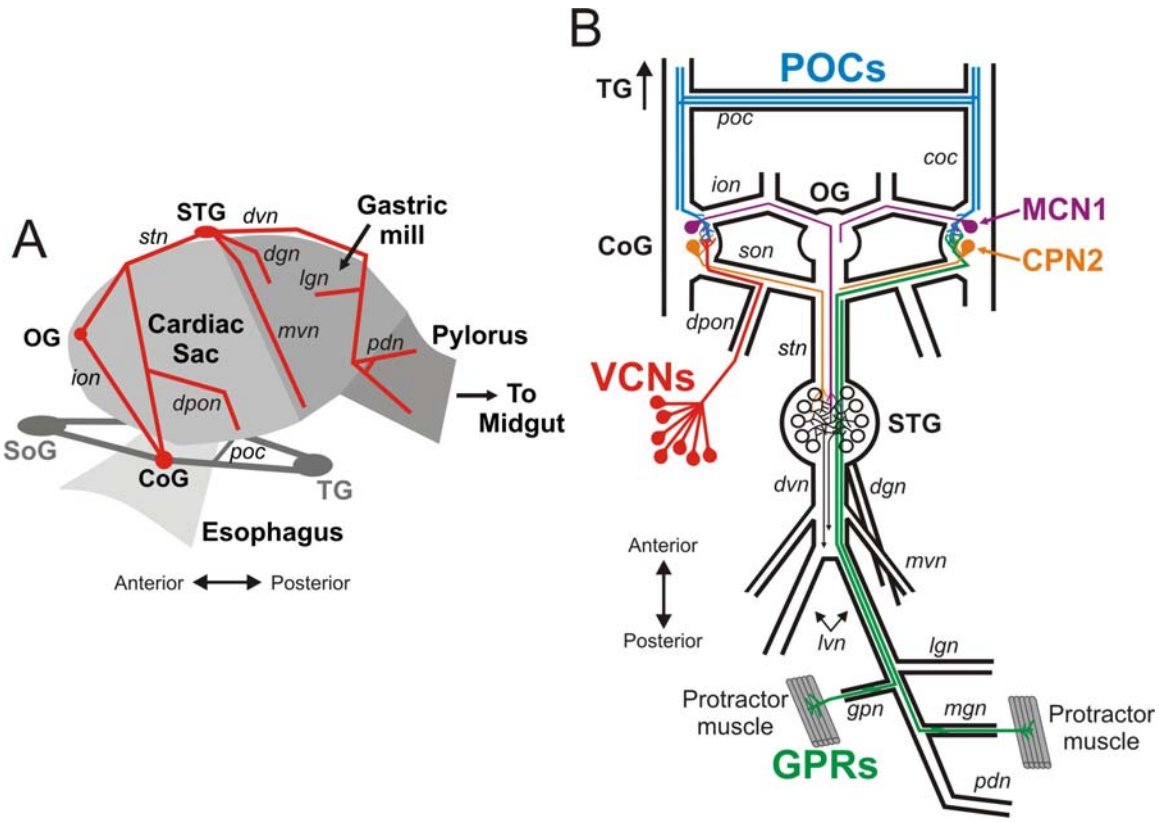

Figure 1. Schematic of the crab foregut and stomatogastric nervous system.

A. Schematic side-view of the crab foregut with the stomatogastric nervous system (STNS) shown in red. The foregut is separated into 4 functional regions, including the oesophagus (swallowing), cardiac sac (storage), gastric mill (chewing) and pylorus (filtering). The STNS receives input from neurons whose somata are located in the SOG and TG (ganglia in gray), and from sensory neurons that project through the same connecting nerves. These extrinsic inputs primarily target projection neurons (CoGs).

B. Schematic of the STNS, including its four ganglia plus their connecting and peripheral nerves. The pyloric and gastric mill CPGs are located in the STG. The paired CoGs and unpaired OG contain projection neurons that regulate the STG circuits.

Abbreviations: Ganglia- CoG, commissural ganglion; OG, oesophageal ganglion; SOG, supraoesphageal ganglion; STG, stomatogastric ganglion; TG, thoracic ganglion.

Nerves– *dgn,* dorsal gastric nerve; *dpon,* dorsal posterior oesophageal nerve; *dvn,* dorsal ventricular nerve; coc, circumoesophageal commissure; *gpn,* gastropyloric nerve; *ion*, inferior oesophageal nerve, *lgn,* lateral gastric nerve; *lvn,* lateral ventricular nerve, *mgn,* medial gastric nerve; *mvn,* medial ventricular nerve; *pdn*, pyloric dilator nerve; *poc,* post-oesophageal commissure; *son*, superior oesophageal nerve; *stn,* stomatogastric nerve. Neurons– CPN2, commissural projection neuron 2; GPRs, gastropyloric receptors; MCN1, modulatory commissural neuron 1; POCs, post-oesophageal commissure neurons; VCNs, ventral cardiac neurons.

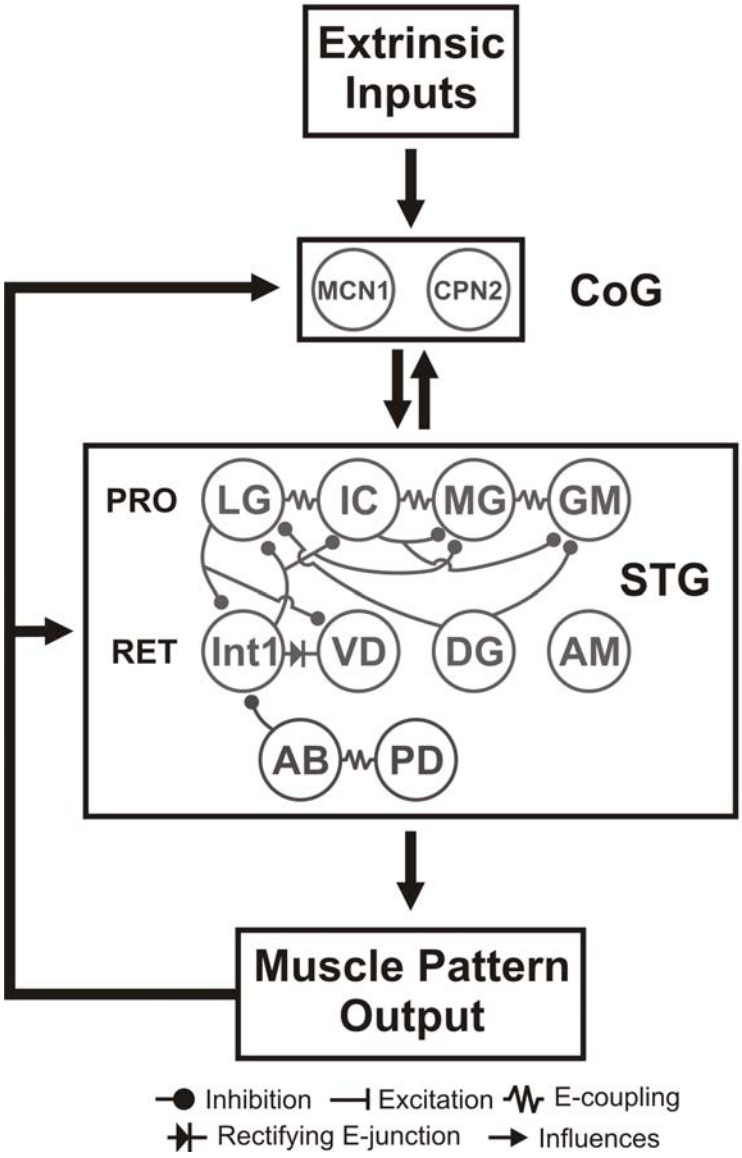

Figure 2. Schematic of the gastric mill motor system, including identified extrinsic inputs, projection neurons and motor circuit neurons. Extrinsic inputs (e.g. POC neurons, VCNs) can each trigger a lasting activation of the projection neurons MCN1 and CPN2, which in turn activate the gastric mill circuit to generate the gastric mill rhythm. As indicated, these projection neurons originate in the CoGs and project to the STG where the gastric mill circuit is located. The top row of gastric mill circuit neurons represent protractor (PRO) phase neurons while the second row represent retractor

(RET) phase neurons. The bottom row shows the pyloric pacemaker neurons, which influence the gastric mill rhythm via synapses in the STG and CoGs. Note that the exact electrical coupling relationship among the protractor neurons is not known, so they are shown simply as being serially coupled. All gastric mill circuit neurons occur as single copies per STG, except for GM (4) and PD (2). Abbreviations: AB, anterior burster; AM, anterior median; DG, dorsal gastric; GM, gastric mill; IC, inferior cardiac; Int1, interneuron 1; MG, medial gastric; LG, lateral gastric; PD, pyloric dilator; VD, ventricular dilator. Other abbreviations as in Fig. 1.

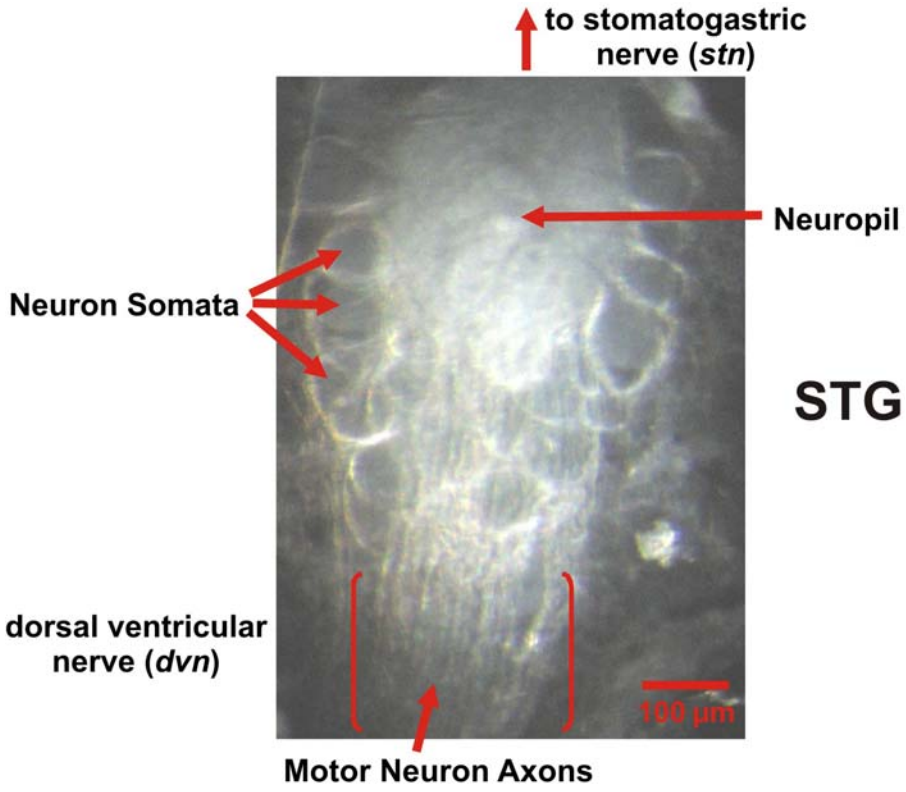

Figure 3. Dark-field image of a desheathed STG from *Cancer borealis.* The neuronal somata form a monolayer around the ganglionic neuropil. All synapses in the STG are located on neuropilar processes. There are no synapses onto the STG somata. The axons in the *stn* include projection neuron and sensory neuron inputs to the STG plus STG neurons projecting towards the CoGs. The axons in the *dvn* are primarily STG motor neurons projecting to their muscle targets and sensory neurons projecting to the STG and more central ganglia. Photograph provided by Jason C. Rodriguez (Nusbaum lab).

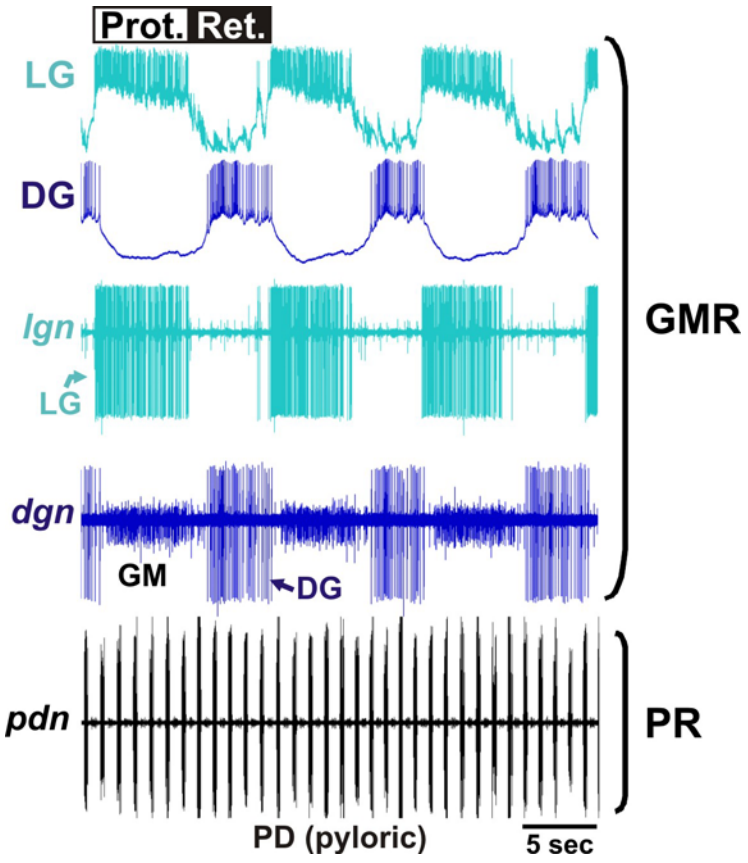

Figure 4. Example recordings during gastric mill and pyloric rhythms. Protractor (LG, GM) and retractor (DG) motor neurons fire in alternation during the gastric mill rhythm. The top two traces are intrasomatic recordings from the protractor LG neuron and the retractor DG neuron. The third and forth traces are extracellular monitors of LG and DG plus GM activity, respectively. The bottom trace is an extracellular recording of PD neuron activity, used to monitor the pyloric rhythm. Note that the pyloric rhythm (cycle period ~1 s) cycles ~10-times faster than the gastric mill rhythm (cycle period ~0.1 s). Abbreviations as in Figs. 1 and 2.

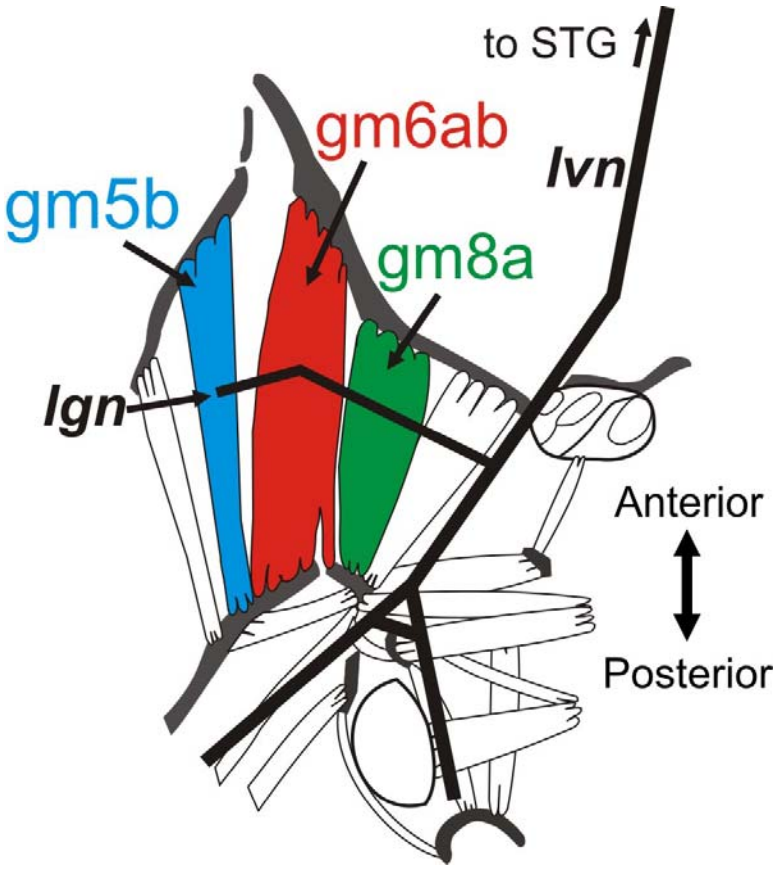

Figure 5. Schematic dorsal view showing some of the muscles in a dissected *C. borealis* posterior foregut. The single LG axon projects from the STG through the *dvn* nerve, bifurcates at the *dvn-lvns* junction (not shown; see Fig. 1A), and continues through the left and right *lvn* and *lgn* nerves to innervate several bilaterally symmetric protractor muscles, including gm5b, gm6ab and gm8a. Only the left side of the posterior foregut is shown (modified from Weimann et al. 1991).

CHAPTER 2

A Newly Identified Extrinsic Input Triggers a Distinct Gastric Mill Rhythm via Activation of Modulatory Projection Neurons

Dawn M. Blitz

Rachel S. White

Shari R. Saideman

Aaron Cook

Andrew E. Christie

Farzan Nadim

Michael P. Nusbaum

Accepted:

Journal of Experimental Biology, 2008

ABSTRACT

Neuronal network flexibility enables animals to respond appropriately to changes in their internal and external states. We are using the isolated crab stomatogastric nervous system to determine how extrinsic inputs contribute to network flexibility. The stomatogastric system includes the well-characterized gastric mill (chewing) and pyloric (filtering of chewed food) motor circuits in the stomatogastric ganglion. Projection neurons with somata in the commissural ganglia (CoGs) regulate these rhythms. Previous work characterized a unique gastric mill rhythm that occurred spontaneously in some preparations, but whose origin remained undetermined. This rhythm includes a distinct protractor phase activity pattern, during which a key gastric mill circuit neuron (LG neuron) and the projection neurons MCN1 and CPN2 fire in a pyloric rhythm-timed activity pattern instead of the tonic firing pattern exhibited by these neurons during previously studied gastric mill rhythms. Here we identify a new extrinsic input, the post-oesophageal commissure (POC) neurons, relatively brief stimulation (30 sec) of which triggers a long-lasting (tens of minutes) activation of this novel gastric mill rhythm at least in part via its lasting activation of MCN1 and CPN2. Immunocytochemical and electrophysiological data suggest that the POC neurons excite MCN1 and CPN2 by release of the neuropeptide *Cancer borealis* tachykinin-related peptide Ia (CabTRP Ia). These data further suggest that the CoG arborization of the POC neurons comprises the previously identified anterior commissural organ (ACO), a CabTRP Ia-containing neurohemal organ. This endocrine organ thus appears to also have paracrine actions, including activation of a novel and lasting gastric mill rhythm.

INTRODUCTION

Neuromodulation enables single motor circuits to generate multiple distinct activity patterns by changing the intrinsic and synaptic properties of circuit neurons (Marder et al., 2005; LeBeau et al., 2005; Kiehn, 2006; Gordon and Whelan 2006; Tryba et al., 2006). Further flexibility in the output of these motor circuits is afforded by modulatory actions at the level of the projection neurons that drive circuit activity (Di Prisco et al., 2000; Beenhakker and Nusbaum, 2004; Blitz et al., 2004; McLean and Sillar, 2004; Brocard et al., 2005; Smetana et al., 2007). However, the extrinsic inputs that provide these modulatory influences on projection neurons are not well-documented in most systems.

We are using the stomatogastric nervous system (STNS) of the crab *Cancer borealis* to identify the extrinsic input responsible for the activation of a previously identified version of the gastric mill (chewing) rhythm (Wood et al., 2004). The stomatogastric nervous system is an extension of the decapod crustacean CNS that includes the unpaired stomatogastric (STG) and oesophageal (OG) ganglia plus the paired commissural ganglia (CoGs) (Nusbaum and Beenhakker, 2002; Marder and Bucher, 2007). Overlapping sets of the 26 neurons in the *C. borealis* STG contribute to the gastric mill and pyloric (filtering of chewed food) rhythms (Marder and Bucher, 2007). In *C. borealis*, these rhythms are regulated by input from no more than 20 projection neurons, most of which are present as single neurons within each CoG (Coleman et al., 1992; Nusbaum et al., 2001). In addition, extrinsic inputs that convey sensory and other information modify these rhythms by influencing circuit neurons and/or projection neurons (Meyrand et al., 1994; Combes et al., 1999; Christie et al., 2004; Beenhakker and Nusbaum 2004; Blitz et al., 2004).

Here we identify a novel extrinsic input to the STNS of *C. borealis*. This input,

called the post-oesophageal commissure (POC) neurons, consists of bilateral peptidergic fiber bundles that project through the post-oesophageal commissure (*poc*) and circumoesophageal connectives (*cocs*) to innervate the CoGs.

Extracellular *poc* stimulation drives the POC neurons to trigger a long-lasting activation of CoG projection neurons, which in turn drive the gastric mill rhythm. Two of these projection neurons are modulatory commissural neuron 1 (MCN1) and commissural projection neuron 2 (CPN2) (Coleman and Nusbaum, 1994; Norris et al., 1994). Interestingly, despite the likely participation of MCN1 and CPN2 in the POC-triggered gastric mill rhythm, the POC-triggered activity pattern of these projection neurons and the associated gastric mill rhythm are distinct from previous versions of this rhythm that are activated by these same two projection neurons (Beenhakker and Nusbaum, 2004; Blitz et al., 2004). Our data further suggest that the POC excitation of MCN1 and CPN2 is mediated by the neuropeptide transmitter *Cancer borealis* tachykinin-related peptide Ia (CabTRP Ia). The POC neurons also appear to be the source of the CabTRP Ia-containing anterior commissural organ (ACO), a dense neurohemal structure in the CoG neuropil (Messinger et al., 2005).

Some of this work was published previously in abstract form (White et al., 2005).

MATERIALS AND METHODS

Animals. Male Jonah crabs (*C. borealis* Stimpson) were obtained from Commercial Lobster and Seafood Co., Boston, MA, USA and the Marine Biological Laboratory, Woods Hole, MA, USA. Before experimentation, crabs were housed in commercial tanks containing recirculating, filtered and aerated artificial seawater (10°C). Crabs were cold anesthetized by packing in ice for at least 30 minutes prior to dissection. The STNS was dissected as described previously (Blitz et al., 2004). Briefly, the foregut was first removed and pinned down in a Sylgard 170 (KR Anderson, Morgan Hill, CA, USA, or World Precision Inc., Sarasota, FL, USA)-coated glass bowl in chilled *C. borealis* saline. The *poc* was bisected under a dissecting microscope, after which the stomach was bisected ventrally and pinned flat with the interior stomach wall against the Sylgard. The STNS, including all four ganglia (2 CoGs, OG, STG) plus their connecting and peripheral nerves (Fig. 1), was next dissected from the surface of the foregut and pinned in a Sylgard 184 (KR Anderson)-coated Petri dish. The foregut and nervous system were maintained in chilled (10-13°C) saline throughout the dissection and subsequent experiment.

All *C. borealis* used for fiber counting, tracing the POC axons to the thoracic ganglion (TG) and axon diameter measurement were collected by hand at Mount Desert Island Biological Laboratory (Salisbury Cove, Maine, USA) and maintained in flow-through natural seawater tanks at ambient water temperature (10-14°C). For ease of dissection and immunoprocessing, these animals were smaller than those used for electrophysiological experiments. As above, for tissue collection these crabs were first anesthetized by packing in ice for at least 30 minutes. The dorsal carapace was then removed and the thoracic ganglion, with the *cocs* and CoGs attached, were isolated by microdissection in chilled (approximately 10°C) *C. borealis* saline.

Solutions. Cancer borealis saline for dissections had the following composition (in mM): 440 NaCl, 26 $MgCl_2$, 13 $CaCl_2$, 11 KCl, 10 Trizma base, and 5 maleic acid (pH 7.4-7.6). During recording, 5 mM dextrose was added to the saline. In high-divalent cation saline (Hi-Di), $MgCl_2$ and $CaCl_2$ were raised to 130 mM and 65 mM, respectively. Phosphoramidon (Sigma, St. Louis, MO, USA) and CabTRP Ia (Biotechnology Center, University of Wisconsin, Madison, WI, USA) were stored as frozen aliquots and diluted in *C. borealis* saline immediately prior to use.

Electrophysiology. Extracellular recordings were made by isolating a section of nerve with petroleum jelly (Vaseline: Medical Accessories and Supply Headquarters, Alabaster, AL, USA) and placing one stainless steel wire of a pair inside the Vaseline compartment and the other wire in the main bath compartment. These recordings were amplified in a 2-stage process (Stage 1: AM Systems Model 1700 AC Amplifier, Carlsborg, WA, USA; Stage 2: Brownlee Precision Model 410 Amplifier, Santa Clara, CA, USA). To facilitate intracellular recordings, ganglia were desheathed and viewed with light transmitted through a darkfield condenser (Nikon, Tokyo, Japan). Intracellular recordings were accomplished using borosilicate microelectrodes filled with 0.6 M K_2SO_4 plus 10 mM KCl (20-25 MΩ). Intracellular signals were amplified using Axoclamp 2B amplifiers (Molecular Devices, Sunnyvale, CA, USA) and digitized at ~5 kHz using a Micro 1401 data acquisition interface and Spike2 software (Cambridge Electronic Design, Cambridge, England).

Network and projection neurons were identified based on their activity patterns, synaptic connectivity and axonal projection patterns (Weimann et al., 1991; Norris et al., 1994; Coleman and Nusbaum 1994; Beenhakker and Nusbaum, 2004; Saideman et al., 2007a,b). In some experiments, the activity of the projection neuron CPN2 was

monitored indirectly, via the presence of excitatory postsynaptic potentials (EPSPs) in the gastric mill (GM) protractor motor neuron (Norris et al., 1994).

Each half of the bisected *poc* was surrounded by a Vaseline well. Axons in the *poc* were stimulated extracellularly using a Grass S88 stimulator (AstroMed, West Warwick, RI, USA) and stimulus isolation unit (SIU5, AstroMed). The *poc* was stimulated tonically, using a range of voltages (4-15 V), at 15-30 Hz for 15-30 seconds. All *poc* stimulations were unilateral. To activate the gastro-pyloric receptor 2 neuron (GPR2: Katz et al., 1989), the gastro-pyloric nerve (*gpn*) was stimulated tonically at 10 Hz for 4 seconds. The ventral cardiac neurons (VCNs: Beenhakker et al., 2004) were activated by stimulating the dorsal posterior oesophageal nerve (*dpon*) in a rhythmic pattern (burst duration: 6 sec, interburst freq.: 0.06 Hz, intraburst freq.: 15 Hz) (Beenhakker et al., 2004; Beenhakker and Nusbaum 2004). CabTRP Ia was pressure ejected (10^{-4} M, 6 - 10 psi, 0.5 - 10 sec) into the desheathed CoG neuropil using a Picospritzer II device (General Valve Corporation, Fairfield, NJ, USA). The dorsal aspect of the CoG is covered with neuronal somata, and the neuropil is underneath these somata. Therefore, to focally apply CabTRP Ia into the CoG neuropil, we inserted the peptide-containing pipette through the soma layer and into the depth of the anterior neuropil (Blitz and Nusbaum, 1999). The endopeptidase inhibitor phosphoramidon (10^{-5} M) was superfused to the anterior portion of the STNS, which was isolated from the STG by a Vaseline wall built across the recording dish. No data collection was made until phosphoramidon superfusion had occurred for at least 25 min.

Immunocytochemistry: Whole-mounts of the isolated STNS and the thoracic ganglion (TG) with attached *cocs* and CoGs were fixed in 4% paraformaldehyde (Electron Microscopy Sciences, Hatfield, PA, USA) for 12-24 hours, rinsed at least 5 times, at one

hour intervals, in phosphate (*P*) buffer (0.1 M) with 0.3 % Triton-X 100 (*P*-Triton) and then incubated for 24-72 hours with a monoclonal rat anti-Substance P antibody (1:300; Accurate Chemical and Scientific Corporation, Westbury, NY, USA; Abcam Incorporated, Cambridge, MA, USA) that has been used previously on this system (Goldberg et al., 1988; Christie et al., 1997; Blitz et al., 1999; Messinger et al., 2005). The nervous system was then again rinsed in *P*-Triton, 5 times at one hour intervals, after which the STNS preparations were incubated with goat anti-rat Alexa Fluor 488 or 647 (1:300; Invitrogen Corporation, Carlsbad, CA, USA) for 12-16 hours. In preparations where the TG was studied, the nervous system was incubated with donkey anti-rat IgG conjugated with either FITC or rhodamine Red-X (Jackson ImmunoResearch, West Grove, PA, USA). In both cases, the preparations were then rinsed at least 5 times at one hour intervals with *P* buffer and then mounted in 80% glycerol/20% 20 mM sodium carbonate and cover-slipped. For the STNS preparations, fluorescence was visualized and photographed with a Leica DMRB microscope, a Leica DC 350 FS camera, and Image-Pro Express software (Leica, version 4.5.1.3) using a L4 or Y5 (Leica) filter set (Leica Microsystems Inc., Bannockburn, IL, USA). The thoracic-CoG preparations were imaged using a Zeiss LSM 510 Meta confocal system (Carl Zeiss MicroImaging Inc., Thornwood, NY, USA), equipped with a Zeiss Observer.Z1 inverted microscope and argon and HeNe lasers. Imaging was done using Zeiss EC plan-NEOFLUAR 10x/0.3 dry, Plan-Apochromat 20x/0.8 dry, EC plan-NEOFLUAR 40x/1.30 oil and Plan-Apochromat 63x/1.4 oil objective lenses, standard FITC and rhodamine filter sets, and manufacturer-supplied software.

Data Analysis: Data analysis was performed with custom written macros using Spike2 ('The Crab Analyzer', freely available at http://www.uni-

ulm.de/~wstein/spike2/index.html). Gastric mill cycle period was measured as the duration from the onset of a lateral gastric (LG) neuron burst to the onset of the subsequent LG burst. An average of 10 consecutive cycles was obtained in each condition. Control MCN1 and CPN2 firing frequencies were measured during 30 continuous seconds prior to stimulation. MCN1 and CPN2 firing frequencies after stimulation were quantified during 10 consecutive protraction and retraction phases of the gastric mill rhythm in each preparation, as the average frequency across the entire protraction or retraction phase. MCN1 pyloric-timed activity was measured as the percentage of time it was active during each pyloric cycle, defined as the duration from the onset of a pyloric dilator (PD) neuron burst until the onset of the subsequent PD burst, for the pyloric cycles occurring during 10 consecutive protraction and retraction phases in each preparation.

The *coc* is a bilateral fiber bundle that connects the TG with the supraoesophageal ganglion (brain), with the CoG being an outpocketing of the *coc* between its two termination points (Fig. 1). The *poc* connects the *cocs* on the TG side of the CoG. To refer specifically to a region of the *coc* relative to the CoG, we label the region of the *coc* projecting from the CoG towards the TG as the coc_{TG}, and the region of the *coc* projecting from the CoG towards the brain as coc_{B} (Fig. 1).

Figures were made using Spike2, CorelDraw (Corel Corporation, Ottawa, Ontario, Canada) and Igor Pro (Wavemetrics, Portland, OR, USA). Statistical analysis was performed with SigmaStat (Systat Software, San Jose, CA, USA). The Paired Student's *t*-test or Repeated Measures (RM) One-Way ANOVA followed by multiple comparisons using the Student-Newman-Keuls method were used as indicated. Significance was considered to be $p<0.05$. Data are expressed as mean ± s.e.m.

RESULTS

The gastric mill rhythm is a two-phase motor pattern driven by descending input

The gastric mill rhythm (cycle period: 5-20 sec) drives the rhythmic protraction and retraction movements of the teeth in the gastric mill stomach compartment, thereby enabling the chewing of food (Heinzel, 1988; Heinzel et al., 1993). In *C. borealis* there are 8 different types of gastric mill neurons, 7 of which are motor neurons (Weimann et al., 1991; Saideman et al., 2007b; Stein et al., 2007). Four of these gastric mill neurons are protractor motor neurons, including the LG, GM, medial gastric (MG) and inferior cardiac (IC) neurons, although the IC and MG neurons can also exhibit retractor phase activity during some versions of the gastric mill rhythm (Beenhakker and Nusbaum, 2004; Blitz et al., 2004; Wood et al., 2004; Saideman et al., 2007b) . There are also three retractor motor neurons, including the dorsal gastric (DG), anterior median (AM) and ventricular dilator (VD) motor neurons, plus interneuron 1 (Int1), which is also active during the retractor phase and is the sole interneuron in this circuit. There is a single neuron of each type per STG, except the GM neurons of which there are four functionally equivalent copies.

In the isolated STNS of *C. borealis*, some of the gastric mill neurons (Int1, MG, IC, VD) are spontaneously active in pyloric rhythm-time, even in the absence of the gastric mill rhythm (e.g. VD and IC in Fig. 2, left panel) (Weimann et al., 1991; Blitz and Nusbaum, 1997). The pyloric rhythm (cycle period 0.5 – 2 sec), which controls the filtering of chewed food in the posterior (pyloric) stomach compartment, is generated by a second motor circuit in the STG and is continuously active both *in vitro* and *in vivo* (Marder and Bucher, 2007).

The gastric mill rhythm is usually silent, in the isolated STNS as well as *in vivo*, unless the projection neurons that drive it are activated (Fleischer 1981; Heinzel et al.,

1993; Nusbaum et al., 2001; Beenhakker and Nusbaum, 2004; Blitz et al., 2004). Wood et al. (2004), however, characterized a version of the gastric mill rhythm that occurred in some preparations without any experimental manipulation of projection neuron activity. This gastric mill rhythm was unusual in that the gastric mill LG neuron and projection neuron MCN1 exhibited a pyloric rhythm-timed activity pattern during the protraction phase, instead of the tonic firing pattern that they exhibit during protraction in all other characterized gastric mill rhythms in *C. borealis* (Coleman and Nusbaum, 1994; Beenhakker et al., 2004; Blitz et al., 2004; Christie et al., 2004; Saideman et al., 2007b). This spontaneously active gastric mill rhythm was driven largely by an unusually high level of spontaneous activity in the projection neuron MCN1. This MCN1 activity was not only pyloric rhythm-timed, but the resulting gastric mill rhythm was largely replicated by pyloric rhythm-timed extracellular stimulation of MCN1 (Wood et al., 2004).

POC stimulation triggers a long-lasting gastric mill rhythm

Stimulating the *poc* nerve (15 Hz tonic stimulation, 30 sec. duration) consistently triggered the gastric mill rhythm, beginning soon after the stimulation was terminated (n=39). In the example shown in Figure 2, this rhythm started approximately two minutes after the end of *poc* stimulation and, as is typical for gastric mill rhythms, there was rhythmic alternating bursting of the protractor (LG neuron) and retractor (DG, VD) neurons. It is also noteworthy that, during these rhythms, the IC neuron was mostly active during the retractor phase instead of the protractor phase (Fig. 2). Across preparations, the *poc*-triggered gastric mill rhythm started approximately 1 minute after the end of *poc* stimulation (mean latency post-stimulation: 0.91 ± 0.05 min, n=39). These rhythms exhibited a cycle period of 13.1 ± 0.9 sec (n=20).

During each protractor phase, the LG neuron exhibited pyloric rhythm-timed

bursts (Fig. 2). Within each pyloric-timed burst, LG activity alternated with activity in the pyloric pacemaker neurons (e.g. PD neuron in Fig. 2), as also occurred in the spontaneously active rhythm characterized by Wood et al. (2004). The protractor motor neuron GM also exhibited pyloric-timed bursts in many preparations (not shown). In all other previously studied gastric mill rhythms, the protractor neuron bursts instead exhibited a tonic firing pattern (Beenhakker and Nusbaum, 2004; Blitz et al., 2004; Christie et al., 2004; Saideman et al., 2007b).

The *poc*-triggered gastric mill rhythm was also long-lasting. After a 30 sec *poc* stimulation, the gastric mill rhythm tended to persist for many minutes, and sometimes for more than one hour (n=39). Specifically, in a few preparations this rhythm lasted for less than 5 minutes (n=4/39), but it often persisted for 5-20 minutes (n=22/39) or longer (n=13/39). The pattern was consistent for the duration of the triggered gastric mill rhythm. For example, there was stable, alternating bursting between the retractor (e.g. DG) and protractor (e.g. LG) neurons, with consistent pyloric-timed interruptions in each LG burst (Fig. 3).

POC stimulation indirectly activates the gastric mill rhythm

Extrinsic inputs can alter STG circuit activity via synaptic actions on circuit neurons and/or descending projection neurons (Hooper and Moulins, 1990; Katz and Harris-Warrick, 1990; Meyrand et al., 1994; Combes et al., 1999; Beenhakker and Nusbaum 2004; Blitz et al., 2004). To determine whether the input(s) activated by *poc* stimulation influenced the gastric mill circuit directly or indirectly, we selectively superfused the CoGs with high divalent cation (Hi-Di: 5 X Ca^{2+}/5 X Mg^{2+}) saline while continuing to supply normal *C. borealis* saline to the STG. The Hi-Di saline raises action potential threshold and reduces the likelihood of polysynaptic transmission (Blitz and

Nusbaum, 1999). This allowed us to reversibly reduce the ability of any *poc*-stimulated synaptic actions to activate CoG projection neurons and thereby determine whether this input activated the gastric mill rhythm via direct actions on STG neurons.

After determining that *poc* stimulation triggered a gastric mill rhythm in control conditions (Fig. 4A), Hi-Di saline was superfused selectively to the CoGs to suppress *poc* activation of CoG projection neurons. Under these conditions, stimulating the *poc* did not activate the gastric mill rhythm (n=6), even when the stimulation voltage was increased by 2 V (Fig. 4B). To ensure that the inability of *poc* stimulation to activate the gastric mill rhythm was not a consequence of a dysfunctional gastric mill circuit, we used extracellular stimulation of the *ion* to drive this rhythm via selective activation of the projection neuron MCN1 (Bartos et al., 1999). Tonic MCN1 stimulation elicits a distinct gastric mill rhythm from the one triggered by *poc* stimulation, but both rhythms involve the same gastric mill circuit neurons (Coleman et al., 1995; Bartos et al., 1999; Wood et al., 2004; Saideman et al., 2007b). Extracellular MCN1 stimulation consistently elicited the gastric mill rhythm despite the presence of high-divalent cation saline to the CoGs (n=3, data not shown). Further, after washing out the Hi-Di saline, *poc* stimulation again triggered the gastric mill rhythm (Fig. 4C) (n=5/6). Thus, axons in the *poc* appear to project into the CoGs to activate projection neurons and thereby indirectly activate the gastric mill rhythm. We have designated the *poc* input that triggers the gastric mill rhythm as the POC neurons (see below).

The POC neurons excite the projection neurons MCN1 and CPN2

Two previously identified CoG projection neurons in *C. borealis*, MCN1 and CPN2, are necessary and sufficient for driving two previously characterized gastric mill rhythms that are elicited by stimulation of a mechanosensory (VCN neurons) or

proprioceptor (GPR neuron) input (Beenhakker and Nusbaum, 2004; Blitz et al., 2004). Further, the spontaneously active gastric mill rhythm studied by Wood et al. (2004) was largely mimicked by direct stimulation of MCN1. We therefore examined the activity of MCN1 and CPN2 before and after *poc* stimulation, and found that this stimulation consistently triggered a long lasting excitatory response in both projection neurons (n=39). This excitatory response included an increased firing rate and pyloric-timed activity (Fig. 5).

The POC-triggered excitation of MCN1 and CPN2 always coincided with the triggering of the gastric mill rhythm (n=39). After *poc* stimulation, the firing frequency of MCN1 was consistently higher than pre-stimulation (pre-*poc* stim.: 4.0 ± 0.5 Hz; post-*poc* stim.: protraction phase (LG burst), 14.5 ± 1.2 Hz, retraction phase (LG inter-burst), 14.7 ± 1.2 Hz, n=10; protraction and retraction significantly different from control, $p<0.05$, protraction not significantly different from retraction, $p>0.05$, RM One-Way ANOVA and Student-Newman-Keuls test of multiple comparisons). Similarly, CPN2 firing frequency was consistently increased after POC stimulation (pre-POC: 2.8 ± 1.1 Hz; post-POC: protraction, 18.2 ± 3.3 Hz; retraction, 15.6 ± 3.3 Hz, n=4; protraction and retraction significantly different from control, $p<0.05$, protraction not significantly different from retraction, $p>0.05$, RM One-Way ANOVA and Student-Newman-Keuls test of multiple comparisons).

A key feature of the MCN1 and CPN2 activity pattern is that their activity was terminated for a portion of each pyloric cycle during both protraction and retraction (Fig. 5). We therefore determined the percentage of the pyloric cycle period during which the projection neurons were active (see Methods). MCN1 and CPN2 were always silent during the pyloric pacemaker neuron burst, which extended from the onset of each pyloric cycle (0%) until approximately the 20% point of each cycle (protraction: 0 - 20.1 ±

0.4%, retraction: 0 - 20.2 ± 0.6%, n=6). During the POC-triggered gastric mill rhythms, activity in these two projection neurons generally commenced with a delay after each pyloric pacemaker neuron burst. For example, MCN1 was active for ~65% of each pyloric cycle during protraction (onset: 34.9 ± 2.9%, offset: 100.0 ± 2.5%) and for ~58% of each pyloric cycle during retraction (onset: 39.4 ± 3.1%, offset: 98.3 ± 0.6%) (n=6). Comparably, CPN2 was active for ~ 72% of each pyloric cycle during protraction (onset: 30.3 ± 0.9%, offset: 102.4 ± 0.8%) and was active for ~47% of each pyloric cycle during retraction (onset: 42.3 ± 1.3%, offset: 88.4 ± 7.2%) (n=3). MCN1 and CPN2 were presumably silent during the pacemaker burst due to feedback inhibition in the CoGs from the anterior burster (AB), the pyloric pacemaker interneuron (Coleman and Nusbaum, 1994; Norris et al., 1994; Wood et al., 2004).

We tested the hypothesis that the AB neuron feedback to MCN1 and CPN2 in the CoGs was responsible for the pyloric-timed activity pattern of these projection neurons during the POC-triggered gastric mill rhythm. Specifically, we used hyperpolarizing current injection into the pyloric pacemaker neurons to suppress their activity and, consequently, that of the pyloric rhythm. The pyloric pacemaker neurons are a group of electrically coupled neurons that include the single AB neuron plus the paired PD and lateral posterior gastric (LPG) neurons (Weimann et al., 1991; Weimann and Marder, 1994). When the pyloric rhythm was suppressed during the POC-triggered gastric mill rhythm, MCN1 and CPN2 activity switched from pyloric-timed to tonic (n=4) (Fig. 6). At these times, the LG neuron activity pattern also switched from pyloric-timed to tonic, presumably because its activity was driven by these projection neurons (Beenhakker and Nusbaum, 2004). There is no direct synapse from the pyloric pacemaker neurons to LG (Bartos et al., 1999). In contrast to our findings, in the European lobster *Homarus gammarus* the pyloric-like activity of some CoG projection

neurons can persist when the pyloric feedback is eliminated (Cardi and Nagy, 1994).

In previously studied gastric mill rhythms (Bartos et al., 1999; Wood et al., 2004), the gastric mill cycle period was regulated by the pyloric rhythm. Specifically, suppressing the pyloric rhythm increased the gastric mill cycle period. This was due to both inter-circuit interactions within the STG and to the pyloric-timing of MCN1 activity. Thus, we tested whether the cycle period of the POC-triggered gastric mill rhythm was also regulated by the pyloric rhythm. We found that the POC-triggered gastric mill cycle period was indeed increased when the pyloric rhythm was suppressed, from 12.3 ± 1.8 sec to 19.4 ± 2.7 sec (n=4; $p<0.05$, Paired *t*-test).

The POC neurons project through the medial aspect of the coc_{TG} to innervate the CoGs

As a step towards localizing the POC neurons, we determined whether their axons preferentially projected through the lateral or medial aspect of the coc_{TG}. We anticipated that the POC neurons projected through the medial coc_{TG}, by analogy with the fact that most projections through the coc_{B} that innervate the CoG do so via the medial coc_{B} (Kirby and Nusbaum, 2007). To determine if this was indeed the case for the POC neurons, we first stimulated the *poc* with the entire coc_{TG} intact, to ensure the ability of this input to trigger the gastric mill rhythm in these preparations (Fig. 7). We then selectively transected either the lateral (n=3) or medial (n=3) aspect of the coc_{TG}, after which we again assessed the ability of *poc* stimulation to trigger the gastric mill rhythm (Fig. 7). There were no landmarks to enable precise transection of exactly one half of each coc_{TG}. Therefore, these transections were done in a fashion to ensure the retention of the lateral-most or medial-most coc_{TG}, with a variable degree of transection of the central aspect of this nerve from preparation to preparation.

The gastric mill rhythm was never triggered by *poc* stimulation after medial coc_{TG}

transection (n=3) (Fig. 7B). In contrast, *poc* stimulation consistently triggered the gastric mill rhythm in every preparation after the lateral coc_{TG} was transected (n=3). The resulting motor pattern retained its characteristic pyloric-timed activity pattern during the protractor phase (Fig. 7C). In these latter experiments, the resulting gastric mill rhythm continued to persist for a long duration, ranging from 8-24 minutes (n=3).

To ensure that the CoG projection neurons and STG circuit neurons were still capable of generating the gastric mill rhythm after medial coc_{TG} transection, we stimulated the VCN neurons (Beenhakker et al., 2004; Beenhakker and Nusbaum, 2004). The VCN-triggered gastric mill rhythm was readily elicited in each of the 3 preparations after the medial coc_{TG} was transected (not shown).

The POC neurons appear to contain the peptide transmitter CabTRP Ia

There is a dense CabTRP Ia-immunoreactive (CabTRP Ia-IR) arborization within the anterior CoG neuropil, called the anterior commissural organ (ACO) (Fig. 8A) (Messinger et al., 2005). The ACO innervates each CoG via a population of small diameter axons that project as a bundle through the medial aspect of the coc_{TG} (Goldberg et al., 1988; Messinger et al., 2005). This CabTRP Ia-IR bundle does not project through the coc_{B} (Fig. 8A) (Goldberg et al., 1988; Messinger et al., 2005). Based on the results of the coc_{TG} transection experiments reported above, and the fact that MCN1 and CPN2 arborize in the anterior CoG neuropil (Coleman and Nusbaum, 1994; Norris et al., 1994), we examined whether the ACO axons projected through the *poc* and therefore might be the axons of the POC neurons.

Wholemount immunocytochemistry revealed that the ACO axon population did indeed project through the *poc* (Fig. 8B). Specifically, at the junction between the coc_{TG} and *poc*, a fraction of the CabTRP Ia-IR axon bundle in the medial coc_{TG} separated and

projected through the *poc*, while the remainder projected posteriorly past the *poc* as a tight bundle along the medial coc_{TG} and terminated as the ACO in the ipsilateral CoG (n=16) (Fig. 8B). This CabTRP Ia-IR fiber bundle projection continued in the medial coc_{TG}, past the *poc*, towards the TG (Fig. 8B) (n=16).

As further support that the POC neurons were likely to be the source of the ACO, we determined whether the CabTRP-IR bundle in the medial coc_{TG} was transected or retained in each of the above coc_{TG} transection experiments. We found that, in each experiment in which the medial coc_{TG} was transected and *poc* stimulation no longer triggered the gastric mill rhythm, the CabTRP Ia-IR bundle had been transected (Fig. 8C; n=3). Conversely, the CabTRP Ia-IR bundle remained intact in preparations in which the lateral coc_{TG} was transected and *poc* stimulation still triggered the gastric mill rhythm (Fig. 8D; n=3).

We also combined CabTRP Ia immunocytochemistry and confocal microscopy to determine the number and distribution of axon diameters for the CabTRP Ia-IR axons in the *poc* and medial coc_{TG} bundle. In the *poc*, as well as in the coc_{TG} adjacent to the CoG, the CabTRP Ia-IR axons were of small diameter (<1 μm) and often tightly fasciculated. Their relatively small diameter and tight fasciculation made it difficult to unambiguously determine the number of individual axons present. However, we counted the fibers to the best of our ability in order to obtain an estimate of the population size. We obtained a distribution of CabTRP Ia-IR axon counts from the left coc_{TG} (88 ± 5, n=5) and right coc_{TG} (83 ± 6, n=5). In the same 5 preparations, the distribution of axon counts in the *poc* suggested a smaller number of CabTRP Ia-IR axons (66 ± 4), supporting our observation that only a subset of the CabTRP Ia-IR bundle in each coc_{TG} projected through the *poc*. In no preparation was branching from the axon bundles seen within the coc_{TG} or *poc*.

In all preparations examined, the CabTRP Ia-IR bundle in the medial coc_{TG} was traced to the junction of the coc_{TG} with the TG (n=5). At this location, the POC axon bundle was less tightly fasciculated, often fanning out and covering a large portion of the nerve (not shown). In 5 separate preparations, we obtained similar axon counts to those from the coc_{TG} near the CoG (left coc_{TG}: 78 ± 4; right coc_{TG}: 73 ± 9). Due to the density and intensity of CabTRP Ia-IR within the TG, it was not possible to localize the destination of the POC axons within this ganglion. Although CabTRP Ia-IR somata within the TG may well be the origin of the POC axons, no discrete clusters of 50-100 CabTRP Ia-IR somata were identified within this ganglion to support that possibility (data not shown).

The POC neurons appear to use the peptide transmitter CabTRP Ia

To determine whether ACO-released CabTRP Ia mediated the long-term actions of the POC neurons on MCN1 and/or CPN2, we examined whether focal application of CabTRP Ia mimicked the POC excitation of these projection neurons. In some of these experiments (e.g. Fig. 9), CPN2 activity was monitored via intracellular GM neuron recordings. CPN2 is the sole source of discrete excitatory postsynaptic potentials in GM (Norris et al., 1994).

Brief, focal application of CabTRP Ia (10^{-4} M: 500 msec) into the anterior CoG neuropil triggered increased activity in MCN1 and CPN2 (n=4) (Fig. 9). This increased activity was consistently pyloric-timed. In some preparations, the CabTRP Ia-triggered excitation of MCN1 and CPN2 led to the equivalent of a single gastric mill cycle, including an action potential burst in the retractor DG neuron preceding a burst in the protractor LG and GM neurons (Fig. 9).

To further assay whether CabTRP Ia mediated the actions of the POC neurons

on MCN1 and/or CPN2, we determined whether suppressing the extracellular peptidase-mediated degradation of this peptide would prolong the POC influence on these projection neurons. To this end, we applied the endopeptidase inhibitor phosphoramidon (10^{-5} M), which effectively prolongs the actions of both focally applied and neuronally released CabTRP Ia (Wood et al., 2000; Stein et al., 2007). Because the *poc* stimulus protocol used to trigger the gastric mill rhythm had such a long-lasting effect, we used briefer *poc* stimulations (15 Hz, 15 sec) to achieve relatively brief control responses. These control stimulations triggered increased activity in MCN1 and CPN2 as well as a relatively short-lasting gastric mill rhythm (duration: 0.5 -13 min, n=5) (Fig. 10A). For example, in Figure 10A the projection neuron activity was subsiding and the gastric mill rhythm had terminated by 90 sec post-POC stimulation (Fig. 10A). Although phosphoramidon alone did not alter CPN2 or LG activity prior to *poc* stimulation (e.g. Fig. 10A, middle left panel), the POC-triggered rhythm during phosphoramidon superfusion persisted for more than 90 sec post-stimulation. After washout of the phosphoramidon, the POC action on CPN2 and the gastric mill rhythm returned to pre-application levels (Fig. 10A). In all cases, when phosphoramidon (10^{-5} M) was superfused selectively to the CoGs, *poc* stimulation triggered a more prolonged excitation of MCN1 (not shown) and CPN2 and triggered a longer-lasting gastric mill rhythm (n=5).

We quantified the influence of phosphoramidon on the duration of POC actions by measuring the duration of time during which the LG neuron generated rhythmic bursts after *poc* stimulation. Specifically, phosphoramidon application reversibly increased the duration of LG bursting by approximately 4-fold (Fig. 10B) (Saline: 6.1 ± 1.9 min, Phosphoramidon: 22.5 ± 6.7 min, Wash: 12.5 ± 4.8 min) (n=5; $p<0.05$, RM One-Way ANOVA and Student-Newman-Keuls test of multiple comparisons).

To control for the specificity of phosphoramidon action, we examined the influence of phosphoramidon on the duration of LG bursting after stimulating the gastro-pyloric receptor neuron (GPR: Katz et al., 1989; Katz and Harris-Warrick, 1990). GPR stimulation excites MCN1 and CPN2 and thereby elicits the gastric mill rhythm (Blitz et al., 2004). GPR does not, however, contain CabTRP Ia but instead contains the co-transmitters acetylcholine, serotonin and allatostatin (Katz and Harris-Warrick, 1990; Skiebe and Schneider 1994). Phosphoramidon (10^{-5} M) superfusion did not change the duration of LG bursting after GPR stimulation (Fig. 10B) **(**n=4, $p>0.5$ RM One-Way ANOVA).

DISCUSSION

We have identified an extrinsic input, the POC neurons, that triggers a long-lasting activation of identified CoG projection neurons and thereby initiates a distinct version of the gastric mill rhythm in the *C. borealis* STG. The POC axons project as a tightly associated bundle through the medial aspect of each coc_{TG}, from the direction of the TG, to innervate the ipsilateral CoG. A subset of these axons also project through the *poc*, enabling them to innervate the contralateral CoG. The long-term activation of the CoG projection neurons MCN1 and CPN2 by POC stimulation is likely mediated by the peptide transmitter CabTRP Ia.

The POC neurons appear to be the source of the extensive CabTRP Ia-IR arborization in the anterior CoG neuropil (Goldberg et al., 1988). This arborization was recently characterized as a neurohemal organ, the ACO, which is well-situated to release CabTRP Ia into the hemolymph as a circulating hormone in the related species *Cancer productus* (Messinger et al., 2005). In that study, the ACO was also studied extensively for the presence of co-transmitters but none were identified. One function of circulating hormones, including CabTRP Ia, is to modulate the properties of muscles that mediate movements of the foregut (Jorge-Rivera and Marder 1996; Messinger et al., 2005). Therefore, POC-mediated release of CabTRP Ia may well coordinately trigger the gastric mill rhythm and modulate the response of gastric mill muscles to the incoming motor pattern. Recently, a second isoform of CabTRP (CabTRP II) was isolated from the STNS, including the CoGs (Stemmler et al., 2007). Both CabTRP isoforms are recognized by the same antibody and have similar actions on the pyloric rhythm (Stemmler et al., 2007). Thus, either or both CabTRP peptides may mediate the POC actions in this system.

The likelihood that the CabTRP Ia released from the ACO terminals locally

excites MCN1 and CPN2 supports the hypothesis that this neuronal population has both paracrine and endocrine functions. Given the sensitivity of MCN1 and CPN2 to relatively brief POC stimulation, there may well be times when this input acts largely or exclusively as a local modulator of neuronal activity, while at other times its activation results in both paracrine and endocrine actions. Previous studies in other systems have established the ability of the same neurons to release signaling molecules that act both locally, in a paracrine fashion, and as circulating hormones (Mayeri 1979; Sigvardt et al., 1986; Jung and Scheller, 1991; Loechner and Kaczmarek, 1994; Ludwig and Pittman, 2003; Fort et al., 2004; Oliet et al., 2007).

We have not yet identified the location of the POC neuronal somata. These somata may be located within the TG, in which the coc_{TG} terminates. In *C. borealis*, the entire ventral nerve cord is compressed into the single TG (Horridge, 1965). However, the POC somata may instead be located within one or more peripheral nerves or related structures, as is common for muscle- and abdominal-stretch sensitive sensory neuron populations in decapod crustaceans (Alexandrowicz, 1951; Cattaert et al., 2002; Katz et al., 1989; Beenhakker et al., 2004). Whether these neurons originate in the TG or a peripheral structure, their point of origin appears likely to be outside the STNS. Thus, the POC neurons may help to coordinate the chewing of food with other behaviors, perhaps acting as a trigger for chewing in response to cues from other regions of the animal. In addition, these neurons may well contribute to the long-term maintenance of chewing in the intact crab and lobster insofar as the gastric mill rhythm can persist for hours after food is ingested (Fleischer 1981; Turrigiano and Selverston 1990). Similarly, there are long-lasting actions of the vertebrate tachykinin peptide, substance P, on rhythmic locomotor activity in the vertebrate CNS (Treptow et al., 1983; Parker and Grillner, 1999). Further, short-duration sensory stimuli can trigger long-term activation of

descending reticulospinal neurons that drive locomotion in lamprey (Di Prisco et al. 1997).

The POC-elicited gastric mill rhythm is qualitatively different from gastric mill rhythms elicited by other extrinsic inputs in *C. borealis*. Specifically, the protraction phase activity pattern of MCN1, CPN2 and LG is pyloric-timed during the POC-triggered rhythm whereas these neurons exhibit tonic protraction phase activity during other gastric mill rhythms (Beenhakker and Nusbaum 2004; Blitz et al., 2004; Christie et al., 2004; Saideman et al., 2007b). The LG-innervated muscles mediate protraction of the lateral teeth within the gastric mill. Thus, the distinct LG neuron activity pattern during the POC-triggered gastric mill rhythm could result in a different mode of chewing relative to the previously characterized gastric mill rhythms. In fact, both smooth protraction and pyloric-timed movements of the lateral teeth occur during *in vivo* endoscopic recordings of these teeth movements in *Cancer* crabs (Heinzel et al., 1993). Future work will be needed to establish whether the pyloric-timed LG neuron pattern is retained at the level of the LG-innervated muscles during the POC-triggered rhythm.

The distinct activity pattern of MCN1 during the POC rhythm also has consequences for motor pattern generation and inter-circuit coordination. For example, the pyloric circuit feedback to MCN1 during the protractor phase of the spontaneous POC-like gastric mill rhythm enables the pyloric rhythm to regulate the speed and pattern of the gastric mill rhythm, as well as its coordination with the pyloric rhythm (Wood et al., 2004). This is also evident in the present study from the change in gastric mill cycle period that occurred when the pyloric rhythm was suppressed. This pyloric regulation of the gastric mill rhythm during the protractor phase, via feedback inhibition of MCN1 and CPN2, occurs only during the POC-type of gastric mill rhythm (Beenhakker and Nusbaum, 2004; Blitz et al., 2004; Christie et al., 2004). Previous work documented

additional cellular and synaptic mechanisms underlying inter-circuit regulation during other versions of the gastric mill rhythm (Bartos and Nusbaum, 1997; Clemens et al., 1998; Bartos et al., 1999; Wood et al., 2004). Although coordination between different behaviors, such as locomotion and respiration, occurs in many animals (Bramble and Carrier 1983; Syed and Winlow 1991; Kawahara et al., 1989; Morin and Viala 2002; Saunders et al., 2004), the underlying cellular mechanisms remain to be determined in these other systems.

It appears likely that the previously studied POC-like gastric mill rhythm by Wood et al. (2004) does represent POC-triggered rhythms, presumably resulting from POC activation that occurred during the dissection. In both cases there was a prominent activation of MCN1, and they further share the distinct pyloric-timed activity pattern during the protractor phase. CPN2 activity, however, was not studied in the earlier work (Wood et al., 2004). Wood et al. (2004) did establish that pyloric-timed MCN1 stimulation elicited a gastric mill rhythm that was comparable to the spontaneous POC-like rhythm.

Given that MCN1 and CPN2 are necessary and sufficient to elicit the VCN- and GPR-elicited gastric mill rhythms (Blitz et al., 2004; Beenhakker and Nusbaum, 2004), it is likely that they play pivotal roles during the POC-triggered rhythm as well. Addressing this issue will provide insight into the extent to which this system uses convergent activation of the same projection neurons to elicit distinct activity patterns. This would contrast to the prevalent hypothesis in other model systems that the generation of distinct but related movements results from the activation of distinct but overlapping sets of projection neurons (Georgopoulos, 1995; Kristan and Shaw, 1997; Lewis and Kristan, 1998; Liu and Fetcho, 1999).

REFERENCES

Alexandrowicz, J.S. (1951). Muscle receptor organs in the abdomen of *Homarus vulgaris* and *Palinurus vulgaris*. *Quart. J. Micr. Sci.* 92:163-199.

Bartos, M. and Nusbaum, M.P. (1997). Intercircuit control of motor pattern modulation by presynaptic inhibition. *J. Neurosci.* 17: 2247-2256.

Bartos, M., Manor, Y., Nadim, F., Marder, E. and Nusbaum, M.P. (1999). Coordination of fast and slow rhythmic neuronal circuits. *J. Neurosci.* 19:6650-6660.

Beenhakker, M.P. and Nusbaum, M.P. (2004). Mechanosensory activation of a motor circuit by coactivation of two projection neurons. *J. Neurosci.* 24:6741-6750.

Beenhakker, M.P., Blitz, D.M. and Nusbaum, M.P. (2004). Long-lasting activation of rhythmic neuronal activity by a novel mechanosensory system in the crustacean stomatogastric nervous system. *J. Neurophysiol.* 91:78-91.

Blitz, D.M. and Nusbaum, M.P. (1997). Motor pattern selection via inhibition of parallel pathways. *J. Neurosci.* 17:4965-4975.

Blitz, D.M. and Nusbaum, M.P. (1999). Distinct functions for cotransmitters mediating motor pattern selection. *J. Neurosci.* 19:6774-6783.

Blitz, D.M., Christie, A.E., Coleman, M.J., Norris, B.J., Marder, E. and Nusbaum, M.P. (1999). Different proctolin neurons elicit distinct motor patterns from a multifunctional neuronal network. *J. Neurosci.* 19:5449-5463.

Blitz, D.M., Beenhakker, M.P. and Nusbaum, M.P. (2004). Different sensory systems share projection neurons but elicit distinct motor patterns. *J. Neurosci.* 24:11381–11390.

Bramble, D.M and Carrier, D.R. (1983). Running and breathing in mammals. *Science*. 219:251-256.

Brocard, F., Bardy, C. and Dubuc, R. (2005). Modulatory effect of substance P to the

brain stem locomotor command in lampreys. *J. Neurophysiol.* 93:2127-2141.

Cardi, P. and Nagy, F. (1994). A rhythmic modulatory gating system in the stomatogastric nervous system of Homarus gammarus. III. Rhythmic control of the pyloric CPG. *J. Neurophysiol.* 71:2503-2516.

Cattaert, D., Le Bon, M. and Le Ray, D. (2002). Efferent controls in crustacean mechanoreceptors. *Microsc. Res. Tech.* 58:312-324.

Christie, A.E., Lundquist, C.T., Nassel, D.R. and Nusbaum, M.P. (1997). Two novel tachykinin-related peptides from the nervous system of the crab *Cancer borealis*. *J. Exp. Biol.* 200:2279-2294.

Christie, A.E., Stein, W., Quinlan, J.E., Beenhakker, M.P., Marder, E. and Nusbaum, M.P. (2004). Actions of a histaminergic/peptidergic projection neuron on rhythmic motor patterns in the stomatogastric nervous system of the crab *Cancer borealis*. *J. Comp. Neurol.* 469:153-169.

Clemens, S., Combes, D., Meyrand, P. and Simmers, J. (1998). Long-term expression of two interacting motor pattern-generating networks in the stomatogastric system of freely behaving lobster. *J. Neurophysiol.* 79:1396-1408.

Coleman, M.J. and Nusbaum, M.P. (1994). Functional consequences of compartmentalization of synaptic input. *J. Neurosci*. 11: 6544-6552.

Coleman, M.J., Meyrand, P. and Nusbaum, M.P. (1995). A switch between two modes of synaptic transmission mediated by presynaptic inhibition. *Nature* 378:502-505.

Coleman, M.J., Nusbaum, M.P., Cournil, I. and Claiborne, B.J. (1992). Distribution of modulatory inputs to the stomatogastric ganglion of the crab, *Cancer borealis*. *J. Comp. Neurol.* 325:581-594.

Combes D., Simmers A.J., Moulins M. (1995). Structural and functional characterization of a muscle tendon proprioceptor in lobster. *J. Comp. Neurol.* 363:221-234.

Combes, D., Meyrand, P. and Simmers, J. (1999). Dynamic restructuring of a rhythmic motor program by a single mechanoreceptor neuron in lobster. *J. Neurosci.* 19:3620-3628.

Di Prisco, G.V., Pearlstein, E., Robitaille, R. and Dubuc, R. (1997). Role of sensory-evoked NMDA plateau potentials in the initiation of locomotion. *Science* 278:1122-1125.

Di Prisco, G.V., Pearlstein, E., Le Ray, D., Robitaille, R. and Dubuc, R. (2000). A cellular mechanism for the transformation of a sensory input into a motor command. *J. Neurosci.* 20:8169-8176.

Fleischer, A.G. (1981). The effect of eyestalk hormones on the gastric mill in the intact lobster *Panulirus interruptus*. *J. Comp. Physiol*. 141:363-368.

Fort, T.J., Brezina, V. and Miller, M.W. (2004). Modulation of an integrated central pattern generator-effector system: dopaminergic regulation of cardiac activity in the blue crab *Callinectes sapidus*. *J. Neurophysiol.* 92:3455-3470.

Georgopoulos, A.P. (1995). Current issues in directional motor control. *Trends Neurosci.* 18:506-510.

Goldberg, D., Nusbaum, M.P. and Marder, E. (1988). Substance P-like immunoreactivity in the stomatogastric nervous systems of the crab *Cancer borealis* and the lobsters *Panulirus interruptus* and *Homarus americanus*. *Cell Tissue Res.* 252:515-522.

Gordon, I.T. and Whelan, P.J. (2006). Deciphering the organization and modulation of spinal locomotor central pattern generators. *J. Exp. Biol.* 209:2007-2014.

Heinzel, H.G. (1988). Gastric mill activity in the lobster. I. Spontaneous modes of chewing. *J. Neurophysiol.* 59:528-550.

Heinzel, H.G., Weimann, J.M. and Marder, E. (1993). The behavioral repertoire of the gastric mill in the crab, *Cancer pagurus*: an in situ endoscopic and

electrophysiological examination. *J. Neurosci.* 13:1793-1803.

Hooper, S.L. and Moulins, M. (1990). Cellular and synaptic mechanisms responsible for a long-lasting restructuring of the lobster pyloric network. *J. Neurophysiol.* 64:1574-1589.

Horridge, G.A. (1965). Arthropoda: General Anatomy. In *Structure and Function in the Nervous System of Invertebrates*. (ed. T.H. Bullock and G.A. Horridge), pp 801-964. San Fransisco: W.H. Freeman and Company.

Jorge-Rivera, J.C. and Marder, E. (1996). TNRNFLRFamide and SDRNFLRFamide modulate muscles of the stomatogastric system of the crab Cancer borealis. *J Comp Physiol [A]*. 179, :741-751.

Jung, L.J. and Scheller, R.H. (1991). Peptide processing and targeting in the neuronal secretory pathway. *Science* 251:1330-1335.

Katz, P.S., Eigg, M.H. and Harris-Warrick, R.M. (1989). Serotonergic/cholinergic muscle receptor cells in the crab stomatogastric nervous system. I. Identification and characterization of the gastropyloric receptor cells. *J. Neurophysiol.* 62:558-570.

Katz, P.S. and Harris-Warrick, R.M. (1990). Neuromodulation of the crab pyloric central pattern generator by serotonergic/cholinergic proprioceptive afferents. *J. Neurosci.* 10:1495-1512.

Kawahara, K., Kumagai, S., Nakazono, Y. and Myamoto, Y. (1989). Coupling between respiratory and stepping rhythms during locomotion in decerebrate cats. *J. Appl. Physiol.* 67:110-115.

Kiehn, O. (2006). Locomotor circuits in the mammalian spinal cord. *Annu. Rev. Neurosci.* 29:279-306.

Kirby, M.S. and Nusbaum, M.P. (2007). Central nervous system projections to and from the commissural ganglion of the crab *Cancer borealis*. *Cell Tissue Res.* 328:625-637.

Kristan, W.B. and Shaw, B.K. (1997). Population coding and behavioral choice. *Curr. Opin. Neurobiol.* 7:826-831.

LeBeau, F.E., El Manira, A., and Grillner, S. (2005). Tuning the network: modulation of neuronal microcircuits in the spinal cord and hippocampus. *Trends Neurosci.* 28:552-561.

Lewis, J.E. and Kristan, W.B. (1998). A neuronal network for computing population vectors in the leech. *Nature* 391:76-79.

Liu, K.S. and Fetcho, J.R. (1999). Laser ablations reveal functional relationships of segmental hindbrain neurons. *Neuron* 23, 325-335.

Loechner, K.J., and Kaczmarek, L.K. (1994). Autoactive peptides act at three distinct receptors to depolarize the bag cell neurons of *Aplysia*. *J. Neurophysiol.* 71:195-203.

Ludwig, M., and Pittman, Q.J. (2003). Talking back: dendritic neurotransmitter release. *Trends Neurosci.* 26, 255-261.

Marder, E., Bucher, D., Schulz, D.J. and Taylor, A.L. (2005). Invertebrate central pattern generation moves along. *Curr. Biol.* 15:R685-R699.

Marder, E. and Bucher, D. (2007). Understanding circuit dynamics using the stomatogastric nervous system of lobsters and crabs. *Annu. Rev. Physiol.* 69:291-316.

Mayeri, E. (1979). Local hormonal modulation of neural activity in *Aplysia*. *Fed. Proc.* 38:2103-2108.

McLean, D.L. and Sillar, K.T. (2004). Metamodulation of a spinal locomotor network by nitric oxide. *J. Neurosci.* 24:9561-9571.

Messinger, D.I., Kutz, K.K., Le, T., Verley, D.R., Hsu, Y.W., Ngo, C.T., Cain, S.D., Birmingham, J.T., Li, L. and Christie, A.E. (2005). Identification and characterization

of a tachykinin-containing neuroendocrine organ in the commissural ganglion of the crab Cancer *productus*. *J. Exp. Biol*. 208:3303-3319.

Meyrand, P., Simmers, J. and Moulins, M. (1994). Dynamic construction of a neural network from multiple pattern generators in the lobster stomatogastric nervous system. *J. Neurosci*. 14:630-644.

Morin, D. and Viala, D. (2002). Coordinations of locomotor and respiratory rhythms in vitro are critically dependent on hindlimb sensory inputs. *J. Neurosci.* 22:4756-4765.

Norris, B.J., Coleman, M.J. and Nusbaum, M.P. (1994). Recruitment of a projection neuron determines gastric mill motor pattern selection in the stomatogastric nervous system of the crab, Cancer borealis. *J. Neurophysiol.* 72:1451-1463.

Nusbaum, M.P. and Beenhakker, M.P. (2002). A small-systems approach to motor pattern generation. *Nature* 417:343-350.

Nusbaum, M.P., Blitz, D.M., Swensen, A.M., Wood, D. and Marder, E. (2001). The roles of co-transmission in neural network modulation. *Trends Neurosci.* 24:146-154.

Oliet, S.H., Baimoukhametova, D.V., Piet, R. and Bains, J.S. (2007). Retrograde regulation of GABA transmission by the tonic release of oxytocin and endocannabinoids governs postsynaptic firing. *J. Neurosci.* 27:1325-1333.

Parker, D. and Grillner, S. (1999). Long-lasting substance-P-mediated modulation of NMDA-induced rhythmic activity in the lamprey locomotor network involves separate RNA- and protein-synthesis-dependent stages. *Eur. J. Neurosci.* 11:1515-1522.

Saideman, S.R., Ma, M., Kutz-Naber, K.K., Cook, A., Torfs, P., Schoofs, L., Li, L. and Nusbaum, M.P. (2007a). Modulation of rhythmic motor activity by pyrokinin peptides. *J. Neurophysiol.* 97:579-595.

Saideman, S.R., Blitz, D.M. and Nusbaum, M.P. (2007b). Convergent motor patterns from divergent circuits. *J. Neurosci.* 27:6664-6674.

Saunders S.W., Rath D. and Hodges P.W. (2004). Postural and respiratory activation of the trunk muscles changes with mode and speed of locomotion. *Gait Posture* 20:280-290.

Sigvardt, K.A., Rothman, B.S., Brown, R.O. and Mayeri, E. (1986). The bag cells of *Aplysia* as a multitransmitter system: identification of alpha bag cell peptide as a second neurotransmitter. *J. Neurosci.* 6:803-813.

Skiebe, P. and Schneider, H. (1994). Allatostatin peptides in the crab stomatogastric nervous system: inhibition of the pyloric motor pattern and distribution of allatostatin-like immunoreactivity. *J. Exp. Biol.* 194, 195-208.

Smarandache C.R. and Stein W. (2007). Sensory-induced modification of two motor patterns in the crab, *Cancer pagurus*. *J. Exp. Biol.* 210:2912-2922.

Smetana, R.W., Alford, S. and Dubuc, R. (2007). Muscarinic receptor activation elicits sustained, recurring depolarizations in reticulospinal neurons. *J. Neurophysiol.* 97:3181-3192.

Stein, W., DeLong, N.D., Wood, D.E. and Nusbaum, M.P. (2007). Divergent co-transmitter actions underlie motor pattern activation by a modulatory projection neuron. *Eur. J. Neurosci.* 26:1148-1165.

Stemmler E.A., Peguero B., Bruns E.A., Dickinson P.S. and Christie A.E. (2007). Identification, physiological actions, and distribution of TPSGFLGMRamide: a novel tachykinin-related peptide from the midgut and stomatogastric nervous system of *Cancer* crabs. *J. Neurochem*. 101:1351-1366.

Syed, N.I. and Winlow, W. (1991). Coordination of locomotor and cardiorespiratory networks of *Lymnaea stagnalis* by a pair of identified interneurones. *J. Exp. Biol.* 158:37-62.

Treptow, K., Oehme, P., Gäbler, E. and Bienert, M. (1983). Modulation of locomotor

activity by substance P in rats. *Regul. Pept.* 5: 343-351.

Tryba, A.K., Pena, F. and Ramirez, J.M. (2006). Gasping activity in vitro: a rhythm dependent on 5-HT2A receptors. *J. Neurosci.* 26:2623-2634.

Turrigiano G. G. and Selverston A. I. (1990). A cholecystokinin-like hormone activates a feeding-related neural circuit in lobster. *Science* 344:866-868.

Weimann, J.M. and Marder, E. (1994). Switching neurons are integral members of multiple oscillatory networks. *Curr. Biol.* 4:896-902.

Weimann, J.M., Meyrand, P. and Marder, E. (1991). Neurons that form multiple pattern generators: identification and multiple activity patterns of gastric/pyloric neurons in the crab stomatogastric system. *J. Neurophysiol.* 65:111-122.

White, R.S., Nadim, F. and Nusbaum, M.P. (2005). Activation of a peripheral modulatory system elicits a distinct gastric mill rhythm. *Soc. Neurosci. Abstr.* Prog. No. 722.52.

Wood, D.E., Stein, W. and Nusbaum, M.P. (2000). Projection neurons with shared cotransmitters elicit different motor patterns from the same neural circuit. *J. Neurosci.* 20:8943-8953.

Wood, D.E., Manor, Y., Nadim, F. and Nusbaum, M.P. (2004). Intercircuit control via rhythmic regulation of projection neuron activity. *J. Neurosci.* 24:7455-7563.

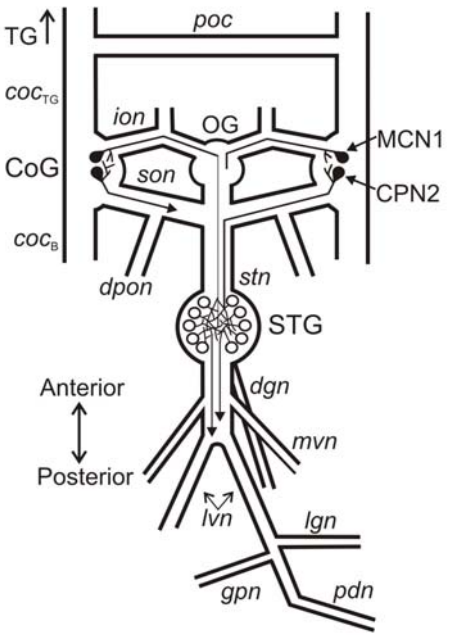

Figure 1. Schematic of the isolated stomatogastric nervous system, including the axon projections of MCN1 and CPN2 to the STG. The two lines with arrowheads projecting posteriorly from the STG neuropil represent the projection pattern of most STG motor neurons. Abbreviations: Ganglia- CoG, commissural ganglion; OG, oesophageal ganglion; STG, stomatogastric ganglion; TG, thoracic ganglion. Nerves- coc_{TG}, circumoesophageal connective from the CoG to the TG; coc_{B}, circumoesophageal connective from the CoG to the brain; *dgn*, dorsal gastric nerve; *dpon*, dorsal posterior oesophageal nerve; *ion*, inferior oesophageal nerve; *lgn*, lateral gastric nerve; *lvn*, lateral ventricular nerve; *mvn*, medial ventricular nerve; *pdn*, pyloric dilator nerve; *poc*, post-oesophageal commissure; *son*, superior oesophageal nerve. Neurons- CPN2, commissural projection neuron 2; MCN1, modulatory commissural neuron 1.

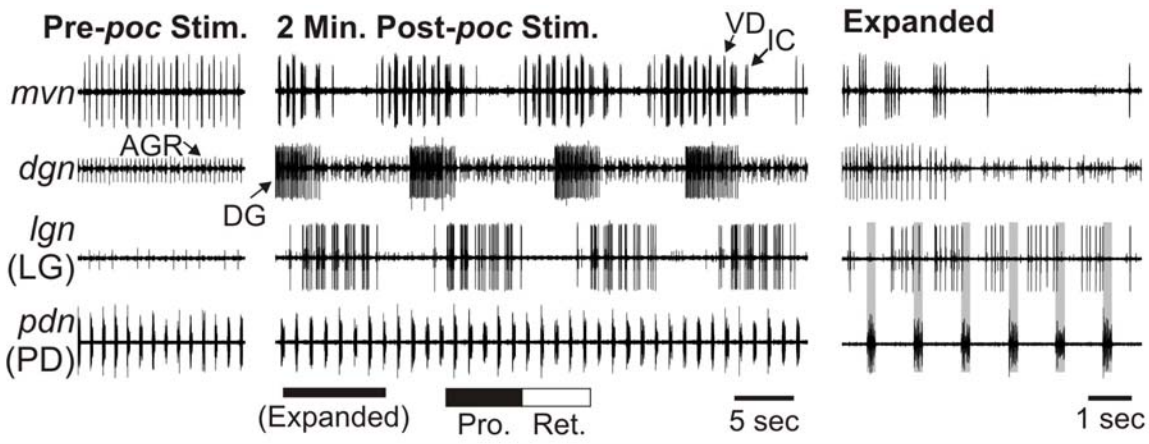

Figure 2. The gastric mill rhythm is triggered by *poc* nerve stimulation. (Left) Prior to *poc* stimulation, there was an ongoing pyloric rhythm (*mvn*, *pdn*), but no gastric mill rhythm (*dgn*, *lgn*). The large, tonically active unit in the *dgn* corresponds to the activity of the anterior gastric receptor (AGR) neuron. AGR is a muscle tendon proprioceptor neuron that is spontaneously active in the isolated STNS (Combes et al., 1995; Smarandache and Stein, 2007). (Middle) Two minutes after tonic *poc* stimulation (15 Hz, 30 sec), the gastric mill rhythm was triggered, as is evident from the rhythmic bursting in the protractor LG neuron that alternated with the retractor phase activity of the DG, VD and IC neurons. Note the pyloric-timed bursting in the LG neuron. (Right) This expanded section of the middle panel shows more explicitly that each protractor LG burst is time-locked to the pyloric rhythm. Each period of inactivity in LG starts with a pyloric dilator (PD) neuron burst (grey bars).

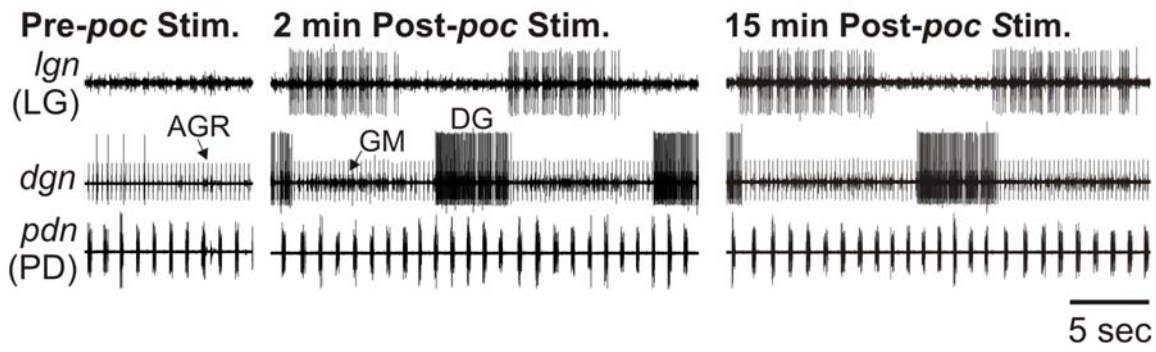

Figure 3. The *poc*-triggered gastric mill rhythm is long-lasting. (Left) Before poc stimulation, there was an ongoing pyloric rhythm (*pdn*) but no gastric mill rhythm (*lgn*, *dgn*). (Middle) Two minutes after tonic *poc* stimulation (15 Hz, 30 sec), the gastric mill rhythm had been triggered and was ongoing. Note the pyloric-timed LG bursts. (Right) This rhythm persisted for more than 15 minutes after *poc* stimulation.

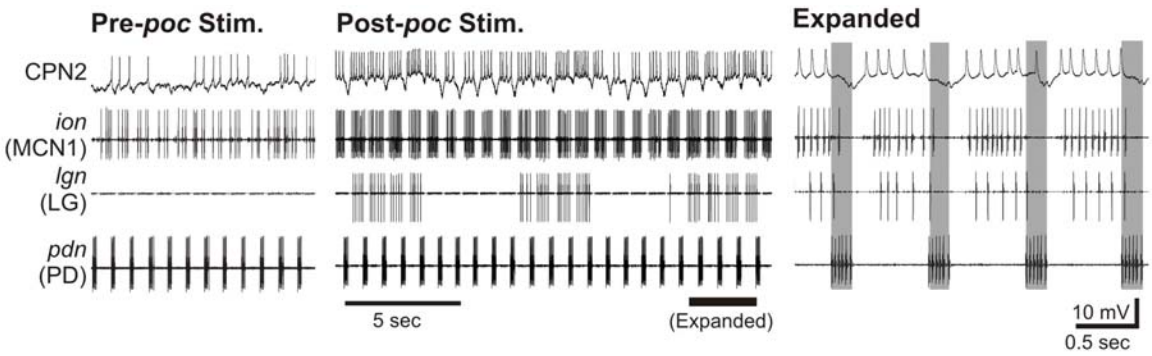

Figure 4. The *poc*-triggered gastric mill rhythm requires the activation of CoG projection neurons. (A) During normal saline superfusion of the CoGs, tonic *poc* stimulation (15 Hz, 30 sec) triggered the gastric mill rhythm. (B) During superfusion of 5X Mg^{2+}/5X Ca^{2+} saline selectively to the CoGs and OG (grey shading in STNS schematic), the same *poc* stimulation did not trigger the gastric mill rhythm. (C) After washout of the 5X Mg^{2+}/5X Ca^{2+} saline, *poc* stimulation again triggered the gastric mill rhythm. Note that the black bar in each STNS schematic represents a Vaseline wall that enabled separate saline superfusion of the anterior (CoGs, OG) and posterior (STG) aspects of the STNS. All panels are from the same preparation.

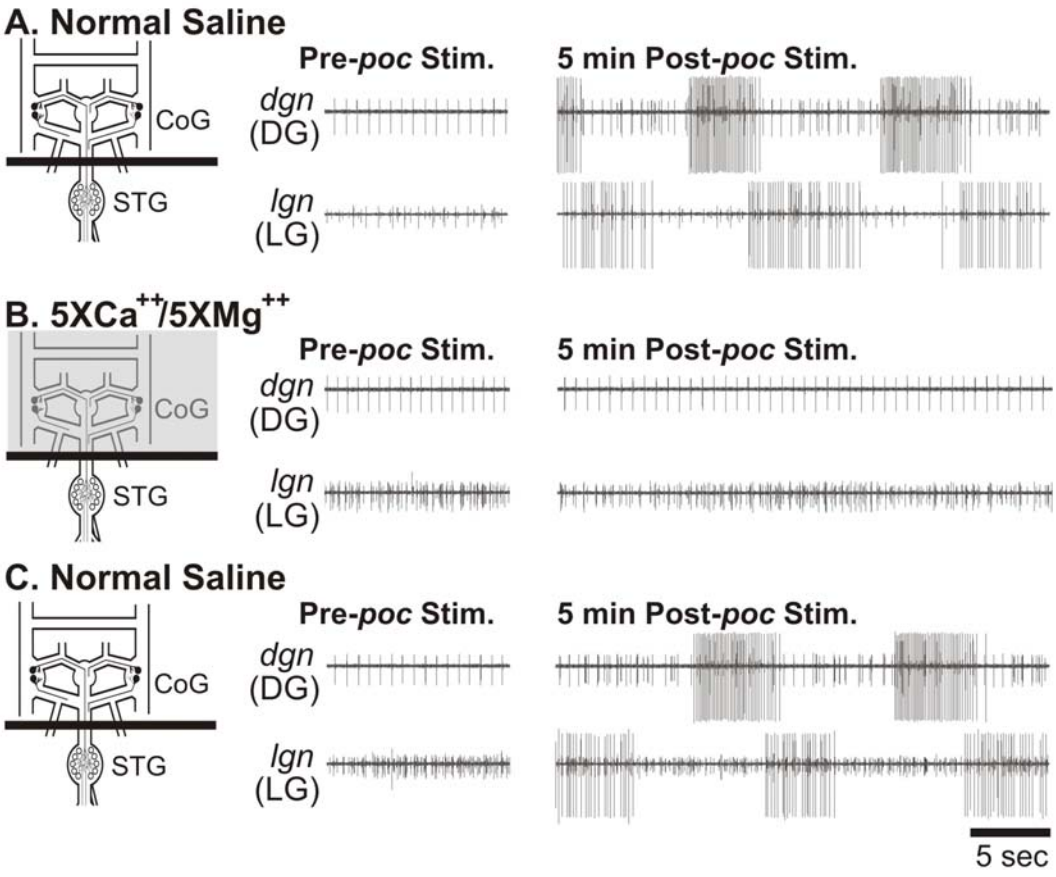

Figure 5. Activation of the CoG projection neurons CPN2 and MCN1, as well as the gastric mill rhythm, is triggered by *poc* stimulation. (Left) Before stimulation, CPN2 and MCN1 were weakly active and there was an ongoing pyloric rhythm (*pdn*) but no gastric mill rhythm (*lgn, dgn*). (Middle) After *poc* stimulation (15 Hz, 30 sec), CPN2 and MCN1 were excited and the gastric mill rhythm was triggered. (Right) Expanded time scale from the middle panel showing that the activity of LG, MCN1 and CPN2 is interrupted in pyloric-time. Note that each such interruption occurs during activity of the pyloric pacemaker PD neuron (grey bars). Most hyperpolarized membrane potential: CPN2, -45 mV.

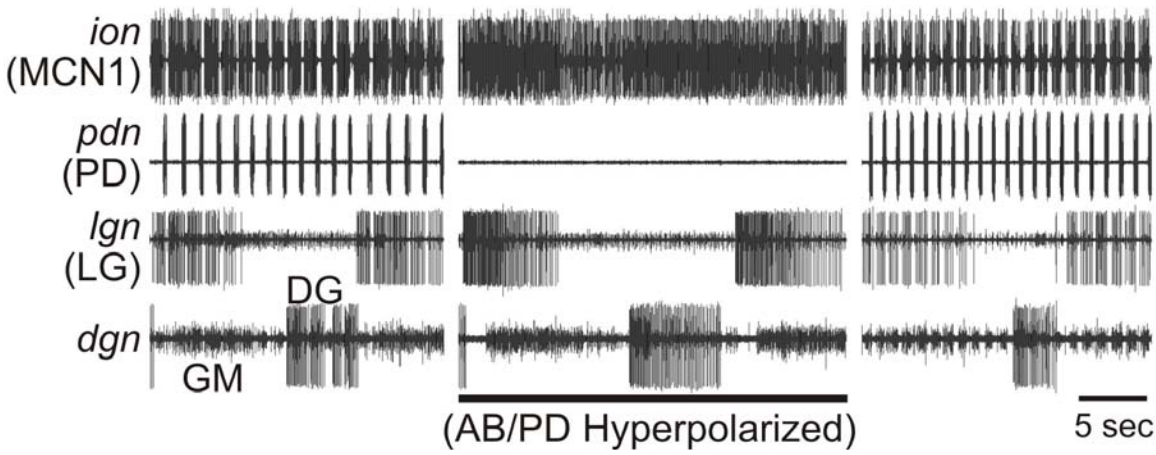

Figure 6. The pyloric rhythm in the STG is responsible for the pyloric-timed activity of the CoG projection neuron MCN1 and the gastric mill protractor neuron LG during the POC-triggered gastric mill rhythm. (Left) During the POC-triggered gastric mill rhythm, MCN1 and LG exhibited pyloric-timed activity. (Middle) When the pyloric rhythm was suppressed, by hyperpolarization of the pyloric pacemaker neurons, the POC-triggered gastric mill rhythm persisted but the activity of MCN1 and LG changed from pyloric-timed to tonic. (Right) After releasing the pyloric pacemaker neurons from hyperpolarization, the pyloric rhythm resumed and MCN1 and LG returned to exhibiting pyloric-timed activity.

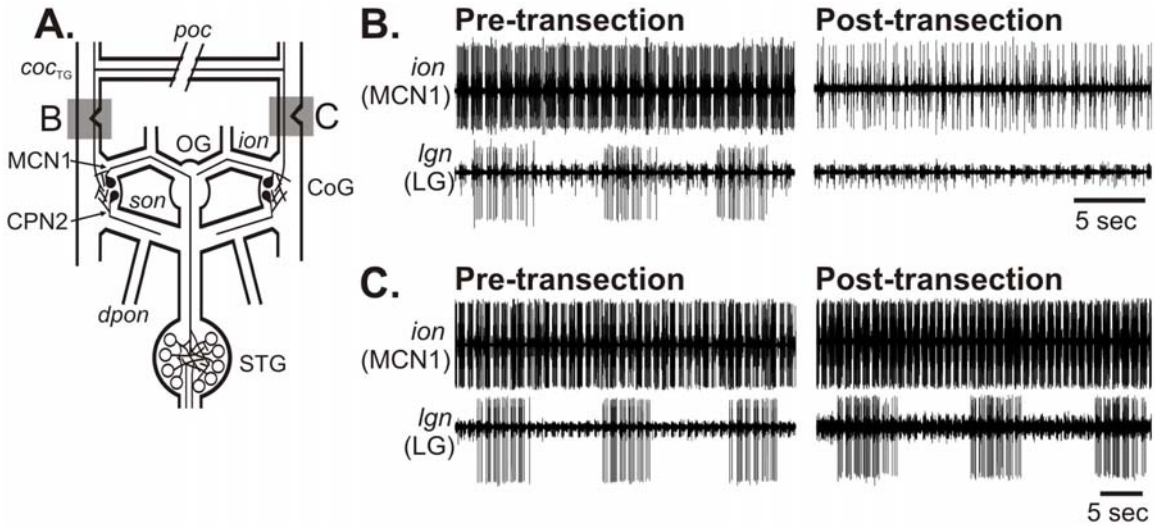

Figure 7. The POC neurons project through the medial aspect of the coc_{TG} to influence MCN1 and CPN2 in the CoG. (A) STNS schematic indicating the location and extent of the coc_{TG} transections that occurred in Panels B and C (grey boxes). (B) Transecting the medial aspect of the coc_{TG} eliminated the ability of *poc* stimulation to trigger the gastric mill rhythm. (Left) Before medial coc_{TG} transection, *poc* stimulation triggered the gastric mill rhythm. (Right) After medial coc_{TG} transection, *poc* stimulation did not trigger the gastric mill rhythm. (C) Transecting the lateral aspect of the coc_{TG} did not alter the ability of *poc* stimulation to trigger the gastric mill rhythm. The gastric mill rhythm was triggered both (Left) before, and (Right) after lateral coc_{TG} transection by *poc* stimulation. B and C are from different preparations.

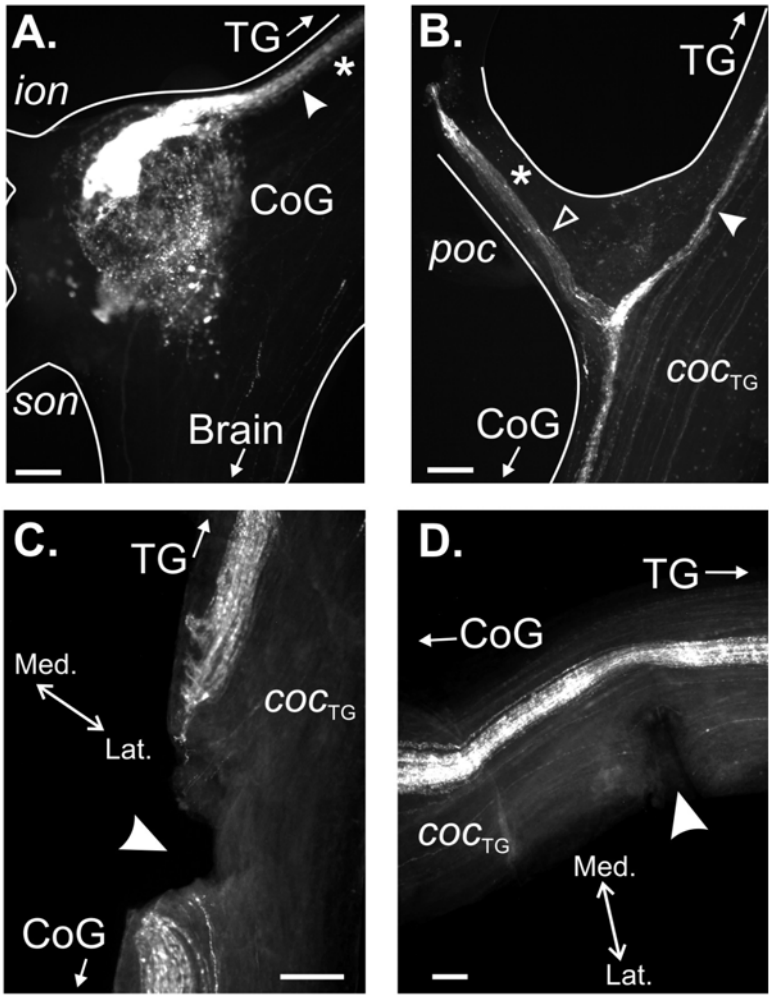

Figure 8. A CabTRP Ia-immunoreactive (IR) axon bundle projects through the *poc* and medial aspect of the anterior coc_{TG} to form terminal arborizations in the CoG. (A) CabTRP Ia-IR occurred in a tightly associated axon bundle in the medial aspect of the coc_{TG} (arrowhead) that terminated as a dense arborization in the antero-medial CoG. There was also more diffuse CabTRP Ia-IR throughout the CoG neuropil and in a subset of CoG neuronal somata. Asterisk indicates area examined to determine the number of CabTRP Ia-IR fibers present in the coc_{TG} (see text). (B) The CabTRP Ia-IR axon bundle in the medial aspect of the coc_{TG} (filled arrowhead) projected past the *poc* towards the TG, and also projected through the *poc* (open arrowhead). Asterisk indicates area

examined to determine the number of CabTRP Ia-IR fibers present in the *poc* (see text). (C) CabTRP Ia-IR bundle was transected in a preparation in which the medial coc_{TG} was transected (arrowhead). (D) CabTRP Ia-IR bundle was not transected in a preparation in which the lateral coc_{TG} was transected (arrowhead). Spatial axes in (C) are for panels A-C. All scale bars: 150 μm.

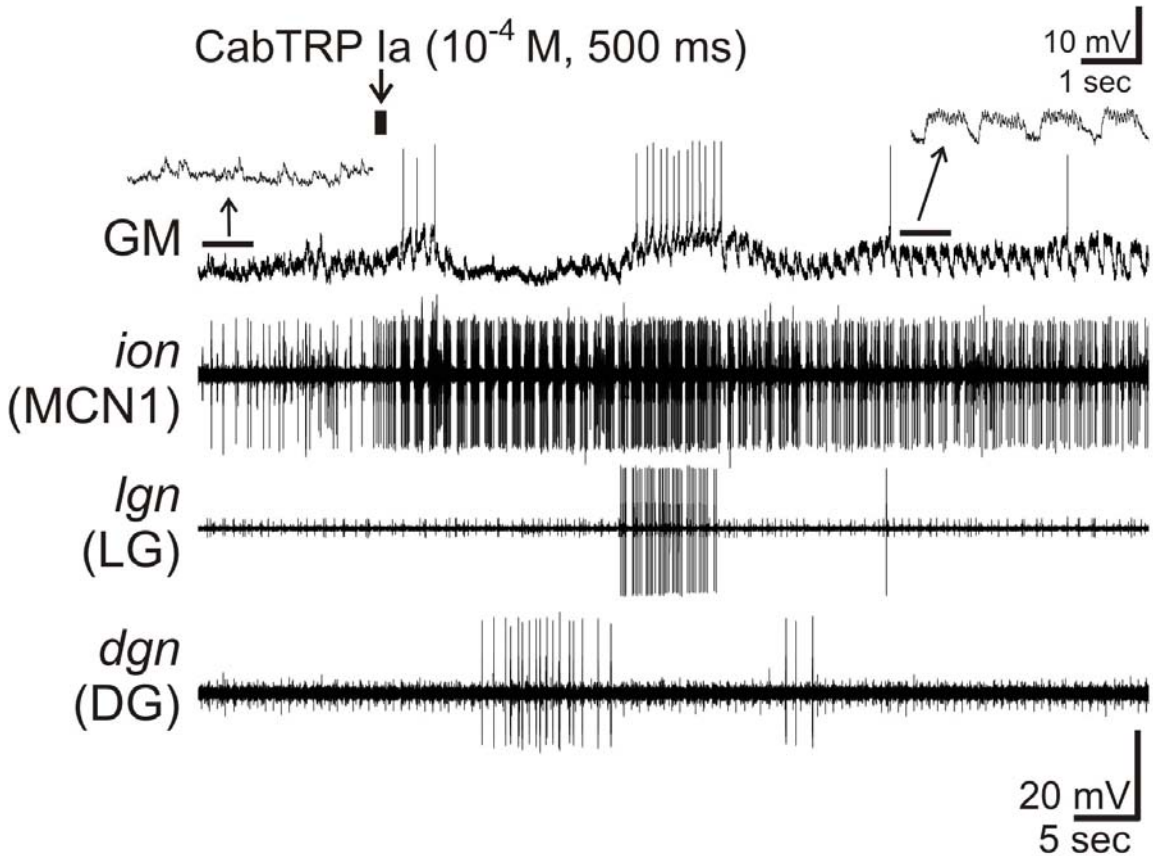

Figure 9. Exogenous CabTRP Ia mimics the POC activation of MCN1 and CPN2. A brief (500 ms) puff of CabTRP Ia (10^{-4} M) into the antero-medial aspect of the CoG neuropil excited MCN1 and CPN2 (monitored as EPSPs in GM; see text), and subsequently activated LG, GM and DG. Note that CabTRP Ia triggered pyloric-timed activity in MCN1, CPN2 and LG. Insets at an expanded time scale indicate that the GM membrane potential was not pyloric-timed before CabTRP Ia application but exhibited barrages of EPSPs that were interrupted in pyloric-time after this application. Most hyperpolarized membrane potential: GM, -67 mV.

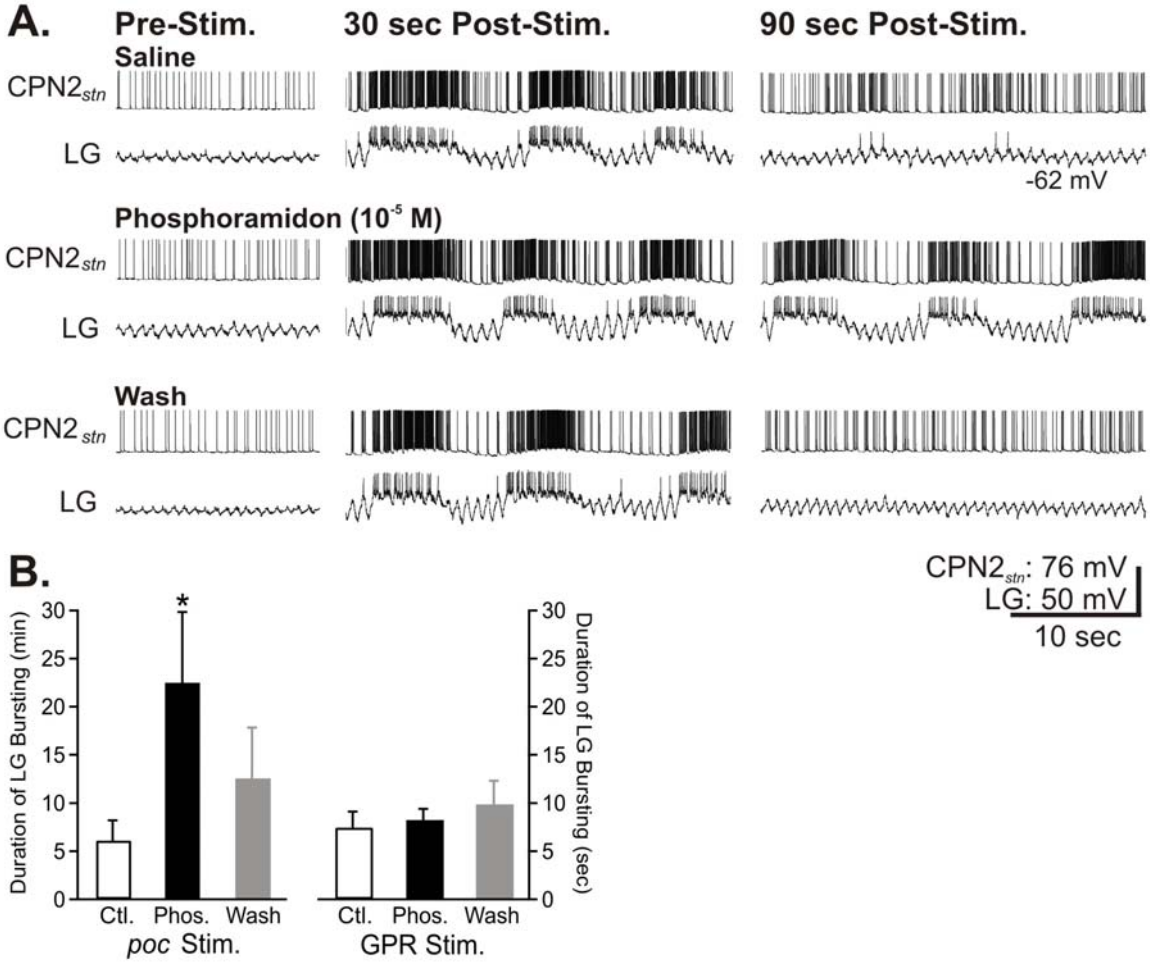

Figure 10. Blocking extracellular peptidase-mediated degradation of CabTRP Ia prolongs the actions of the POC neurons. (A) Before, during and after superfusion of the endopeptidase inhibitor phosphoramidon (10^{-5} M) to the CoGs, CPN2 was weakly active before *poc* stimulation and LG was silent (Left Panel: Top, Middle, Bottom). CPN2 activity was monitored with an intra-axonal recording near the entrance to the STG (Beenhakker and Nusbaum, 2004). Thirty seconds after *poc* stimulation (15 Hz, 15 sec), the gastric mill rhythm was triggered (as indicated by the rhythmic LG bursting) and CPN2 activity was strengthened (Middle Panel: Top, Middle, Bottom). Ninety seconds after *poc* stimulation, the gastric mill rhythm had terminated and CPN2 activity had subsided during saline superfusion, both before and after phosphoramidon application

(Right Panel: Top, Bottom). In contrast, ninety seconds after *poc* stimulation during phosphoramidon superfusion, CPN2 activity remained strong and the gastric mill rhythm persisted. (B, Left) There was a significant increase in the duration of LG bursting after *poc* stimulation in the presence of phoshoramidon (10^{-5} M) ($p<0.05$, n=5), compared to its bursting duration in saline before phosphoramidon application. (B, Right) In contrast, phosphoramidon (10^{-5} M) did not alter the duration of LG bursting after stimulation of the proprioceptor sensory GPR neuron. Most hyperpolarized membrane potentials: $CPN2_{stn}$, -73 mV; LG, -63 mV.

CHAPTER 3

The Same Core Rhythm Generator Underlies Different Rhythmic Motor Patterns

Rachel S. White

Michael P. Nusbaum

Dept. of Neuroscience, University of Pennsylvania School of Medicine, 215 Stemmler Hall, Philadelphia, PA 19104-6074

Submitted to Journal of Neuroscience (04-14-11)

Running Title: Distinct patterns paced by one rhythm generator

Text Pages: 42

Figures: 10

Tables: 0

Abstract: 241/250 Words

Introduction: 500/500 Words

Discussion: 1369/1500 Words

Acknowledgments: This work was supported by National Institutes of Neurological Disorders and Stroke Grants R37-NS 29436 and R01-NS 42813 (M.P.N.). We thank Dawn M. Blitz for helpful discussions and comments on previous versions of this paper, and Dirk Bucher and Joshua Gold for assistance with data analysis.

Keywords: Central pattern generator; stomatogastric; modulation; intercircuit regulation; projection neurons

ABSTRACT

Rhythmically active motor circuits can generate different activity patterns in response to different inputs. In most systems, however, it is not known whether the same neurons generate the underlying rhythm for each different pattern. Thus far, information regarding the degree of conservation of rhythm generator neurons is limited to a few pacemaker-driven circuits, in most of which the core rhythm generator is unchanged across different output patterns. We are addressing this issue in the network-driven, gastric mill (chewing) circuit in the crab stomatogastric nervous system. We first establish that distinct gastric mill motor patterns are triggered by separate stimulation of two extrinsic input pathways, the ventral cardiac neurons (VCNs) and post-oesophageal commissure (POC) neurons. A prominent feature that distinguishes these gastric mill motor patterns is the LG protractor motor neuron activity pattern, which is tonic during the VCN-rhythm and exhibits fast rhythmic bursting during the POC-rhythm. These two motor patterns also differed in their cycle period and some motor neuron phase relationships, duty cycles and burst durations. Despite the POC- and VCN-motor patterns being distinct, rhythm generation during each motor pattern required the activity of the same two, reciprocally inhibitory gastric mill neurons (LG, Int1). Specifically, reversibly hyperpolarizing LG or Int1, but no other gastric mill neuron, delayed the start of the next gastric mill cycle until after the imposed hyperpolarization. Thus, the same circuit neurons can comprise the core rhythm generator during different versions of a network-driven rhythmic motor pattern.

INTRODUCTION

Rhythm generation is a key feature of many neuronal networks, including central pattern generators (CPGs) (Marder and Calabrese, 1996; Huguenard and McCormick, 2007; Mann and Paulsen, 2007; Welsh et al., 2010). Individual CPGs can generate different activity patterns when influenced by distinct inputs (Marder et al., 2005; Doi and Ramirez, 2008; Briggman and Kristan, 2008; Rauscent et al., 2009; Klein et al., 2010). The different motor patterns generated by a CPG involve changes in the relative timing, firing rate, burst duration and/or burst pattern of one, some or all of the associated motor neurons (Marder and Calabrese, 1996; Marder and Bucher, 2001; Buschges et al., 2008; Friedman et al., 2009; Rosenbaum et al., 2010). These different patterns underlie different variants of a behavior (e.g. different chewing patterns) or distinct behaviors (e.g. ingestion vs. egestion).

The different patterns generated by a network often result, at least partly, from activating overlapping but distinct sets of network neurons (Jing and Weiss, 2002; Popescu and Frost, 2002; Proekt et al., 2007; Briggman and Kristan, 2008; Berkowitz et al., 2010; Weaver et al., 2010), although the same network neurons can also generate distinct motor patterns (Marder and Bucher, 2007). For some CPGs, some or all of the core rhythm generating neurons for a particular motor pattern are also identified (Selverston and Miller, 1980; Hooper and Marder, 1987; Masino and Calabrese, 2002; Cangiano and Grillner, 2003, 2005; Saideman et al., 2007; Li et al., 2010). Less is known regarding whether the different motor patterns generated by any single network are driven by the same rhythm generating neurons. Thus far, this latter issue has been addressed primarily in CPGs driven by endogenously oscillatory neurons (pacemaker-driven CPGs). Work from these circuits provide counter-examples, including preservation of the rhythm generator neurons across distinct motor patterns (Marder and

Bucher, 2007; Weaver et al., 2010) and an apparent switch in the rhythm generator neurons (Peña et al., 2004). The flexibility of rhythm generator neurons in CPGs with no endogenously oscillatory neurons (network-driven CPGs) remains unexplored.

Here we assess the degree of preservation of the rhythm generator underlying different motor patterns generated by the network-driven gastric mill (chewing) circuit in the isolated crab stomatogastric nervous system (STNS). Qualitatively distinct gastric mill motor patterns are triggered by the ventral cardiac neurons (VCNs) and post-oesophageal commissure (POC) neurons (Beenhakker et al., 2004; Blitz et al., 2008).

We first establish that the VCN- and POC-gastric mill motor patterns are quantitatively distinct in their cycle period, phase durations, protractor LG neuron burst pattern, and the burst parameters of several other motor neurons. We then show that these differences result partly from the distinct influence of the pyloric rhythm on these two gastric mill rhythms. Lastly, we determine that, among the eight types of gastric mill neurons, only the reciprocally inhibitory LG and Int1 (interneuron 1) are necessary for gastric mill rhythm generation after VCN- or POC-stimulation. These results illustrate that the same core rhythm generator can pace different motor patterns generated by a network-driven motor circuit.

MATERIALS AND METHODS

Animals. Male Jonah crabs (*Cancer borealis*) were obtained from commercial suppliers (Yankee Lobster; Marine Biological Laboratory) and maintained in aerated, filtered artificial seawater at 10 – 12°C. Animals were cold anesthetized by packing in ice for at least 30 min before dissection. The foregut was removed from the animal, and the dissection of the STNS from the foregut was performed in physiological saline at ~4°C.

Solutions. C. borealis physiological saline contained the following (in mM): 440 NaCl, 26 $MgCl_2$, 13 $CaCl_2$, 11 KCl, 10 Trisma base, 5 maleic acid, 5 glucose, pH 7.4 – 7.6. All preparations were superfused continuously with *C. borealis* saline (8-12°C).

Electrophysiology. Electrophysiology experiments were performed using standard techniques for this system (Beenhakker and Nusbaum, 2004). The isolated STNS (Fig. 1*A*) was pinned down in a silicone elastomer-lined (Sylgard 184, KR Anderson) Petri dish. Each extracellular nerve recording was made using a pair of stainless steel wire electrodes (reference and recording) whose ends were pressed into the Sylgard-coated dish. A differential AC amplifier (Model 1700: AM Systems) amplified the voltage difference between the reference wire, placed in the bath, and the recording wire, placed near an individual nerve and isolated from the bath by petroleum jelly (Vaseline, Lab Safety Supply). This signal was then further amplified and filtered (Model 410 Amplifier: Brownlee Precision). Extracellular nerve stimulation was accomplished by placing the pair of wires used to record nerve activity into a stimulus isolation unit (SIU 5: Astromed/Grass Instruments) that was connected to a stimulator (Model S88: Astromed/Grass Instruments).

Stimulation of the POC neurons was performed via extracellular stimulation of

the post-oesophageal commissure (*poc*) (Fig. 1), using a tonic stimulation pattern (duration: 15 – 30 s, intraburst frequency: 15 – 30 Hz) (Blitz et al. 2008). In all experiments, the *poc* was bisected and each half was surrounded by a petroleum jelly well to stimulate them separately. However, the left and right *pocs* were stimulated simultaneously in all experiments. The ventral cardiac neurons (VCNs) were activated by stimulating one or both of the dorsal posterior oesophageal nerves (*dpons*: Fig. 1) in a rhythmic pattern (interburst freq.: 0.06 Hz, burst duration: 6 s, intraburst freq.: 15 Hz) (Beenhakker et al., 2004). However, the same gastric mill motor pattern (e.g. cycle period, LG duty cycle) is triggered when the VCNs are stimulated in (a) the aforementioned rhythmic pattern, (b) a faster, pyloric rhythm-like pattern, or (c) a tonic pattern (Beenhakker et al., 2004).

Intrasomatic recordings were made with sharp glass microelectrodes (15-30 MΩ) filled with 0.6M K_2SO_4 plus 10mM KCl. Intracellular signals were amplified using Axoclamp 2B amplifiers (Molecular Devices), then further amplified and filtered (Brownlee Model 410 Amplifier). Current injections were performed in single-electrode discontinuous current-clamp (DCC) mode with sampling rates between 2 and 3 kHz. To facilitate intracellular recording, the desheathed ganglia were viewed with light transmitted through a dark-field condenser (Nikon). STG neurons were identified on the basis of their axonal projections, activity patterns and interactions with other STG neurons (Weimann et al. 1991; Blitz et al. 2008).

Data analysis. Data were collected in parallel onto a chart recorder (Astro-Med Everest) and computer. Acquisition onto computer (sampling rate ~5 kHz) used the Spike2 data acquisition and analysis system (Cambridge Electronic Design). Some analyses, including cycle period, burst durations, duty cycle, number of action potentials per burst,

inter-spike interval durations, intraburst firing frequency and phase relationships were conducted on the digitized data using a custom-written Spike2 program (The Crab Analyzer: freely available at http://www.uni-ulm.de/~wstein/spike2/index.html).

Unless otherwise stated, each data point in a data set was derived by determining the mean for the analyzed parameter from 10 consecutive gastric mill cycles. One gastric mill cycle was defined as extending from the onset of consecutive LG neuron action potential bursts (Beenhakker and Nusbaum, 2004; Wood et al., 2004). Thus, the gastric mill cycle period was measured as the duration (s) between the onset of two successive LG neuron bursts. The protractor phase was measured as the LG burst duration, while the retractor phase was measured as the LG interburst duration. A gastric mill rhythm-timed burst duration was defined as the duration (s) between the onset of the first and last action potential within an impulse burst, during which no inter-spike interval was longer than 2 s (approximately twice the pyloric cycle period during the gastric mill rhythm and no more than half the duration of each gastric mill phase; Beenhakker et al., 2004). The intraburst firing rate of a neuron was defined as the number of action potentials minus one, divided by the burst duration. The instantaneous spike frequency was defined as the inverse of each successive interspike interval within a burst. Duty cycle, defined as the fraction of a gastric mill cycle during which a particular neuron fired its burst, was determined by dividing each burst duration by the cycle period during which that burst occurred. The burst relationship among gastric mill neurons was expressed in terms of phase. Phase relationships were determined by measuring the phase of burst onset and offset for each gastric mill neuron relative to the gastric mill cycle. The onset and offset phase of each gastric mill neuron was determined as the latency from cycle onset to the start and endpoint, respectively, of a gastric mill neuron burst, divided by the cycle period.

We determined the LG burst pattern during the POC- and VCN-gastric mill rhythms with respect to the pyloric rhythm by determining its relationship to the activity of the pyloric dilator (PD) neuron, a member of the pyloric pacemaker ensemble, during normalized pyloric cycles. The normalized pyloric cycle extended from PD neuron burst onset to the start of the next PD burst, as is standard for the pyloric rhythm (Bucher et al., 2006). Specifically, we separated the LG recording during each normalized pyloric cycle into 100 equal bins (1 bin = 1% normalized pyloric cycle) and determined the fraction of the LG spikes during each pyloric cycle that occurred in each bin (Bucher et al., 2006). In general, there are several pyloric cycles per LG burst, insofar as the LG burst is ~5 s duration and the pyloric cycle period during these gastric mill rhythms is ~1 s (Beenhakker et al., 2004; Beenhakker and Nusbaum, 2004; Blitz et al., 2008).

To determine whether each type of gastric mill neuron was necessary for gastric mill rhythm generation, activity in a gastric mill neuron was reversibly suppressed by hyperpolarizing current (range: -0.5 nA to -4.0 nA) during an ongoing VCN- or POC-gastric mill rhythm. These hyperpolarizing current injections typically hyperpolarized the injected neuron to –65 mV to – 90 mV. This range of current injections was not sufficient to alter the activity of any neurons to which the hyperpolarized neuron is electrically coupled (see circuit diagram in Fig. 1*A*). All gastric mill neurons except for the gastric mill (GM) motor neurons are present as single copies in each STG (Kilman and Marder, 1996). There are 4 GM neurons per STG. Hence, for these experiments, 3 of 4 GM neurons were recorded intracellularly and hyperpolarizing current was injected simultaneously into each one.

We determined whether a particular hyperpolarizing current injection altered the ongoing gastric mill rhythm by tracking the gastric mill cycle period via the rhythmic bursting in the LG neuron, except during LG hyperpolarizations when we also tracked

Int1 activity. To this end, we determined the mean gastric mill cycle period (successive LG burst onsets) for the five cycles prior to a hyperpolarizing current injection, and then labeled the expected onset time of the next several gastric mill cycles in the absence of any perturbation of the ongoing rhythm. We then determined whether the first gastric mill cycle onset (LG burst onset) after the start of a hyperpolarizing current injection occurred at the expected time in the absence of the hyperpolarization.

Data were plotted with Excel (version 2002, Microsoft), Prism (version 3.0, GraphPad) and MatLab (Mathworks). Figures were produced by using CorelDraw (version 13.0 for Windows). Statistical analyses were performed with Microsoft Excel (Microsoft), SigmaStat 3.0 (SPSS) and MatLab. Comparisons were made to determine statistical significance using the paired Student's *t*-test, with the following exceptions. The Chi-square goodness of fit test (two-tailed) with Yates' correction was used to compare the percentage of pyloric cycles associated with a LG interspike-interval pause of at least 200 ms during the POC- and VCN-gastric mill rhythms. The two-sample Kolmogorov-Smirnov goodness-of-fit test (K-S Test) was used to determine the likelihood that the distribution of LG spikes across the pyloric cycle during the POC- and VCN-gastric mill rhythms was the same. As internal controls for the K-S test analysis, we divided each data set in half and compared them to each other (i.e. POC-data to POC-data, and VCN-data to VCN-data).

In all experiments, the effect of each manipulation was reversible, and there was no significant difference between the pre- and post-manipulation groups. Data are expressed as the mean ± standard error (SE).

RESULTS

The VCN- and POC-triggered gastric mill rhythms

The gastric mill rhythm is a two-phase motor pattern that underlies chewing behavior by alternately driving the protraction and retraction of the teeth, which are located in the gastric mill stomach compartment (Heinzel et al., 1993). This rhythm is generated by a CPG circuit in the STG. The gastric mill neurons are all identified and their synaptic interactions characterized (Nusbaum and Beenhakker, 2002; Marder and Bucher 2007; Stein, 2009). This circuit includes 4 types of protractor motor neurons (LG, GM, medial gastric [MG], inferior cardiac [IC]), 3 types of retractor motor neurons (DG, ventricular dilator [VD], anterior median [AM]) and a single interneuron (Int1) (Figs. 1*A*,*B*). The motor neurons also have synaptic actions within the circuit (Fig. 1*B*), enabling some of them to influence at least some versions of the gastric mill rhythm (Coleman et al., 1995; Bartos et al., 1999; Saideman et al., 2007). The gastric mill rhythm is an episodic motor pattern, in vivo and in vitro, that is driven primarily by projection neurons whose somata are located in the commissural ganglia (CoGs) (Fig. 1*A*) (Coleman and Nusbaum, 1994; Combes et al., 1999; Beenhakker and Nusbaum, 2004).

In the isolated crab STNS, relatively brief stimulation of the VCN- or POC neurons triggers a gastric mill rhythm that commonly persists for tens of minutes post-stimulation (Beenhakker et al., 2004; Blitz et al., 2008). The VCNs are a bilateral population (~60 neurons per side) of stretch receptor neurons located in the lining of the cardiac sac stomach compartment, a food storage organ just anterior to the gastric mill compartment (Beenhakker et al., 2004). The VCNs project to the CoGs, where their activity triggers a long-lasting activation of the projection neurons MCN1 and CPN2 (Figs. 1*A*-*C*) (Beenhakker et al., 2004). VCN activation of these two projection neurons

is necessary and sufficient to drive the VCN-gastric mill rhythm (Beenhakker and Nusbaum, 2004). All gastric mill neurons participate in the VCN-gastric mill rhythm.

The POCs are a bilateral population of peptidergic neurons (~100 per side) that innervate the CoGs via the circumoesophageal commissure (*coc*), by which the thoracic ganglion (TG) communicates with each CoG (Fig. 1*A*) (Kirby and Nusbaum, 2007; Blitz et al., 2008). A subset of the POC axons cross to the contralateral *coc* via the post-oesophageal commissure (*poc*) (Fig. 1*A*) (Blitz et al., 2008). Like the VCNs, POC stimulation causes a long-lasting activation of MCN1 and CPN2 which drives the gastric mill rhythm (Fig. 1*B,C*) (Blitz et al., 2008). All gastric mill neurons except AM participate in the POC-gastric mill rhythm.

Another distinction between the VCN- and POC-gastric mill motor patterns, besides the AM neuron only participating in the VCN-rhythm, is the burst pattern of the protractor neuron LG (Fig. 1*C*). This neuron commonly fires tonically during the protraction phase of the VCN-gastric mill rhythm, while it exhibits a fast, rhythmic burst pattern during POC-protraction. These distinct patterns result from the comparable patterns in MCN1 and CPN2 during each rhythm, because these projection neurons drive LG activity (Fig. 1*C*) (Coleman and Nusbaum, 1994; Norris et al., 1994; Blitz and Nusbaum, 2008). The fast rhythmic pattern in these projection neurons during POC-protraction results from the fast rhythmic feedback inhibition they receive from the pyloric pacemaker interneuron AB (anterior burster) in the CoGs (Blitz and Nusbaum, 2008). Thus, the fast rhythmic LG burst pattern during the POC-gastric mill rhythm is also pyloric rhythm-timed. The tonic pattern in the projection neurons and, thus, in LG during VCN-protraction results from the AB feedback being gated out within the CoGs during this time (Blitz and Nusbaum, 2008). Insofar as AB is electrically-coupled to and coactive with the paired PD neurons in the STG (Fig. 1*B*), the more readily recorded PD

motor neurons serve as a useful monitor of AB activity (Fig. 1*C*).

Comparison of the VCN- and POC-triggered gastric mill motor patterns

Previous studies provided only a qualitative evaluation of the distinct LG burst pattern during the VCN- and POC-gastric mill rhythms. Thus, to more firmly establish this distinction, we analyzed the LG burst structure during each type of gastric mill rhythm. To this end, we determined its within-burst spike distribution relative to the AB/PD burst of the pyloric rhythm (see Methods). When plotted as a function of the phase of the pyloric rhythm, during the POC-gastric mill rhythm there was a consistent drop in LG activity that began during the PD burst and continued afterwards for another approximately 20% of each pyloric cycle (n=10/10 preparations) (Fig. 2*A*,*B*). In contrast, there was no evident PD-related decline in LG activity during VCN-gastric mill rhythms (n=10/10 preparations) (Fig 2*C*,*D*). The overall distribution of LG spikes across the pyloric cycle was significantly different during these two gastric mill rhythms ($p=9.2 \times 10^{-5}$). In contrast, the distribution of LG spikes across the pyloric cycle was not different when either the POC-data set (n=5 each, p=0.89) or VCN-data set (n=5 each, p=0.68) was divided in half and compared.

We also determined the distribution of these same LG spikes during each pyloric cycle as a function of time instead of pyloric phase, by binning these spikes (10 ms/bin; ~1% of the pyloric cycle), starting with PD burst onset. With this approach, during the POC-gastric mill rhythm the biggest decline in the PD-timed activity of LG, wherein each bin contained ≤0.2% of the total LG spikes during the pyloric cycle, commonly lasted for at least 200 ms. We therefore determined the fraction of PD neuron bursts during each LG burst that were associated with a pause in LG firing of at least 200 ms. During the POC-gastric mill rhythm, there were such pauses in LG activity during 90% of all pyloric cycles

(404 of 448 pyloric cycles, n=10 preparations). Additionally, in all of the remaining 44 cycles, a briefer, PD-timed pause was still evident in LG activity. In contrast, during the VCN-gastric mill rhythm, comparable pauses of at least 200 ms in LG activity occurred in a significantly smaller percentage of pyloric cycles (5%: 23 of 466 pyloric cycles, n=10 preparations; $p<0.0001$ relative to the POC-gastric mill rhythm). Further, in every case where this pause did occur (n=23/23), there was only one per LG burst and it took place at the end of the burst when the LG firing rate was waning.

We also compared several parameters that define the gastric mill motor pattern and found additional distinctions between the VCN- and POC-gastric mill rhythms. One such distinction was that the cycle period was briefer during the VCN-gastric mill rhythm (VCN: 10.36 s ± 0.4 s, n=10; POC: 13.39 s ± 1.1 s, n=10; p=0.02) (Fig. 3*A*). The longer cycle period for the POC-rhythm resulted from a prolongation of both the protractor phase (i.e. LG burst duration) (VCN: 4.47 ± 0.2 s, n=10; POC: 5.61 ± 0.5 s, n=10; p=0.04) and the retractor phase (VCN: 5.89 ± 0.3 s, n=10; POC: 7.82 ± 0.7 s, n=10; p=0.03) (Fig. 3*A,B*).

In parallel with the increased protractor phase duration during the POC-gastric mill rhythm, the protractor neurons GM (POC: n=10; VCN: n=10, p=0.02) and MG (POC: n=10; VCN: n=10, p=0.03) exhibited longer duration bursts during this version of the gastric mill rhythm (Fig. 3*B*). In contrast, despite the longer retractor phase duration during the POC-rhythm, the retractor motor neuron DG burst duration was not different during the POC- and VCN-rhythms (each rhythm: n=10, p=0.98) (Fig. 3*B*). During both rhythms, the DG burst began part-way through the retractor phase and terminated near the time of LG burst onset (e.g. Figs. 1*C*, 3*C*). Lastly, there was no difference in the duration of the gastro-pyloric motor neuron IC and VD bursts (each rhythm: n=10, p=0.3) (Fig. 3*B*). IC and VD activity spanned the retractor phase and overlapped the initial part

of protraction (Figs. 1*C*,3*C*).

There were also some differences in duty cycle and phase relationships during the VCN- and POC-rhythms. Specifically, the retractor neuron DG duty cycle was larger during the VCN-rhythm (each rhythm: n=10, p=0.01) while the duty cycle of the protractor neuron MG was larger during the POC-rhythm (each rhythm: n=10, p=0.049). With respect to phase, relative to its burst onset during the POC-rhythm, during the VCN-rhythm the burst onset of the protractor GM (each rhythm: n=10, p=0.0001) and MG (each rhythm: n=10, p=0.009) neurons were consistently phase-delayed (Fig. 3*C*). DG burst offset was also phase delayed during the VCN-rhythm (each rhythm: n=10, p=0.02) (Fig. 3*C*).

Thus, the POC-and VCN-gastric mill rhythms were distinct with respect to their cycle periods and many aspects of their patterns. The most prominent distinctions spanned 5 of the 8 types of gastric mill neurons, including AM neuron participation only during the VCN-gastric mill rhythm and the distinct LG neuron burst structure, DG neuron duty cycle and burst onset phase of the GM and MG neurons.

Influence of the pyloric rhythm on the VCN- and POC-triggered gastric mill motor patterns

One clear distinction between the VCN- and POC-gastric mill rhythms is the relative influence of the pyloric rhythm on the projection neurons MCN1 and CPN2 during the gastric mill protractor phase (Blitz and Nusbaum, 2008), and the resulting distinction in the LG burst pattern during these two motor patterns (Figs. 1*C*, 2). Thus, we tested the hypothesis that all of the identified differences between these two gastric mill motor patterns resulted from this distinct influence of the pyloric rhythm. To this end, we compared VCN- and POC-gastric mill motor patterns in preparations where we

suppressed the pyloric rhythm by injecting constant amplitude hyperpolarizing current into the pyloric pacemaker neurons (AB and PD neurons). We continuously monitored the pyloric rhythm by extracellular recordings of all pyloric motor neurons, including the PD neurons.

Suppressing the pyloric rhythm did not terminate either type of gastric mill rhythm (POC-rhythm, n=6; VCN-rhythm, n=8) (Fig. 4*A,B*). Thus, the pyloric rhythm was not necessary for POC- or VCN-gastric mill rhythm generation. However, as anticipated, it did alter many aspects of these gastric mill motor patterns. For example, for both gastric mill rhythms, suppressing the pyloric rhythm increased the cycle period (POC: pyloric rhythm [PR] on, 14.1 ± 0.8 s; PR off, 21.6 ± 1.0 s, n=6, p=0.001; VCN: PR on, 11.0 ± 0.9 s; PR off, 13.9 ± 1.6 s, n=9, p=0.03) and retraction duration (POC: PR on, 7.9 ± 0.5 s; PR off, 12.8 ± 1.4 s, n=6, p=0.001; VCN: PR on, 6.0 ± 0.7 s; PR off, 8.5 ± 1.1 s, n=9, p=0.02).

Suppressing the pyloric rhythm also altered the burst structure of those gastric mill neurons whose gastric mill rhythm-related burst normally exhibited pyloric-timed interruptions in firing. For example, as first reported qualitatively by Blitz et al. (2008), the pyloric-timed LG burst pattern during the POC-rhythm changed to a tonic pattern when the pyloric rhythm was suppressed (6/6 preparations) (Fig. 4*A,C*). We analyzed the LG burst pattern in POC-gastric mill rhythms before and after the pyloric rhythm was suppressed and determined that there was an approximately 9-fold decrease in the number of events (PR on: 245; PR off: 27) in the instantaneous spike frequency range (1.5 – 3 Hz) where most pyloric-timed interruptions in LG activity occurred (245 of 298: 82%) (Fig. 4*C*). The LG burst also exhibited a broader peak distribution of instantaneous spike frequencies when the pyloric rhythm was suppressed (n=6) (Fig. 4*C*). In general, at these times the first half of each LG burst exhibited higher frequency

firing than the latter half (Fig. 4*A*).

Although the LG intraburst structure was changed by suppressing the pyloric rhythm during the POC-gastric mill rhythm, its mean intraburst firing frequency (excluding the pyloric-timed interruptions) did not change (PR on: 10.0 ± 0.4 Hz; PR off: 11.5 ± 1.5 Hz, n=6, p=0.21). However, its burst duration increased (PR on: 6.8 ± 0.5 s; PR off: 9.0 ± 0.7 s, n=6, p=0.002). The combination of the increased LG burst duration plus the elimination of pyloric-timed interruptions contributed to a considerable increase in the number of LG spikes per burst when the pyloric rhythm was suppressed (PR on: 58.5 ± 0.5 spikes; PR off: 102.1 ± 10.9 spikes, n=9, p=0.004). In contrast, during the VCN-gastric mill rhythm the mean LG intraburst spike frequency increased when the pyloric rhythm was suppressed (PR on: 10.7 ± 1.3 Hz; PR off: 11.6 ± 1.5 Hz, n=9, p=0.01), but its burst duration did not change (PR on: 5.0 ± 0.5 s; PR off: 5.4 ± 0.8 s, n=9, p=0.18). Consequently, the number of LG spikes per burst during the VCN-gastric mill rhythm did not change when the pyloric rhythm was suppressed (PR on: 57.1 ± 9.5 spikes; PR off: 59.7 ± 9.6 spikes, n=9, p=0.34). The influence of removing the pyloric rhythm on LG burst duration and retraction duration advanced the off phase of the LG burst during the VCN-gastric mill rhythm (PR on: 0.47 ± 0.04; PR off: 0.40 ± 0.04 n=9, p=0.02), but did not change this parameter during the POC-rhythm (PR on: 0.46 ± 0.02; PR off: 0.43 ± 0.03, n=6, p=0.08).

Suppressing the pyloric rhythm also changed the burst pattern from fast rhythmic to tonic for the GM neurons during the POC-gastric mill rhythm (Fig. 4*A*) and during both rhythms for the Int1, MG, IC and VD neurons (data not shown). Thus, with the pyloric rhythm suppressed during the VCN- and POC-gastric mill rhythms, the burst structure of many gastric mill neurons converged to a tonic bursting pattern.

Despite the overall convergence of the gastric mill neuron burst structures to a

tonic firing pattern when the pyloric rhythm was suppressed, the VCN- and POC-gastric mill motor patterns remained distinct with respect to other parameters. This was the case, for example, for the POC- and VCN-cycle period, protraction duration and retraction duration (Fig. 5*A*-*C*). For some parameters there was an increased level of significant difference, including the cycle period (PR on: $p<0.05$; PR off: $p<0.001$) and protraction duration (i.e. LG burst duration) (PR on: $p<0.05$; PR off: $p<0.01$) (Figs. 3,5). In contrast, some parameters that had been distinct between these two gastric mill rhythms became comparable when the pyloric rhythm was suppressed, such as the DG duty cycle (PR on: $p=0.01$; PR off: $p=0.16$) and the phase of its burst termination (PR on: $p=0.02$; PR off: $p=0.16$) (Figs. 3*C*, 5*D,E*). Lastly, at least one parameter that was comparable during both gastric mill rhythms with the pyloric rhythm on, the number of LG spikes/burst, diverged when the pyloric rhythm was suppressed (PR on: $p=0.452$; PR off: $p=0.005$). Consequently, although the pyloric rhythm was responsible for the fast rhythmic burst pattern in many gastric mill neurons, it was not the source of all the gastric mill rhythm parameters that distinguished the POC- and VCN-gastric mill motor patterns.

Identifying the core rhythm-generating neurons during the VCN- and POC-gastric mill rhythms

The core rhythm generating neurons for the version of the gastric mill motor pattern driven by tonic MCN1 stimulation in reduced preparations, with the CoGs removed, include LG and Int1 (Coleman et al., 1995; Bartos et al., 1999; Saideman et al., 2007). The same gastric mill motor pattern is elicited by bath applying *Cancer borealis* pyrokinin (CabPK) peptide, again in the isolated STG, although in this latter condition the core rhythm generator includes LG, Int1 and AB (Saideman et al., 2007).

This version of the gastric mill motor pattern is distinct from those triggered by VCN or POC stimulation. For example, neither the GM nor AM neurons participate in the MCN1/CabPK-elicited gastric mill rhythm, the VD neuron is active only during retraction, and the IC neuron is predominantly active during protraction (Saideman et al., 2007). We therefore aimed to determine whether LG and Int1 also comprised the core rhythm generator for the gastric mill rhythms triggered by VCN- and POC stimulation. To this end, we selectively and reversibly suppressed activity in each gastric mill neuron during VCN- and POC-rhythms for durations that were longer than their normal interburst duration, and determined whether doing so interfered with the ongoing rhythm (see Methods).

Transiently hyperpolarizing either LG (n=8) or Int1 (n=5) consistently and reversibly disrupted the VCN-gastric mill rhythm. For example, as shown in Figure 6, the gastric mill cycle period was regular from cycle-to-cycle before each hyperpolarization. In contrast, during the maintained LG or Int1 hyperpolarization, the start of the next gastric mill cycle did not occur at the anticipated time. Instead, the next cycle onset was consistently delayed until some time after the hyperpolarizing current injection was removed (cycle period: LG control, 13.2 ± 1.2 s; LG hyperpolarized, 26.5 ± 2.4 s, $p=0.0001$, n=8; Int1 control, 11.5 ± 2.7s; Int1 hyperpolarized, 23.4 ± 1.6 s, $p=0.002$, n=5) (Figs. 6,7). Resumption of the gastric mill rhythm always began with a burst in the previously hyperpolarized neuron (Fig. 6). Moreover, after each hyperpolarizing current injection, the rhythm was reset in that the start of each subsequent gastric mill cycle (i.e. LG burst onset) did not return to occurring at its expected onset time in the absence of current injection (Fig. 6). The same results were obtained when LG or Int1 was reversibly hyperpolarized during the POC-gastric mill rhythm (LG: $p=0.002$, n=6; Int1: $p=0.017$, n=7) (Figs. 7,8).

When LG activity was suppressed by hyperpolarizing current injection, the retractor phase was not simply prolonged. For example, whereas the retractor phase neuron Int1 did consistently maintain its retractor activity pattern, the retractor DG motor neuron burst was prolonged but not for the duration of the LG hyperpolarization (n=8/8) (Figs. 6*A*, 8*A*). Additionally, the protractor phase neurons exhibited relatively weak activity during prolonged LG hyperpolarizations (Fig. 6*A*). Similarly, the protractor phase was not well-maintained during Int1 hyperpolarization. For example, the LG activity waned over time (n=5/5) (Fig. 6*B*). The retractor neurons, such as DG, were weakly active or silent (Figs. 6*B*, 8*B*). The disruption and subsequent resumption of the ongoing motor pattern occurred consistently across the approximately 10-fold range of current injection durations used for LG and Int1 (Fig. 7).

Given the pivotal influence of LG and Int1 on rhythm generation during the VCN- and POC-motor patterns, we determined whether there was a difference in the range of their membrane potential oscillations during each rhythm, insofar as it might contribute to the differences in the motor patterns. Across preparations, there was no difference between these gastric mill rhythms in terms of the slow wave membrane potential in LG at the peak (VCN: -39.0 ± 1.2 mV, n=6; POC: -39.6 ± 1.5 mV, n=7, p=0.09) and trough (VCN: -63.0 ± 0.8 mV, n=6; POC: -61.3 ± 0.1 mV, n=7, p=0.4) of its gastric mill-timed profile. This was also the case for the Int1 peak (VCN: -37.7 ± 4.8 mV, n=4; POC: -43.4 ± 3.6 mV, n=6, p=0.2) and trough (VCN: -63.2 ± 2.0 mV, n=4; POC: -62.4 ± 2.9 mV, n=6; p=0.4) membrane potentials.

In contrast to the ability of LG and Int1 to influence gastric mill rhythm generation after VCN or POC stimulation, reversibly suppressing the activity any one of the other gastric mill neurons never altered these ongoing rhythms, regardless of the duration of the hyperpolarizing current injection ($p>0.05$ for all 6 neuron types, n=3–10, both gastric

mill rhythms) (Fig. 7). One example of this result is shown in Figure 9 for hyperpolarization of the retractor neuron DG. In neither the VCN- nor POC-gastric mill rhythm did suppressing DG activity alter the expected onset time of the next gastric mill cycle. This result was not necessarily a foregone conclusion, because the DG neuron does influence the gastric mill rhythm activated by bath applying CabPK (Saideman et al., 2007).

DISCUSSION

In this paper we have shown that the same core rhythm generator underlies different versions of a rhythmic motor pattern triggered by different input pathways. Specifically, the reciprocally inhibitory neurons LG and Int1 are the only gastric mill circuit neurons necessary for rhythm generation during the distinct, VCN- and POC-triggered gastric mill rhythms in the crab *C. borealis* (Fig. 10). It is not a foregone conclusion that different motor patterns generated by the same motor circuit would have the same rhythm generator. One reason for this uncertainty is that, for many CPGs, the different motor patterns they generate often result at least partly from a change in the set of participating neurons (Jing and Weiss, 2002; Popescu and Frost, 2002; Proekt et al., 2007; Briggman and Kristan, 2008; Berkowitz et al., 2010; Weaver et al., 2010). In contrast, one might anticipate that the same motor pattern elicited by different inputs would be driven by the same core rhythm generator, yet distinct albeit overlapping sets of neurons are necessary for generating the comparable MCN1- and CabPK-elicited gastric mill motor patterns. Specifically, they both include LG and Int1, but the pyloric pacemaker neuron AB is also necessary for CabPK-gastric mill rhythm generation (Coleman et al., 1995; Bartos et al., 1999; Saideman et al., 2007). The gastric mill motor pattern activated by MCN1 and CabPK is also distinct from the ones triggered by the POC and VCN pathways (Saideman et al., 2007).

The basis of rhythm generation in CPGs is classically separated into networks paced by intrinsically oscillatory neurons, often called pacemaker-driven CPGs, and those in which rhythm generation results from a combination of non-oscillatory intrinsic properties and synaptic interactions (network-driven CPGs) (Marder and Bucher, 2001; Marder et al., 2005; Selverston 2010). A common synaptic interaction motif in network-driven CPGs is reciprocal inhibition, as between the LG neuron and Int1. Some or all of

the rhythm generating neurons for at least one version of a rhythmic motor pattern are identified in a number of rhythmic motor systems (Selverston and Miller, 1980; Getting and Dekin, 1985; Masino and Calabrese, 2002; Cangiano and Grillner, 2003, 2005; Katz et al., 2004; Peña et al., 2004; Pirtle and Satterlie, 2006; Saideman et al., 2007; Li et al., 2010; Selverston, 2010).

With respect to the degree of preservation of the core rhythm generator when a CPG produces different motor patterns, the pacemaker-driven pyloric circuit is the most extensively studied. Under the different modulatory conditions where the pyloric rhythm generator has been identified, the pyloric pacemaker group (AB, PDs) retains this role (Hooper and Marder, 1987; Ayali and Harris-Warrick, 1999; Marder and Bucher, 2007). Similarly, the pacemaker-driven timing network for leech heartbeat is unchanged when each side of the system reciprocally switches its pattern between peristaltic and synchronous mode (Masino and Calabrese, 2002; Weaver et al., 2010). In contrast, work in the mammalian respiratory system suggests that its core rhythm generator switches between different types of pacemaker neurons during different respiratory behaviors (Peña et al., 2004). Less is known regarding preservation of the rhythm generator during different versions of a network-driven motor pattern. As discussed above, for the network-driven crab gastric mill CPG, the core rhythm generator group had been identified for one gastric mill motor pattern, driven by either tonic MCN1 stimulation or bath applied CabPK (Saideman et al., 2007). Our current work establishes that the gastric mill rhythm generator can persist during different versions of this motor pattern. Although the number of systems studied remains limited, it appears that the neurons contributing to the core rhythm generator for a particular motor system can either persist or be modified when different versions of the motor pattern are elicited. This provisional conclusion suggests that this feature has more flexibility than other,

more extensively characterized general principles of CPG organization (Marder and Calabrese, 1996; Marder and Bucher, 2001; Selverston, 2010).

Different versions of a particular motor pattern commonly result either from modulating the properties of the same set of pattern generating neurons or altering the set responsible for pattern generation (Marder et al., 2005; Marder and Bucher, 2007; Briggman and Kristan, 2008; Sasaki et al., 2009; Berkowitz et al., 2010). In contrast, the distinctions between the VCN- and POC-gastric mill rhythms appear to result at least partly from a selective gating-out of the feedback inhibition from the pyloric pacemaker neuron AB to MCN1 and CPN2 during the VCN-gastric mill protractor phase (Blitz and Nusbaum, 2008). This gating mechanism underlies the tonic vs. pyloric-timed activity of MCN1 and CPN2 during the VCN- and POC-gastric mill rhythms, respectively, which in turn determines the LG activity pattern. There must, however, be additional differences mediated by the POC- and VCN pathways, insofar as the two gastric mill rhythms remained distinct in at least several respects when the pyloric rhythm was suppressed.

The fact that LG and Int1 were the only gastric mill neurons necessary for generating the VCN- and POC-gastric mill rhythms does not necessarily mean that other gastric mill neurons cannot influence rhythm generation. For example, the other protractor motor neurons are electrically coupled to LG. Consequently, whereas individual manipulations of these neurons did not interfere with the ongoing rhythm, coincident membrane potential changes in several of these neurons might produce such a change. Within the pyloric pacemaker group, electrical coupling enables the paired PD neurons to regulate the cycle period of the intrinsically oscillatory AB neuron, and manipulating both PD neurons has a stronger influence than either one alone on the AB cycle period (Hooper and Marder, 1987; Ayali and Harris-Warrick, 1999).

The fact that the POC- and VCN-gastric mill motor patterns were both altered by

suppressing the pyloric rhythm indicates that the pyloric pacemaker neurons are pattern generator neurons for the gastric mill rhythm, in parallel with their well established roles as rhythm generator- and pattern generator neurons for the pyloric rhythm (Marder and Bucher, 2007). For example, suppressing AB and PD neuron activity switched the activity pattern of all gastric mill neurons that normally exhibit pyloric-timed activity during the VCN- and POC-gastric mill rhythms to a tonic bursting pattern. This pattern change in the gastric mill motor neurons will likely influence both the pattern and strength of contraction of the muscles that they innervate (Heinzel et al., 1993; Stein et al., 2006; White et al., 2007). Earlier work by Weimann and Marder (1984), using gastric mill rhythms elicited by bath-applied modulators, drew the similar conclusion that current injection into some pyloric neurons could reset the gastric mill cycle period as could some gastric mill neurons for the pyloric cycle period. This observation adds to the previously established, intertwined nature of the gastric mill and pyloric circuits, which exhibit coordinated activity and regulate each others cycle period, despite functioning with mean cycle periods that are ~10-fold different (Bartos and Nusbaum, 1997; Clemens et al., 1998; Nadim et al., 1998; Bartos et al., 1999; Wood et al., 2004; Bucher et al. 2006). Many complex behaviors involve coordination between separate motor networks, as occurs for example between locomotion and respiration (Kawahara et al., 1989; Syed and Winlow, 1991; Bernasconi and Kohl, 1993; Morin and Viala, 2002; Saunders et al., 2004; Gariépy et al., 2010). Thus far, however, in most of these systems it remains to be determined whether the coordination results from interactions between the two CPGs or is imposed on them from descending and/or ascending inputs (Ezure and Tanaka, 1997; Morin and Viala, 2002; Steriade, 2006).

Whether there are separate conditions in vivo that selectively activate the POC or VCN pathway to drive their two distinct gastric mill motor patterns is not yet known,

although VCN-like gastric mill rhythms have been recorded in vivo (Heinzel et al., 1993). However, in vivo endoscope analysis has shown that the LG neuron-driven lateral teeth protract either smoothly or in a pyloric-timed pattern, supporting a natural behavioral role for the VCN- and POC-gastric mill patterns (Heinzel et al., 1993). As methodological developments for in vivo recordings and manipulations continue to be refined (Hedrich et al., 2011), it will become possible to determine whether the preservation of the gastric mill rhythm generator during different versions of the gastric mill motor pattern that occurs in the isolated STNS accurately reflects the comparable situation in the behaving animal.

REFERENCES

Ayali A, Harris-Warrick RM (1999) Monoamine control of the pacemaker kernel and cycle frequency in the lobster pyloric network. J Neurosci 19:6712 – 6722.

Bartos M, Nusbaum MP (1997) Intercircuit control of motor pattern modulation by presynaptic inhibition. J Neurosci 17:2247 – 2256.

Bartos M, Manor Y, Nadim F, Marder E, Nusbaum MP (1999) Coordination of fast and slow rhythmic neuronal circuits. J Neurosci 19:6650 – 6660.

Beenhakker MP, Nusbaum MP (2004) Mechanosensory activation of a motor circuit by coactivation of two projection neurons. J Neurosci 24:6741 – 6750.

Beenhakker MP, Blitz DM, Nusbaum MP (2004) Long-lasting activation of rhythmic neuronal activity by a novel mechanosensory system in the crustacean stomatogastric nervous system. J Neurophysiol 91:78 – 91.

Bernasconi P, Kohl J (1993) Analysis of co-ordination between breathing and exercise rhythms in man. J Physiol 471:693-706.

Berkowitz A, Roberts A, Soffe SR (2010) Roles for multifunctional and specialized spinal interneurons during motor pattern generation in tadpoles, zebrafish larvae, and turtles. Front Behav Neurosci 4:pp. 18.

Blitz DM, Nusbaum MP (2008) State-dependent presynaptic inhibition regulates central pattern generator feedback to descending inputs. J Neurosci 28:9564 – 9574.

Blitz DM, White RS, Saideman SR, Cook A, Christie AE, Nadim F, Nusbaum MP (2008) A newly identified extrinsic input triggers a distinct gastric mill rhythm via activation of modulatory projection neurons. J Exp Biol 211:1000 – 1011.

Briggman KL, Kristan WB (2008) Multifunctional pattern-generating circuits. Annu Rev Neurosci 31:271 – 294.

Bucher D, Taylor AL, Marder E (2006) Central pattern generating neurons

simultaneously express fast and slow rhythmic activities in the stomatogastric ganglion. J Neurophysiol 95:3617 – 3632.

Büschges A, Akay T, Gabriel JP, Schmidt J (2008) Organizing network action for locomotion: insights from studying insect walking. Brain Res Rev 57:162 – 171.

Cangiano L, Grillner S (2003) Fast and slow locomotor burst generation in the hemispinal cord of the lamprey. J Neurophysiol 89:2931 – 2942.

Cangiano L, Grillner S (2005) Mechanisms of rhythm generation in a spinal locomotor network deprived of crossed connections: the lamprey hemicord. J Neurosci 25:923 – 935.

Clemens S, Combes D, Meyrand P, Simmers J (1998) Long-term expression of two interacting motor pattern-generating networks in the stomatogastric system of freely behaving lobster. J Neurophysiol 79:1396 – 1408.

Coleman MJ, Nusbaum MP (1994) Functional consequences of compartmentalization of synaptic input. J Neurosci 14:6544 – 6552.

Coleman MJ, Meyrand P, Nusbaum MP (1995) Presynaptic inhibition mediates a switch between two modes of synaptic transmission. Nature 378:502 – 505.

Combes D, Meyrand P, Simmers J (1999) Motor pattern specification by dual descending pathways to a lobster rhythm-generating network. J Neurosci 19:3610 – 3619.

Doi A, Ramirez JM (2008) Neuromodulation and the orchestration of the respiratory rhythm. Respir Physiol Neurobiol 164:96 – 104.

Ezure K, Tanaka I (1997) Convergence of central respiratory and locomotor rhythms onto single neurons of the lateral reticular nucleus. Exp Brain Res 113:230 – 242.

Friedman AK, Zhurov Y, Ludwar BCh, Weiss KR (2009) Motor outputs in a multitasking network: relative contributions of inputs and experience-dependent network states. J

Neurophysiol 102:3711 – 3727.

Gariépy J-F, Missaghi K, Dubuc R (2010) The interactions between locomotion and respiration. Prog Brain Res 187:173 – 188.

Getting PA, Dekin MS (1985) Mechanisms of pattern generation underlying swimming in *Tritonia*. IV. Gating of central pattern generator. J Neurophysiol, 53:466 – 480.

Hedrich UB, Diehl F, Stein W (2011) Gastric and pyloric motor pattern control by a modulatory projection neuron in the intact crab, *Cancer pagurus*. J Neurophysiol, in press.

Heinzel HG, Weimann JM, Marder E (1993) The behavioral repertoire of the gastric mill in the crab, *Cancer pagurus*: an in situ endoscopic and electrophysiological examination. J Neurosci 13:1793 – 1803.

Hooper SL, Marder E (1987) Modulation of the lobster pyloric rhythm by the peptide proctolin. J Neurosci 7:2097 – 2112.

Huguenard JR, McCormick DA (2007) Thalamic synchrony and dynamic regulation of global forebrain oscillations. Trends Neurosci 30: 350 – 356.

Jing J, Weiss KR (2002) Interneuronal basis of the generation of related but distinct motor programs in *Aplysia*: implications for current neuronal models of vertebrate intralimb coordination. J Neurosci 22:6228 – 6238.

Katz PS, Sakurai A, Clemens S, Davis D (2004) Cycle period of a network oscillator is independent of membrane potential and spiking activity in individual central pattern generator neurons. J Neurophysiol, 92:1904 – 1917.

Kawahara K, Kumagai S, Nakazono Y, Miyamoto Y (1989) Coupling between respiratory and stepping rhythms during locomotion in decerebrate cats. J Appl Physiol 67:110 – 115.

Kilman VL, Marder E (1996) Ultrastructure of the stomatogastric ganglion neuropil of the

crab, *Cancer borealis*. J Comp Neurol 374:362 – 375.

Kirby MS, Nusbaum MP (2007) Central nervous system projections to and from the commissural ganglion of the crab *Cancer borealis*. Cell Tissue Res 328:625 – 637.

Klein DA, Patino A, Tresch MC (2010) Flexibility of motor pattern generation across stimulation conditions by the neonatal rat spinal cord. J Neurophysiol 103:1580 – 1590.

Li WC, Roberts A, Soffe SR (2010) Specific brainstem neurons switch each other into pacemaker mode to drive movement by activating NMDA receptors. J Neurosci 30:16609 – 16620.

Mann EO, Paulsen O (2007) Role of GABAergic inhibition in hippocampal network oscillations. Trends Neurosci 30:343 – 349.

Marder E, Bucher D (2001) Central pattern generators and the control of rhythmic movements. Curr Biol 11: R986 – R996.

Marder E, Bucher D (2007) Understanding circuit dynamics using the stomatogastric nervous system of lobsters and crabs. Annu Rev Physiol 69:291 – 316.

Marder E, Calabrese RL (1996) Principles of rhythmic motor pattern generation. Physiol Rev 76:687 – 717.

Marder E, Bucher D, Schulz DJ, Taylor AL (2005) Invertebrate central pattern generation moves along. Curr Biol 15:R685 – R699.

Masino M, Calabrese RL (2002) A functional asymmetry in the leech heartbeat timing network is revealed by driving the network across various cycle periods. J Neurosci 22:4418 – 4427.

Morin D, Viala D (2002) Coordinations of locomotor and respiratory rhythms in vitro are critically dependent on hindlimb sensory inputs. J Neurosci 22:4756 – 4765.

Nadim F, Manor Y, Nusbaum MP, Marder E (1998) Frequency regulation of a slow

rhythm by a fast periodic input. J Neurosci 18:5053 – 5067.

Norris BJ, Coleman MJ, Nusbaum MP (1994) Recruitment of a projection neuron determines gastric mill motor pattern selection in the stomatogastric nervous system of the crab, *Cancer borealis*. J Neurophysiol 72:1451 – 1463.

Nusbaum MP, Beenhakker MP (2002) A small systems approach to motor pattern generation. Nature 417:343 – 350.

Peña F, Parkis MA, Tryba AK, Ramirez JM (2004) Differential contribution of pacemaker properties to the generation of respiratory rhythms during normoxia and hypoxia. Neuron 43:105 – 117.

Pirtle TJ, Satterlie RA (2006) The contribution of the pleural type 12 interneuron to swim acceleration in *Clione limacina*. Invert Neurosci 6:161 – 168.

Popescu IR, Frost WN (2002) Highly dissimilar behaviors mediated by a multifunctional network in the marine mollusk *Tritonia diomedea*. J Neurosci 22:1985 – 1993.

Proekt A, Jing J, Weiss KR (2007) Multiple contributions of an input-representing neuron to the dynamics of the *Aplysia* feeding network. J Neurophysiol 97:3046 – 3056.

Rauscent A, Einum J, Le Ray D, Simmers J, Combes D (2009) Opposing aminergic modulation of distinct spinal locomotor circuits and their functional coupling during amphibian metamorphosis. J Neurosci 29:1163 – 1174.

Rosenbaum P, Wosnitza A, Büschges A, Gruhn M (2010) Activity patterns and timing of muscle activity in the forward walking and backward walking stick insect *Carausius morosus*. J Neurophysiol 104:1681-1695.

Saideman SR, Blitz DM, Nusbaum MP (2007) Convergent motor patterns from divergent circuits. J Neurosci 27:6664 – 6674.

Sasaki K, Brezina V, Weiss KR, Jing J (2009) Distinct inhibitory neurons exert temporally specific control over activity of a motoneuron receiving concurrent excitation and

inhibition. J Neurosci 29:11732 – 11744.

Saunders SW, Rath D, Hodges PW (2004) Postural and respiratory activation of the trunk muscles changes with mode and speed of locomotion. Gait Posture 20:280 – 290.

Selverston AI (2010) Invertebrate central pattern generator circuits. Philos Trans R Soc Lond B 365:2329 – 2345.

Selverston AI, Miller JP (1980) Mechanisms underlying pattern generation in lobster stomatogastric ganglion as determined by selective inactivation of identified neurons. I. Pyloric system. J Neurophysiol, 44:1102 – 1121.

Stein W (2009) Modulation of stomatogastric rhythms. J Comp Physiol A 195: 989 – 1009.

Stein W, Smarandache CR, Nickmann M, Hedrich UB (2006) Functional consequences of activity-dependent synaptic enhancement at a crustacean neuromuscular junction. J Exp Biol, 209:1285 – 1300.

Steriade M (2006) Grouping of brain rhythms in corticothalamic systems. Neurosci 137:1087 – 1106.

Syed NI, Winlow W (1991) Coordination of locomotor and cardiorespiratory networks of *Lymnaea stagnalis* by a pair of identified interneurones. J Exp Biol 158:37 – 62.

Weaver AL, Roffman RC, Norris BJ, Calabrese RL (2010) A role for compromise: synaptic inhibition and electrical coupling interact to control phasing in the leech heartbeat CPG. Front Behav Neurosci 4: pp. 17.

Weimann JM, Marder E (1984) Switching neurons are integral members of multiple oscillatory networks. Curr Biol 4:896 – 902.

Weimann JM, Meyrand P, Marder E (1991) Neurons that form multiple pattern generators: identification and multiple activity patterns of gastric/pyloric neurons in

the crab stomatogastric system. J Neurophysiol 65:111 – 122.

Welsh DK, Takahashi JS, Kay SA (2010) Suprachiasmatic nucleus: cell-autonomy and network properties. Annu Rev Physiol 72:551 – 577.

White RS, Blitz DM, Nusbaum MP (2007) Different outputs from the same CPG elicit distinct muscle activity patterns. Program No. 924.22, Neurosci Mtg Planner. San Diego, CA: Society for Neuroscience. Online.

Wood DE, Manor Y, Nadim F, Nusbaum MP (2004) Intercircuit control via rhythmic regulation of projection neuron activity. J Neurosci 24:7455 – 7463.

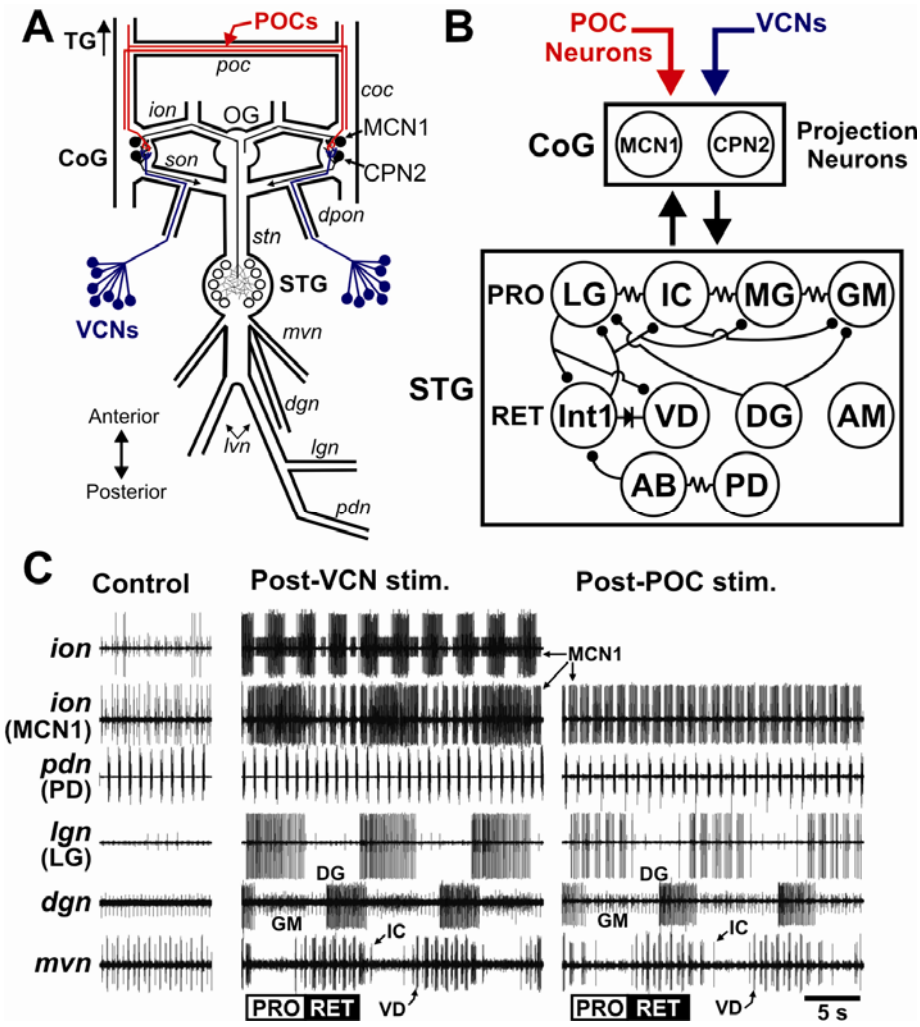

Figure 1. The VCN- and POC-pathways each trigger a gastric mill motor pattern. ***A,*** Schematic of the isolated STNS, including its four ganglia plus their connecting- and peripheral nerves. The VCNs project into the CoGs from the cardiac sac stomach compartment via the *dpon* and *son* nerves. The POC neurons project into the CoGs via the *coc* and *poc* nerves. The single MCN1 and CPN2 projection neurons in each CoG extend their axons to the STG via the *ion* and *son*, respectively, and then converge to reach the STG via the *stn* nerve. Abbreviations- Ganglia: CoG, commissural ganglion; OG, oesophageal ganglion; STG, stomatogastric ganglion; TG, thoracic ganglion. Nerves: *coc*, circumoesophageal commissure; *dgn*, dorsal gastric nerve; *dpon*, dorsal

posterior oesophageal nerve; *ion*, inferior oesophageal nerve; *lgn*, lateral gastric nerve; *lvn*, lateral ventricular nerve; *mvn*, medial ventricular nerve; *pdn*, pyloric dilator nerve; *poc*, post-oesophageal commissure; *son*, superior oesophageal nerve; *stn*, stomatogastric nerve. Neurons: CPN2, commissural projection neuron 2; MCN1, modulatory commissural neuron 1; POCs, post-oesophageal commissure neurons; VCNs, ventral cardiac neurons. ***B,*** Schematic of the gastric mill circuit activated by the VCN- and POC pathways. As indicated, the top row of gastric mill neurons in the STG represent protractor (PRO) phase neurons while the second row represent retractor (RET) phase neurons. Bottom row shows the pyloric pacemaker neurons. The exact electrical coupling relationship among the protractor neurons is not known, so they are shown simply as being serially coupled. All STG circuit neurons occur as single copies per STG, except for GM (4) and PD (2). Symbols: downward arrows, activation of the system within the target box; upward arrow, synaptic feedback; filled circles, fast synaptic inhibition; resistor, non-rectifying electrical coupling; diode, rectifying electrical coupling. ***C,*** Gastric mill motor patterns triggered by brief stimulation of the VCN- and POC pathways and recorded extracellularly from nerve branches shown schematically in Panel *A*. No gastric mill rhythm was in progress before either pathway was stimulated, but the pyloric rhythm was ongoing (*pdn*, *mvn*: Control) and there was modest MCN1 activity (*ion*). In the Control and Post-VCN stimulation panels, which came from the same experiment, the lower *ion* recording is the same as the upper *ion* recording except that the large unit (an oesophageal rhythm motor neuron) was digitally subtracted to more explicitly show the MCN1 activity pattern (see Blitz and Nusbaum, 2008). Also, the gain was increased in the lower *ion* recording to increase the amplitude of the MCN1 spikes. This large unit was not active during the POC-rhythm. Note that the protraction phase burst pattern of MCN1 and LG (*lgn*) was tonic during the VCN-gastric mill rhythm

but was pyloric rhythm-timed (see *pdn*) during the POC-gastric mill rhythm. The CPN2 burst pattern during each rhythm is the same as the MCN1 pattern (not shown) (Beenhakker and Nusbaum, 2004; Blitz and Nusbaum, 2008). The POC- and VCN-gastric mill rhythms were recorded in separate preparations.

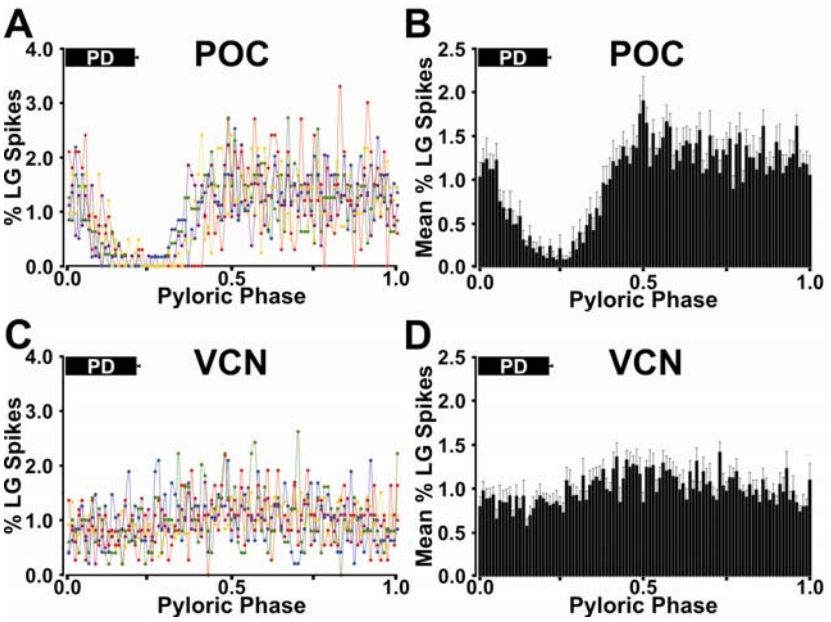

Figure 2. Quantitative analysis of the LG burst structure during the POC- and VCN-gastric mill rhythms relative to PD neuron activity. ***A,*** Mean percentage of LG spikes per bin across the normalized pyloric cycle during the POC-gastric mill rhythm, plotted separately for 5 different preparations, 10 LG bursts/preparation (see Methods). The mean fraction of the normalized cycle during which PD was active is shown by the PD bar at the top of the graph. Note the consistent drop in LG activity during and immediately after the PD burst. Each color represents a single experiment. ***B,*** Mean ± SE percentage of the total LG spikes across the normalized pyloric cycle for POC-gastric mill rhythms from 10 separate preparations, including the 5 experiments shown in Panel *A*. ***C,*** Mean percentage of LG spikes per bin across the normalized pyloric cycle during the VCN-gastric mill rhythm, plotted separately for 5 different preparations, 10 LG bursts/preparation. Note the consistent absence of a drop in LG activity during and after the PD burst. ***D,*** Mean ± SE percentage of LG spikes per bin across the normalized pyloric cycle from 10 separate VCN-gastric mill rhythms, including the 5 experiments shown in Panel *C*.

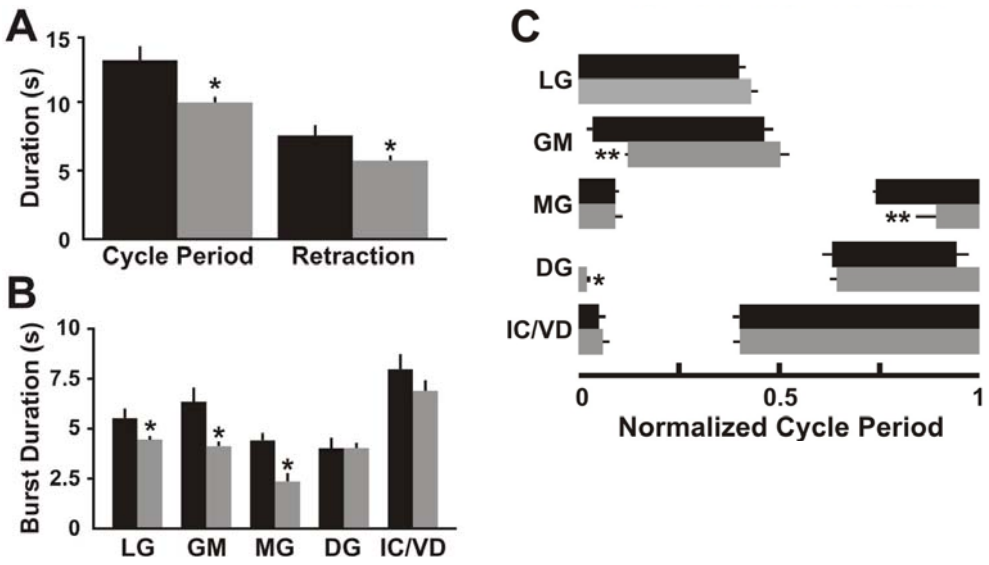

Figure 3. Comparison of POC- and VCN-gastric mill rhythm parameters. ***A,*** The POC-gastric mill cycle period and retraction duration are longer than those for the VCN-rhythm. ***B,*** The burst duration of the protractor neurons LG, GM and MG is longer during the POC-gastric mill rhythm. Note that the LG burst duration also represents the protraction duration. ***C,*** The burst onset phase of the GM and MG neurons occurs sooner in the normalized cycle during the POC-gastric mill rhythm, while the burst offset phase of the DG neuron occurs sooner during the VCN-rhythm. All panels: Black bars, POC-rhythm (n=10); Grey bars, VCN-rhythm (n=10); *p<0.05; **p<0.01.

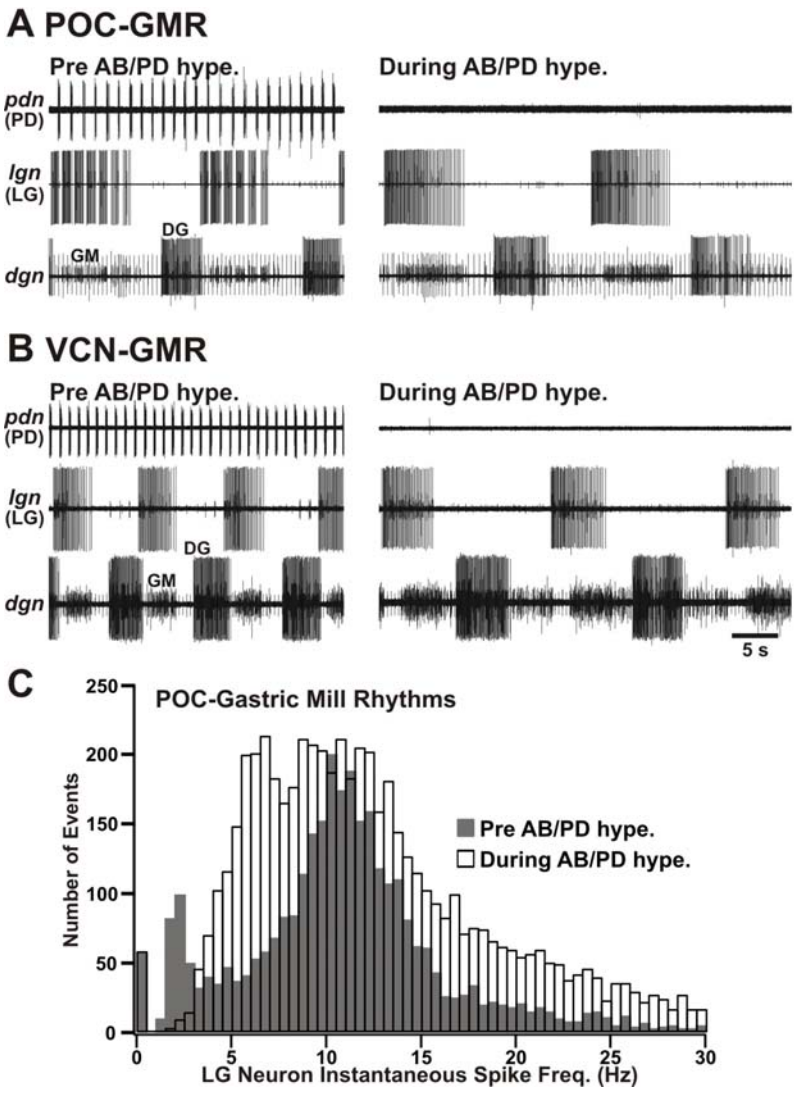

Figure 4. Suppressing the pyloric rhythm did not eliminate the POC- or VCN-gastric mill rhythm but did change the fast rhythmic LG burst pattern to a tonic pattern during the POC-rhythm. ***A,*** The POC-gastric mill rhythm persisted when the pyloric rhythm was suppressed by hyperpolarizing the pyloric pacemaker (AB/PD) neurons, but it slowed and the pyloric-timed LG burst pattern (Left) was changed to a tonic pattern (Right). ***B,*** The VCN-gastric mill rhythm persisted, albeit with a longer cycle period, when the pyloric rhythm was suppressed. Note that the LG burst pattern remained tonic in the absence of the pyloric rhythm. ***C,*** Comparison of the LG instantaneous spike frequency

distribution during the POC-gastric mill rhythm in the presence vs. absence of the pyloric rhythm. Note that suppressing the pyloric rhythm resulted in an approximately 9-fold decrease in the number of events between 1.5 – 3 Hz (PR on: 245 events; PR off: 27 events). This range included most (82%: 245 of 298) of the pyloric rhythm (PD neuron)-timed interruptions in the LG burst. The first bar (0 – 0.5 Hz) for each condition represents the retractor phase. Bin width is 0.5 Hz. Data are from 6 preparations (10 LG bursts per preparation for each condition).

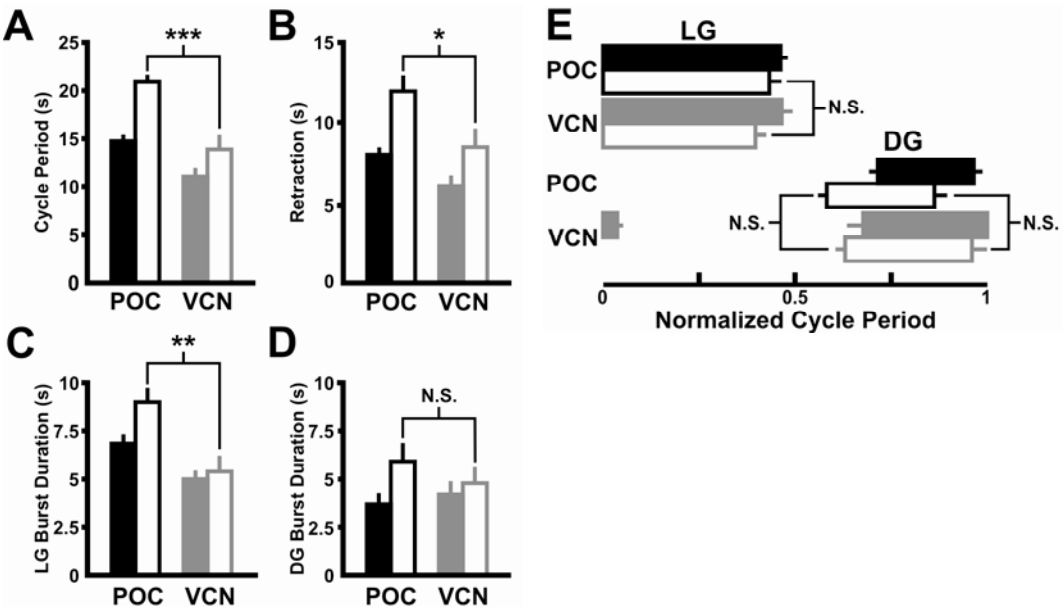

Figure 5. Suppressing the pyloric rhythm did not eliminate all of the differences between the POC- and VCN-gastric mill motor patterns. ***A,B:*** The POC- and VCN-gastric mill cycle period and retraction burst duration remained distinct when the pyloric rhythm was suppressed. ***C,D:*** The LG burst duration remained distinct, while the DG burst duration remained comparable, during the POC- and VCN-gastric mill rhythms when the pyloric rhythm was suppressed. ***E,*** The LG burst offset phase remained comparable, while that of the DG neuron became comparable during the POC- and VCN-gastric mill motor patterns when the pyloric rhythm was suppressed. All panels: POC-rhythm, n=6; VCN-rhythm, n=8. Symbols: Filled bars, pyloric rhythm active; Unfilled bars, pyloric rhythm suppressed; *p<0.05; **p<0.01; ***p<0.001; N.S., not significant (p>0.05).

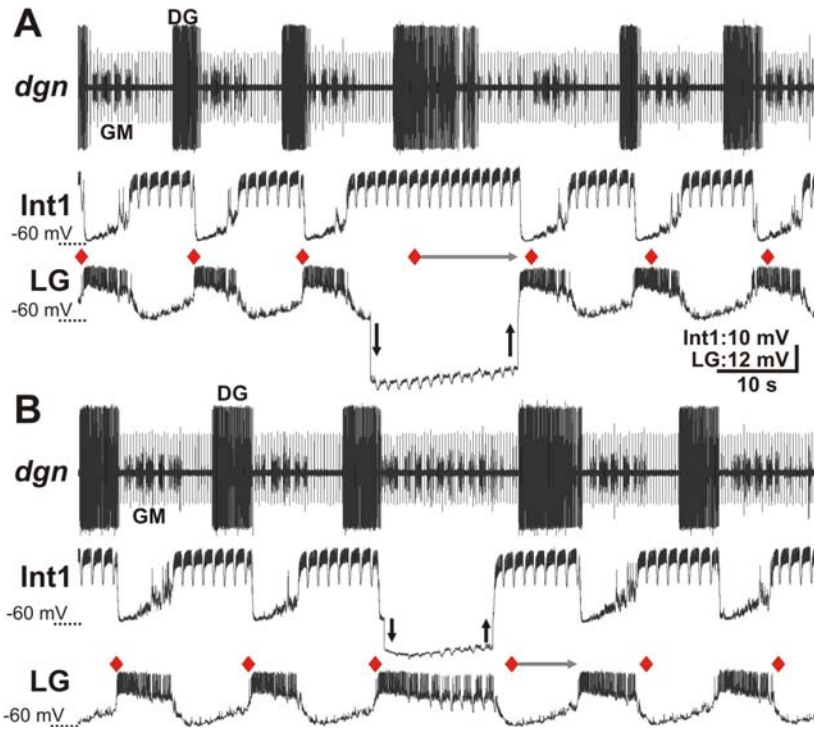

Figure 6. LG and Int1 are necessary for VCN-gastric mill rhythm generation. ***A,*** During a VCN-gastric mill rhythm, the LG neuron was hyperpolarized (arrows) for longer than its gastric mill rhythm-timed inhibition by Int1. Red diamonds indicate the expected LG burst onset, based on the 5 successive gastric mill cycles prior to the LG hyperpolarization. Note that, during the LG hyperpolarization, Int1 did not exhibit its anticipated, protractor phase-associated hyperpolarization starting at the red diamond, as should have occurred if the gastric mill rhythm was not influenced by suppressing LG activity. As indicated by the horizontal grey arrow, the next Int1 hyperpolarization, and associated LG burst, was delayed until after the LG hyperpolarization. Note also that the DG burst duration was prolonged, but not for the duration of the LG hyperpolarization. Downward and upward arrows indicate the start and end of hyperpolarizing current injection, respectively. ***B,*** During a VCN-gastric mill rhythm, suppressing Int1 activity by hyperpolarizing current injection (arrows) for longer than the duration of its inhibition by LG delayed the LG burst termination until after the period of hyperpolarization. Thus, the

next gastric mill cycle onset (i.e. LG burst onset: red triangle) after the start of Int1 hyperpolarization was delayed until well after the period of hyperpolarization (grey arrow). Both panels are from the same preparation.

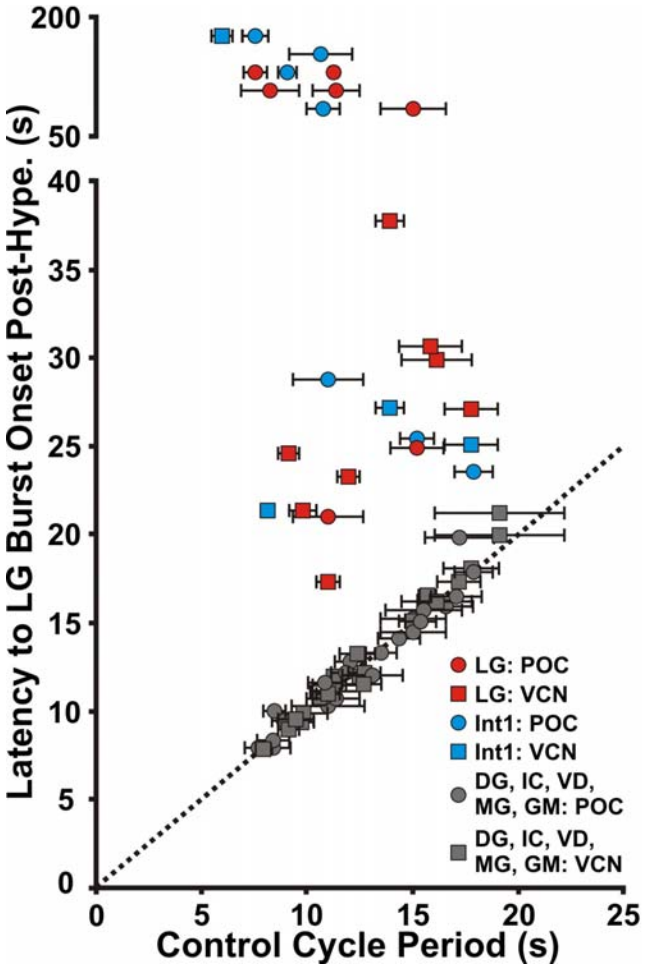

Figure 7. LG and Int1, but no other gastric mill circuit neuron, are necessary for POC- and VCN-gastric mill rhythm generation. Reversibly hyperpolarizing either LG or Int1 during the VCN- or POC-gastric mill rhythm consistently delayed the onset of the next gastric mill cycle until after the period of imposed hyperpolarization. In contrast, hyperpolarizing any of the other gastric mill neurons did not alter the gastric mill cycle period. Number of experiments per neuron: POC-gastric mill rhythm: LG, 6; Int1, 7; MG, 3; IC, 7; GM, 2; VD, 5; DG, 7; VCN-gastric mill rhythm: LG, 8; Int1, 5; MG, 3; IC, 4; GM, 3; VD: 3; DG, 6. For all neurons, the hyperpolarizing current injections ranged in duration from 10 s – 180 s. Dotted line: slope = 1. Data points on the dotted line indicate equivalent values on the x- and y-axis.

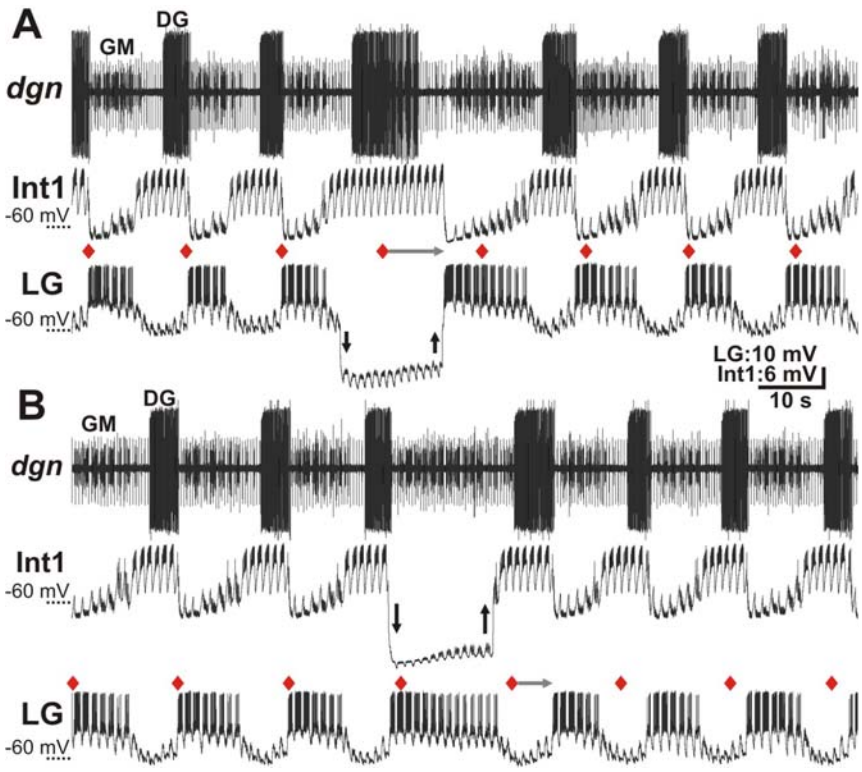

Figure 8. LG and Int1 are necessary for POC-gastric mill rhythm generation. ***A,*** During a POC-gastric mill rhythm, hyperpolarizing the LG neuron (arrows) for longer than the duration of its inhibition by Int1 delayed the start of the next episode of protraction-related Int1 hyperpolarization (i.e. start of the next gastric mill cycle) until after the current injection (grey arrow). Int1 remained active for the entire LG hyperpolarization, and the DG burst duration was also prolonged. The next expected gastric mill cycle onset (i.e. LG burst onset) after the start of hyperpolarizing current injection, in the absence of that current injection, is indicated by the red diamond. ***B,*** During a POC-gastric mill rhythm, suppressing Int1 activity by hyperpolarizing current injection (arrows) for longer than its inhibition by LG delayed the start of the next gastric mill cycle until after the period of current injection (grey arrow). The start of the next anticipated gastric mill cycle (i.e. LG burst onset) after the beginning of current injection into Int1 is indicated by the red diamond. Both panels are from the same preparation.

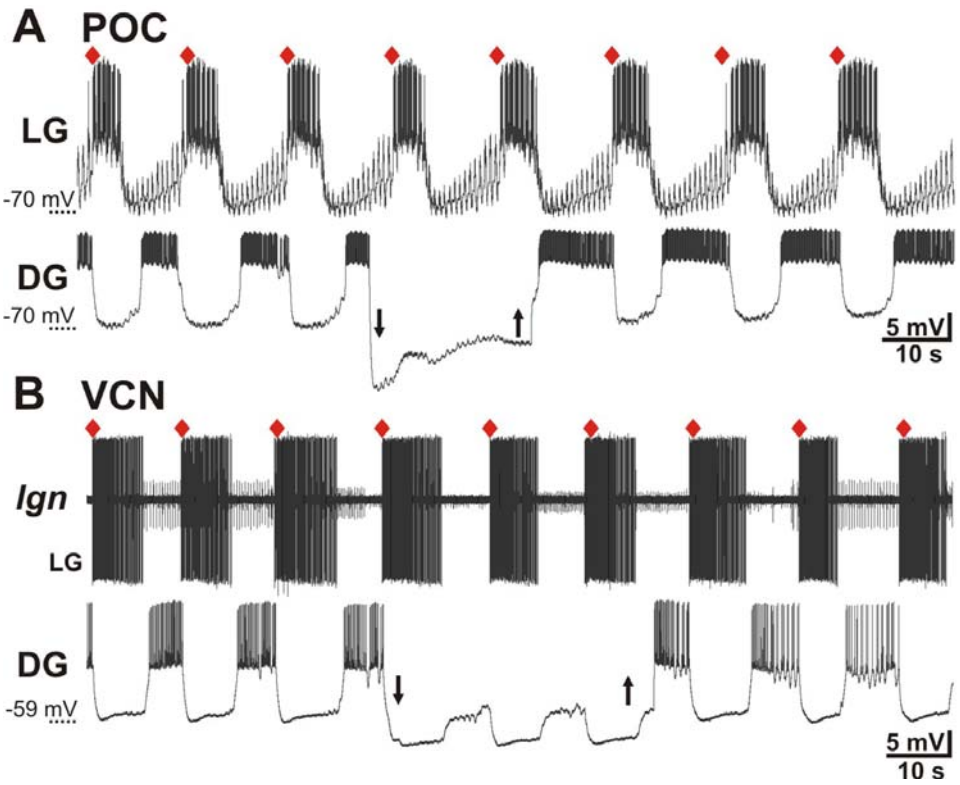

Figure 9. DG is not necessary for POC- or VCN-gastric mill rhythm generation. ***A,*** During a POC-gastric mill rhythm, DG was hyperpolarized (arrows) for a duration that was longer than its normal gastric mill interburst period, but doing so did not delay the next expected LG burst onset (red diamond). ***B,*** Suppressing DG activity with hyperpolarizing current injection (arrows) did not delay the next expected LG burst onset during a VCN-gastric mill rhythm. Panels A and B are from different preparations.

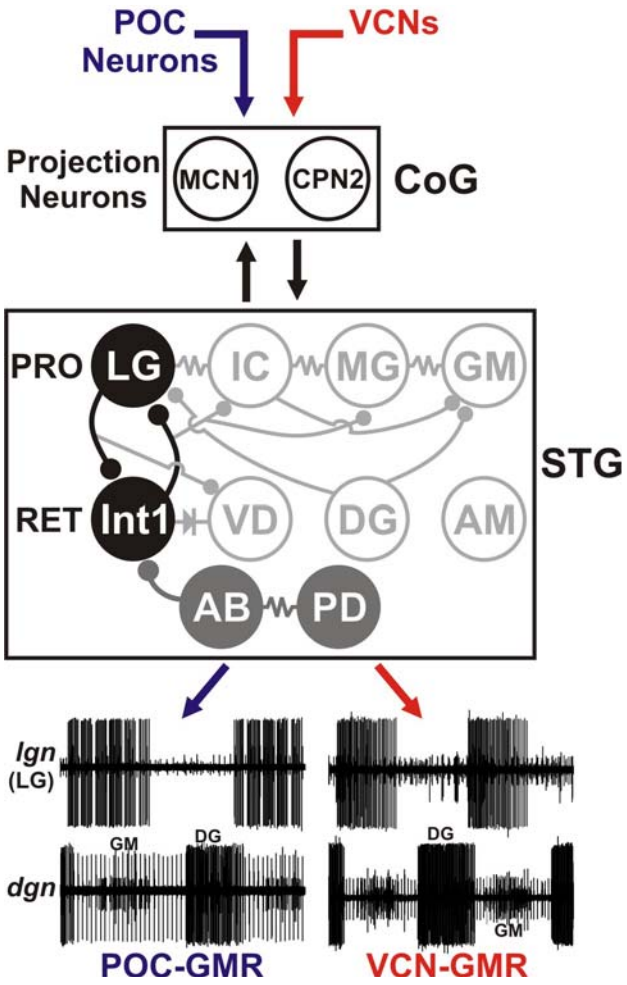

Figure 10. The gastric mill circuit neurons LG and Int1 form the core rhythm generator for the POC- and VCN-gastric mill rhythms. Two different extrinsic inputs, POC- and VCN neurons, trigger different gastric mill motor patterns by activating the same CoG projection neurons (MCN1, CPN2). LG and Int1 are the only gastric mill neurons necessary for generating the POC- and VCN-gastric mill rhythms. The pyloric pacemaker neurons (AB, PD), however, regulate the cycle period and pattern of both gastric mill rhythms. Hence, in parallel with their pivotal role in generating the pyloric rhythm, AB and PD are pattern generator neurons for these gastric mill rhythms. The POC- and VCN-gastric mill rhythms (GMRs) are represented by extracellular recordings of the LG (*lgn*) and GM (*dgn*, small units) protractor neurons firing their rhythmic bursts

in alternation with those of the DG retractor neuron (*dgn*, large unit). Note the fast rhythmic LG burst pattern during the POC-GMR and its tonic burst pattern during the VCN-GMR. The pyloric pacemaker neuron inhibition of other gastric mill neurons (VD, IC, MG) is omitted for clarity. Symbols: STG neurons- Black filled circles, core POC- and VCN-gastric mill rhythm generator neurons; grey filled circles, POC- and VCN-gastric mill pattern generator neurons; clear circles, gastric mill follower motor neurons. Synapse symbols as in Figure 1.

CHAPTER 4

Different Motor Neuron Patterns Drive Different Muscle Patterns During Distinct Gastric Mill Rhythms

Rachel S. White

Michael P. Nusbaum

Dept. of Neuroscience, University of Pennsylvania School of Medicine, 215 Stemmler Hall, Philadelphia, PA 19104.

Abstract: 259 Words

Introduction: 586 Words

Discussion: 988 Words

Running Title: Different motor neuron patterns drive different muscle patterns

Acknowledgments: We thank Dr. Dawn Blitz for informative discussions and Dr. Joshua Gold for assistance with statistical analysis. This research was supported by National Institute of Neurological Disease and Stroke Grants NS29436 and NS42813 (M.P.N.).

Keywords: Central pattern generator; stomatogastric; modulation; projection neuron; excitatory junction potentials; tension

ABSTRACT

Different inputs enable individual motor circuits to generate different motor patterns in the isolated CNS. These distinct patterns sometimes include altered motor neuron burst patterns, but whether these different burst patterns are retained by the associated neuromuscular system is not known in most systems. The possibility that muscles transform their motor neuron input pattern is particularly plausible in systems with slow contraction dynamics, which increases the likelihood of filtering across cycles. We are addressing this issue in the crab stomatogastric system by determining if slowly contracting muscles innervated by the lateral gastric (LG) protractor motor neuron retain the distinct LG activity patterns that occur during different versions of the biphasic (protraction, retraction) gastric mill (chewing) rhythm. These different rhythms are triggered by the post-oesophageal commissure (POC) neurons and the ventral cardiac neurons (VCNs). The LG neuron burst is tonic during the VCN-rhythm while its burst is separated into brief duration burstlets during the POC-rhythm. The LG burst and interburst durations are also longer during the POC-rhythm. Intracellular muscle fiber recordings and tension measurements of LG-innervated muscles indicate that, at both these levels, these muscles retain the distinct VCN- and POC-patterns. Additionally, although their excitatory junction potential amplitudes are comparable, the LG burst-generating muscle tension during the VCN-pattern is considerably larger than during the POC-pattern. This difference appears to result at least partly from the distinct LG burst patterns. Thus, different LG burst patterns occurring during distinct gastric mill rhythms in the isolated CNS are retained by the LG-innervated muscles, suggesting that they drive distinct chewing movements in the animal.

INTRODUCTION

Central pattern generators (CPGs) are multifunctional motor circuits that generate distinct rhythmic motor patterns in the isolated CNS when influenced by different inputs (Marder and Calabrese, 1996; Marder and Bucher, 2001; Selverston 2010). The cellular and synaptic mechanisms by which CPGs generate distinct outputs have been studied extensively (Kristan et al., 2005; Marder and Bucher, 2007; Buschges et al., 2008; Friedman et al., 2009; Sakurai and Katz, 2009; Kiehn, 2010; Selverston, 2010; Weaver et al., 2010). Thus far, less attention has focused on the extent to which different versions of a centrally generated motor pattern remain distinct at the level of the muscles that mediate the behavior (Thuma et al., 2003; Wenning et al., 2004; Neustadter et al., 2007). This issue is particularly relevant for systems in which muscle contractions are relatively slow and hence might not always maintain the rhythmic nature of their motor neuronal input pattern (Carrier, 1989; Morris and Hooper, 1997, 1998; Hooper and Weaver, 2000; Zhurov and Brezina, 2006). Thus far, it is clear in such systems that the motor patterns underlying different behaviors can drive different contraction patterns in the same muscles (Morris et al., 2000; Thuma et al., 2003; Kristan et al., 2005; Zhurov et al., 2005; Neustadter et al., 2007). Less information is available regarding the ability of such muscles to express the distinct, centrally-generated versions of the same motor pattern (Rosenbaum et al., 2010), particularly when there are considerable changes in motor neuron burst structure (Marder and Calabrese, 1996; Friedman et al., 2009).

We are examining the extent to which slowly contracting muscles retain the distinct motor neuron patterns that drive them during different versions of a rhythmic motor pattern in the crab stomatogastric nervous system (STNS). Specifically, we compare the response of muscles innervated by an identified motor neuron during the

distinct gastric mill (chewing) motor patterns triggered by two extrinsic inputs, the post-oesophageal commissure (POC) neurons and ventral cardiac neurons (VCNs) (White and Nusbaum, 2011). In the isolated STNS, stimulating either input triggers a long-lasting activation of two projection neurons, MCN1 (modulatory commissural neuron 1) and CPN2 (commissural projection neuron 2), in the paired commissural ganglia (CoGs) (Beenhakker et al., 2004; Beenhakker and Nusbaum, 2004; Blitz et al., 2008). These projection neurons activate the gastric mill CPG, which is located in the stomatogastric ganglion (STG). One distinction between the VCN- and POC-triggered gastric mill rhythms is the activity pattern of the protraction phase motor neuron LG (lateral gastric). During VCN-protraction, LG fires a tonic burst while during POC-protraction its burst is divided into a series of separate, brief duration burstlets.

Here, we kept the LG-innervated muscles connected with the otherwise isolated STNS to determine if the different LG neuron activity patterns during the VCN- and POC-gastric mill rhythms is maintained by the LG-innervated muscles. Using intracellular muscle fiber recordings, we establish that three LG-innervated muscles (gm5b, gm6ab, gm8a) exhibit VCN- and POC-specific activity patterns, although the peak excitatory junction potential (EJP) amplitude was comparable during both rhythms. Tension measurements from the gm6ab muscle indicate that the distinct VCN- and POC-patterns are also maintained during rhythmic contractions. Despite the shared peak EJP amplitude during the two patterns, there was a larger tension increase during the VCN-pattern, presumably due at least partly to the associated LG burst pattern. Our data indicate that different gastric mill CPG-generated motor patterns remain distinct at the level of the gastric mill muscles, supporting the hypothesis that these distinct centrally generated rhythms drive different versions of the resulting behavior in the intact animal.

MATERIALS AND METHODS

Animals. Male Jonah crabs (*C. borealis*) were obtained from commercial suppliers (Commercial Lobster and Seafood, Boston, MA; Marine Biological Laboratory, Woods Hole, MA) and were maintained in aerated artificial seawater at 10-12° C. Animals were cold anesthetized by packing them in ice for at least 30 min before dissection. The foregut was then removed from the animal, and the dissection of the STNS from the foregut was performed in physiological saline at ~4°C.

Solutions. C. borealis physiological saline contained the following (in mM): 440 NaCl, 26 $MgCl_2$, 13 $CaCl_2$, 11 KCl, 10 Trisma base, 5 maleic acid, pH 7.4 -7.6, 5 dextrose. All preparations were superfused continuously with *C. borealis* saline (8-12°C).

Electrophysiology. Electrophysiology experiments were performed by using standard techniques for this system (Weimann et al., 1991; Beenhakker et al., 2004). The STNS, with the LG-driven muscles still innervated (Fig. 1A,B), was pinned down in a silicone elastomer-lined (Sylgard 184, KR Anderson, Santa Clara, CA) Petri dish. All other motor nerve branches were bisected, preventing the motor neurons from regulating their muscle targets. The only exception was the gm8b muscle, which is innervated by the medial gastric (MG) motor neuron in addition to the LG neuron (Weimann et al., 1991).

Extracellular recordings were made by isolating a region of nerve with petroleum jelly and pressing one of a pair of stainless steel wire electrodes into the Sylgard within the well, with the second electrode pressed into the Sylgard in the electrically-grounded main bath compartment. Extracellular nerve stimulation was accomplished by placing the pair of wires used to record nerve activity into a stimulus isolation unit (Model SIU5: Astromed/Grass Instruments, West Warwick, RI) that was connected to a stimulator

(Model S88: Astromed/Grass Instruments).

Intrasomatic recordings were made with microelectrodes (15-30 MΩ) filled with 0.6M K_2SO_4 plus 10mM KCl. Intracellular recordings from muscle fibers were made with microelectrodes (10-15MΩ) filled 0.6M K_2SO_4 plus 10mM KCl. To facilitate intracellular recording, we viewed the desheathed ganglia with light transmitted through a dark-field condenser (Nikon, Tokyo, Japan). Intracellular signals were amplified using Axoclamp 2B amplifiers (Molecular Devices, Sunnyvale, CA) and digitized at ~5 kHz using a Micro 1401 data acquisition interface and Spike2 software (Cambridge Electronic Design, Cambridge, England). Current injections were performed in single-electrode discontinuous current-clamp (DCC) mode with sampling rates between 2 and 3 kHz. STG neurons were identified on the basis of their axonal projections, activity patterns, and interactions with other STG neurons (Weimann et al., 1991; Beenhakker and Nusbaum, 2004; Blitz and Nusbaum, 1997).

To stimulate the POC neurons, each half of the bisected *poc* nerve was surrounded by a Vaseline well. The POC axons in the *poc* nerve were stimulated using a tonic stimulation pattern (frequency: 15 – 30 Hz; duration: 15 – 30 s) (Blitz et al., 2008). Threshold for extracellular activation of the POC neurons was determined by monitoring the activity of the projection neuron MCN1 in the ipsilateral *ion* nerve (Fig. 1A). The POC neurons cause a long-lasting activation of MCN1 (Blitz et al., 2008). In this paper, *poc* stimulations were either uni- or bilateral. The ventral cardiac neurons (VCNs) were activated by stimulating the dorsal posterior oesophageal nerve (*dpon*) (Fig. 1A). The *dpon* stimulations were done using a rhythmic pattern (burst duration: 6 s, interburst freq.: 0.06 Hz, intraburst freq.: 15 Hz) (Beenhakker et al., 2004). However, previous work showed that this rhythmic pattern had the same influence on the gastric mill circuit as did stimulation patterns that were either tonic or time-locked to the pyloric

rhythm (Beenhakker et al., 2004). To avoid cross-pathway influences, we elicited POC- and VCN-gastric mill rhythms in different preparations. Specifically, when one pathway was stimulated after the other in the same preparation, a hybrid gastric mill motor pattern was often triggered which exhibited, to varying degrees, features of both types of rhythms (data not shown).

Muscles were identified based on their attachment points and relationship to identified motor nerves (Hooper et al., 1986; Weimann et al., 1991). To minimize movement artifacts and prematurely lost recordings due to muscle contractions, intracellular muscle fiber recordings were obtained by removing the tissue covering a portion of the muscle near one of its attachment points. In some experiments, the LG-innervated muscles were isolated from the STNS ganglia by bisecting the lateral ventricular nerves (*lvns*: see Fig. 1), and the LG neuron was stimulated via the *lvn* or lateral gastric nerve (*lgn*), using a standardized POC-like or VCN-like gastric mill rhythm LG pattern. The stimulus patterns were as follows: POC-like: burst duration: 5.1s, stimulus frequency: 10Hz, interburst duration: 8s; VCN-like: burst duration: 4.8s, stimulus frequency: 10Hz, interburst duration: 5.7.

Muscle tension recordings were done using an isometric transducer (Harvard Apparatus, Holliston, MA) and isolating the portion of the stomach that contains the LG-innervated muscles. The gm6ab muscle was secured with pins at its anterior insertion site, without damaging the muscle. The muscle was then stretched vertically to its original length and attached to the recording device. The *lvn* or *lgn* was stimulated in the same pattern as above and force measurements were recorded and stored on computer using the SPIKE2 data acquisition and analysis system (Cambridge Electronic Design, Cambridge, UK).

Data analysis. Data were collected in parallel on chart recorder (Everest model: Astro-Med, West Warwick, RI) and computer, via SPIKE2, with a sampling rate of 5 kHz. Some data analyses, including neuron burst duration, number of action potentials per burst, intraburst firing frequency, duty cycle and neuron phase relationships were conducted on the digitized data with a custom-written SPIKE2 program called "The Crab Analyzer" (freely available at http://www.uni-ulm.de/~wstein/spike2/index.html). Data were plotted with Excel (version 2002, Microsoft, Redmond, WA). Final figures were produced using CorelDraw (version 13.0 for Windows).

Unless otherwise stated, each data point in a data set was derived by determining the mean for the analyzed parameter from 10 consecutive gastric mill cycles during the steady-state region of the motor pattern, starting ~30 s – 60 s after gastric mill rhythm onset. One gastric mill cycle is defined as extending from the onset of consecutive LG neuron action potential bursts (Beenhakker and Nusbaum, 2004; Wood et al., 2004). The protractor phase was measured as the LG burst duration, while the retractor phase was measured as the LG interburst duration. Instantaneous EJP frequency, determined for 10 consecutive steady-state bursts during each gastric mill rhythm, was defined as 1 divided by the inter-EJP interval.

We determined the relationship of the EJP burst pattern in gm6ab to the pyloric rhythm during the POC-gastric mill rhythm by determining the EJP distribution during each normalized pyloric cycle. The pyloric cycle period (~1 s) is ~10-fold shorter than the gastric mill cycle period (~10 s), so there are several pyloric cycles per gastric mill protractor phase (Blitz et al., 2008). The LG neuron, which provides the EJPs to gm6ab, is active during the protractor phase (Heinzel et al., 1993). We used the activity of the projection neuron MCN1 as the monitor of the pyloric rhythm, because MCN1 activity is explicitly pyloric-timed during the POC-gastric mill rhythm (Blitz et al., 2008). Each

normalized pyloric cycle extended from the start of a MCN1 burst to the start of the next MCN1 burst. Specifically, for 10 consecutive gastric mill rhythm-timed gm6ab EJP bursts per experiment, we separated the gm6ab recording during each normalized pyloric cycle into 50 equal bins (1 bin = 2% normalized pyloric cycle) and determined the fraction of the EJPs during each pyloric cycle that occurred in each bin (Bucher et al., 2006).

We also determined the amount of decay that occurred after each EJP during VCN- and POC-gastric mill rhythms and during standardized versions of these motor patterns in nerve-muscle preparations (see above). During each protraction phase, each EJP decay from its peak membrane potential was normalized to the maximum possible decay amplitude during that phase. The maximum possible decay amplitude was defined as the peak membrane potential of the largest amplitude EJP minus the baseline resting potential. The last EJP of each burst was omitted in this analysis.

Statistical analyses were performed with Microsoft Excel (Microsoft), SigmaStat 3.0 (SPSS) and MatLab (Mathworks, Natick, MA). Comparisons were made to determine statistical significance using primarily the paired Student's *t*-test. To determine whether the distribution of EJP instantaneous frequencies and EJP decay amplitudes during the POC- and VCN-gastric mill rhythms, or during their standardized equivalents in nerve-muscle experiments, were likely to correspond to a single population distribution, we compared them using the Two-sample Kolmogorov-Smirnov goodness-of-fit hypothesis test (K-S Test). As an internal control for each comparison of distributions (i.e. POC- vs. VCN-patterns), we divided each group in half and used the K-S Test to determine whether each population was likely to represent a single distribution. In all experiments, the effect of each manipulation was reversible, and there was no significant difference between the pre-manipulation and post-manipulation groups. Data

are expressed as the mean ± standard error (SE).

RESULTS

LG-innervated muscle fibers exhibit distinct EJP patterns during the VCN- and POC-gastric mill rhythms

The VCN- and POC-triggered gastric mill motor patterns are distinct with respect to the activity of several motor neurons (White and Nusbaum, 2011). Among these motor neurons, the protractor LG neuron exhibits the most distinct pattern during these two rhythms. Specifically, LG exhibits a tonic burst pattern during VCN-protraction while its POC-protraction burst pattern is divided into relatively short duration, pyloric rhythm-timed burstlets (Fig. 1C) (Beenhakker and Nusbaum, 2004; Blitz et al., 2008; White and Nusbaum, 2011). The LG neuron burst- and interburst durations are also longer during the POC-gastric mill rhythm, while its intraburst firing frequency is similar during both rhythms, although as indicated above its POC-related activity is separated by pyloric-timed silent periods (Fig. 1C) (White and Nusbaum, 2011). Therefore, to assess whether these distinct LG patterns that occur in the isolated STNS underlie distinct muscle patterns, and hence likely underlie distinct chewing movements, we studied the electrophysiological and tension responses of LG-innervated muscles during the VCN- and POC-gastric mill rhythms.

Intracellular recordings from individual muscle fibers in gm5b (n=8 fibers, 8 crabs), gm6ab (n=8 fibers, 8 crabs) and gm8a (n=4 fibers, 4 crabs) resulted in a comparable value of ~-70 mV for the resting potential (POC-preps: gm5b, -73.2 ± 1.9 mV; gm6ab, -69.3 ± 1.4 mV; gm8a, -68.0 ± 1.1 mV; VCN-preps: gm5b, -72.3 ± 1.0 mV; gm6ab, -69.6 ± 1.4 mV; gm8a, -68.8 ± 1.9 mV). These values were comparable to previous recordings from these fibers (Stein et al., 2006). Action potentials were rarely generated in these fibers, as is typical for STNS muscles (Hooper et al., 1986; Weimann et al., 1991; Stein et al., 2006).

For each muscle type, the EJP pattern matched the LG neuron pattern during both gastric mill rhythms. Specifically, the EJP pattern in each muscle type was tonic during the VCN-gastric mill rhythm while it was pyloric rhythm-timed during the POC-gastric mill rhythm (Fig. 2). Across preparations, the distribution of instantaneous EJP rates was distinct during these two gastric mill rhythms (K-S Test, $p=1.7 \times 10^{-29}$) (Fig. 3A). The within group comparisons indicated that the distribution of EJP rates for each rhythm likely represents a single, albeit separate population (K-S Test: POC-rhythm, p=0.35; VCN-rhythm, p=0.48). One clearly distinct region of these distributions occurred between 2 – 5 Hz. Within this range, there were 273 instantaneous EJP frequencies that occurred during the POC-rhythm but only 25 during the VCN-rhythm, despite the fact that overall there were more total events analyzed during the VCN-rhythm (POC: 2225 events, n=6; VCN: 2427 events, n=6).

The 2 – 5 Hz range represents the range of pyloric rhythm-timed interruptions in LG activity during the POC-gastric mill rhythm (White and Nusbaum, 2011). To determine whether the distinct instantaneous EJP distribution in this range that occurred during the POC-gastric mill rhythm likely resulted from the pyloric-timed interruptions in LG activity, we determined the distribution of the LG-mediated EJPs in the LG-innervated muscles relative to the pyloric rhythm. We monitored the pyloric rhythm via extracellular recording of the projection neuron MCN1 in the *ion* nerve, because the extracellular recordings that directly monitor pyloric motor neuron activity were unavailable as the peripheral nerves were not dissected from the posterior region of the foregut in these preparations (Fig. 1A) (Coleman and Nusbaum, 1994). During the POC-gastric mill rhythm, MCN1 maintains a pyloric rhythm-timed activity pattern that is comparable to that exhibited by LG (Blitz et al., 2008). Specifically, during this motor pattern the MCN1 activity is inhibited during each burst in the pyloric pacemaker neurons (AB, PD) (Wood

et al., 2004; Blitz et al., 2008). LG shows the same pyloric-timed pattern largely because it is driven by input from MCN1 (Wood et al., 2000; White and Nusbaum, 2011). As shown from the cumulative data in Figure 3B, there was a steady number of LG-mediated EJPs during most of each pyloric-timed MCN1 burst, but this number dropped soon after the end of the MCN1 active period and did not increase again until after MCN1 activity resumed. Thus, the LG-mediated EJPs did indeed exhibit a pyloric-timed activity pattern during the POC-gastric mill rhythm. We did not perform the comparable analysis during the VCN-gastric mill rhythm because there is no pyloric timing within the LG burst during this motor pattern (White and Nusbaum, 2011).

The fact that the LG-mediated EJP patterns during each LG burst were distinct during the POC- and VCN-gastric mill rhythms suggested that they exhibited different degrees of summation during each burst (Fig. 4*A*,*B*). To assess the within-burst summation, we determined the extent to which each EJP amplitude decayed towards the baseline resting potential after its peak during each gastric mill rhythm (see Methods). As indicated above, the resting potential across fibers for the different gastric mill rhythms were equivalent. The presence of a skewed distribution during one of these rhythms such that there were more large amplitude EJP decays would support the hypothesis that this population exhibited less summation across each burst. Comparing the distribution of EJP decays between the two gastric mill rhythms indicated that they were quite likely to represent different populations (K-S Test, $p=2.9 \times 10^{-36}$, n=6 fibers for each rhythm) (Fig. 4*C*). As for the instantaneous EJP rates reported above, the within group comparisons indicated that the distribution of EJP decays for each rhythm represented a single, albeit different distribution (K-S Test: POC: p=0.95; VCN: p=0.84). Focusing on the section of the distribution containing the largest amplitude decays (0.6 – 1.0), in which 1.0 represents the decline of the largest amplitude EJP in a burst back to

the baseline resting potential, there were more than twice as many large amplitude declines during the POC-rhythm (VCN: 328; POC: 761, n=6 each). This was the case despite the fact that there were more total events analyzed during the VCN-rhythm (VCN: 3597 events; POC: 3185 events). This result supports the hypothesis that more within-burst summation occurred during the VCN-gastric mill rhythm. The presence of increased EJP summation could contribute to increased tension generated during those bursts (see below).

LG-innervated muscle fiber responses remain distinct during standardized VCN- and POC-like stimulations

As a prelude to determining whether LG-innervated muscles retain distinct VCN- and POC-patterns during tension generation in nerve-muscle preparations, we generated standardized VCN- and POC-like gastric mill rhythm stimulation protocols. These protocols were based on LG burst parameters determined previously during these gastric mill rhythms (White and Nusbaum, 2011). These patterns were the same with respect to intraburst stimulation rate (10 Hz), slightly different for burst duration (VCN: 4.8 s; POC: 5.1 s), and more different for the interburst duration (VCN: 5.7 s; POC: 8 s). Additionally, unlike the actual rhythms, we used a constant inter-stimulus interval (100 ms) during the intraburst 10 Hz stimulations. Lastly, because we used direct nerve stimulations to drive LG activity, we elicited these distinct rhythmic patterns in the same experiments.

The resulting VCN- and POC-like EJP patterns reflected the comparable patterns during the actual gastric mill rhythms. Specifically, using gm6ab muscle fibers, rhythmic stimulation with the VCN-like pattern elicited tonic EJP bursts, while using the POC-like pattern elicited EJP bursts with regular, pyloric-like interruptions (n=5) (Fig. 5). I

obtained the same results with intracellular recordings from gm5b, gm8a and gm8b muscle fibers (data not shown). There was a small but significant difference between the peak EJP amplitude during each stimulated pattern (VCN: 25 ± 2 mV; POC: 23.9 ± 2.1 mV, n=5, p=0.02). As was the case in the actual gastric mill rhythms, there was a consistent difference in the distribution of EJP decays during the two artificial rhythms (K-S Test, $p=6.8 \times 10^{-42}$) (Fig. 6). During both rhythms there was a predominant peak of EJP decays between 0.4 – 0.6 in each fiber assayed (Fig. 6B). In contrast, there were consistently considerably more large amplitude decays (0.6 – 1.0) during the POC-like rhythm (VCN-like: 17; POC-like: 284) (Fig. 6A, B). This was the case despite the larger number of sampled events during the VCN-like stimulations (VCN-like: 2772; POC-like: 2106). The large amplitude decays during the POC-like stimulations resulted primarily from the pyloric-like interruptions during each stimulated burst. As for the natural rhythms, the larger number of large amplitude decays during the POC-like rhythm suggested that there was less within-burst summation occurring during this pattern.

LG-innervated muscle tension patterns are distinct during VCN- and POC-like gastric mill rhythm stimulation patterns

We obtained tension measurements using the isolated, LG-innervated gm6ab muscle and the above-indicated VCN- and POC-like stimulation protocols in nerve-muscle preparations. As was the case for the EJP recordings, the within-burst tension pattern followed the stimulation pattern. Specifically, each gm6ab muscle generated smooth, rhythmic increases and decreases in tension during the VCN-like stimulations while its rhythmic tension increases were divided into short-duration, pyloric-like episodes during the POC-like stimulation (n=9) (Fig. 7A,B). Thus far, however, most of these preparations were compromised by movement artifacts and/or a slowly but

continually changing baseline (drop in tension) that prevented our using them for a quantitative analysis of peak tension amplitude. The data from 2 experiments, however, support the hypothesis that the gm6ab muscle generates a considerably larger peak tension during the VCN-like stimulation pattern (Fig. 7A-D). This distinction was not entirely a consequence of the difference in the interburst interval, which is shorter during the VCN-like pattern, because the amplitude of the first burst in a train was already larger for the VCN-like stimulation pattern (Fig. 7B). The shorter interburst interval could enable the preceding burst(s) to enhance the amplitude of each subsequent burst, a process called augmentation (Stein et al., 2006). There did appear to be some contribution from the distinct interburst durations, because the initial contraction slope prior to the first pyloric-timed interruption was the same for the first burst in each train during the VCN- and POC-like rhythms, whereas this slope was steeper during the VCN-like rhythm for subsequent bursts in the train (Fig. 7B,C).

DISCUSSION

In this Chapter we show that the distinct neuronal patterns that occur in an identified motor neuron during two different versions of a rhythmic motor pattern in the isolated crab STNS are maintained as distinct patterns in the associated muscle. Specifically, the tonic vs. pyloric-timed burst patterns exhibited by the LG neuron during the VCN- and POC-gastric mill rhythms also occurred in LG-innervated muscle at the level of both EJPs and tension. A previous study of the LG-innervated muscle gm6ab during gastric mill rhythms that had the same LG burst pattern (tonic), but differed in the LG burst and interburst durations and intraburst firing rate, showed that the EJP and tension response in this muscle is also sensitive to changes in these parameters (Stein et al., 2006).

Previous studies have established that muscles can generate contraction patterns that do not accurately mimic their neuronal input pattern. This is best established for muscles with slow contraction dynamics, and that are regulated by EJPs instead of action potentials (Hooper and Weaver, 2000; Morris et al., 2000; Thuma et al., 2003; Zhurov et al., 2005; Hooper et al., 2007). Such muscles tend to exhibit considerable summation and/or facilitation across motor neuron bursts, which can minimize their ability to generate discrete contractions in response to a relatively fast rhythmic input. One particularly clear example comes from a lobster muscle innervated by the pyloric dilator (PD) motor neuron, whose contraction dynamics are sufficiently slow that it maintains a relatively constant level of tension in response to its rhythmic motor neuron input (Morris et al., 2000). Less information is available regarding the ability of a muscle, particularly slowly contracting ones, to generate distinct within-burst patterns during different versions of the same behavior or different behaviors, although changes in burst amplitude and duration clearly occur under these conditions (Morris et

al., 2000; Thuma et al., 2003; Zhurov et al., 2005; Zhurov and Brezina, 2006). A recent example of a muscle generating a distinct burst pattern was documented during forward and backward insect walking (Rosenbaum et al., 2010).

There is an extensive literature establishing the ability of individual CPGs to generate many distinct motor patterns, largely due to changes in the intrinsic and synaptic properties of the CPG neurons and in the subset of active neurons during each motor pattern (Marder and Calabrese, 1996; Marder and Bucher, 2001; Marder et al., 2005; Dickinson, 2006; Doi and Ramirez, 2008). Most of these studies, however, were performed in the isolated CNS, leaving as an implication that the different patterns generated by a CPG do drive different muscle patterns and hence different versions of the behavior. Insofar as the most detailed of such studies have been performed in invertebrate motor systems with slowly contracting muscles, this implication might not necessary be valid. The ability of the LG-innervated muscles to follow the distinct LG burst patterns during the VCN- and POC-gastric mill rhythms provides one of the first examples that such patterns are retained at the muscle level, despite the slow dynamics of the muscles.

Our data supporting the presence of less EJP summation during the POC-gastric mill rhythm than the VCN-rhythm suggests that there would be a smaller build-up of intracellular Ca^{2+} in the muscle fibers during the POC-rhythm. One consequence of this distinction would be the build-up of less tension during the POC-rhythm, as we observed during our tension measurements. However, whether there truly is less build-up of intracellular Ca^{2+} in the LG-innervated muscle fibers during the POC-rhythm than the VCN-rhythm is not yet known. Future voltage-clamp and/or Ca^{2+}-imaging studies will resolve this issue. One clear contributor to the larger amplitude tension level in the LG-muscles during the VCN-rhythm was the pattern difference relative to the POC-rhythm.

As is evident in Figure 7A-C, during each pyloric-timed interruption in the LG burst during the POC-rhythm there was considerable tension decay. The shorter LG interburst interval during the VCN-rhythm may also contribute to its larger tension response, as suggested by comparing the first burst in each train to the subsequent bursts (Fig. 7B,C).

The fact that the LG-innervated muscles generate different patterns during these two gastric mill rhythms is not sufficient to conclude that they cause distinct movements during chewing. This cautionary note results from the fact that the muscles in this system only indirectly move the teeth (Turrigiano and Heinzel, 1992). In between the muscles and teeth are ossicles (cartilaginous support structures), and the quantitative relationship between muscle contraction and tooth movement remains to be determined in this system. For example, the LG-innervated muscles attach to two ossicles (Fig. 1B). When these muscles contract, they change the position of the attached ossicles which in turn cause the lateral teeth to pivot and move towards the midline (protract). Nonetheless, there is support for these distinct gm6ab tension patterns contributing to different chewing movements from previous work combining endoscopic video monitoring of tooth movements with recordings of gastric mill neuron activity (Heinzel, 1988a,b; Heinzel et al., 1993). These studies have shown that the lateral teeth, which are controlled by LG neuron activity, can make both smooth, large amplitude movements and briefer, smaller amplitude pyloric-timed movements.

In conclusion, the gastric mill CPG can generate different versions of the gastric mill rhythm in the isolated STNS when different extrinsic inputs are stimulated (Beenhakker et al., 2004; Blitz et al., 2008; White and Nusbaum, 2011). Here, we assessed the ability of one gastric mill neuromuscular system to retain these distinct activity patterns, thereby starting the process of determining if these distinct CNS

rhythms are effectively conveyed to the muscles and thereby generate distinct versions of the resulting behavior. At both the EJP and tension levels, the LG-innervated muscles did generate both VCN-like and POC-like patterns, despite the fact that the gastric mill muscles have slow contraction dynamics. These results are among the first to show that distinct, biologically-relevant burst patterns in a single motor neuron can drive different contraction patterns in the associated muscles.

REFERENCES

Beenhakker MP, Nusbaum MP (2004) Mechanosensory activation of a motor circuit by coactivation of two projection neurons. J Neurosci 24:6741-6750.

Beenhakker MP, Blitz DM, Nusbaum MP (2004) Long-lasting activation of rhythmic neuronal activity by a novel mechanosensory system in the crustacean stomatogastric nervous system. J Neurophysiol 91:78-91.

Blitz DM, Nusbaum MP (1997) Motor pattern selection via inhibition of parallel pathways. J Neurosci 17:4965-4975.

Blitz DM, White RS, Saideman SR, Cook A, Christie AE, Nadim F, Nusbaum MP (2008) A newly identified extrinsic input triggers a distinct gastric mill rhythm via activation of modulatory projection neurons. J Exp Biol. 211:1000-1011.

Bucher D, Taylor AL, Marder E (2006) Central pattern generating neurons simultaneously express fast and slow rhythmic activities in the stomatogastric ganglion. J Neurophysiol 95:3617-3632.

Buschges A, Akay T, Gabriel JP, Schmidt J (2008) Organizing network action for locomotion: insights from studying insect walking. Brain Res Rev 57:162-171.

Carrier (1989) Ventilatory action of the hypaxial muscles of the lizard *Iguana iguana*: a function of slow muscle. J Exp Biol. 143:435-457.

Coleman MJ, Nusbaum MP (1994) Functional consequences of compartmentalization of synaptic input. J Neurosci 14:6544-6552.

Dickinson PS (2006) Neuromodulation of central pattern generators in invertebrates and vertebrates. Curr Opin Neurobiol 16:604-614.

Doi A, Ramirez JM (2008) Neuromodulation and the orchestration of the respiratory rhythm. Respir Physiol Neurobiol 164:96-104.

Friedman AK, Zhurov Y, Ludwar BCh, Weiss KR (2009) Motor outputs in a multitasking

network: relative contributions of inputs and experience dependent network states. J Neurophysiol 102:3711–3727.

Heinzel HG, Weimann JM, Marder E (1993) The behavioral repertoire of the gastric mill in the crab, *Cancer pagurus*: an in situ endoscopic and electrophysiological examination. J Neurosci 13:1793-1803.

Heinzel HG (1988) Gastric mill activity in the lobster. I. Spontaneous modes of chewing. J Neurophysiol 59:528-550.

Heinzel HG (1988) Gastric mill activity in the lobster. II. Proctolin and octopamine initiate and modulate chewing. J Neurophysiol 59:551-565.

Hooper SL, Guschlbauer C, von Uckermann G, Büschges A. (2007) Different motor neuron spike patterns produce contractions with very similar rises in graded slow muscles. J Neurophysiol 97:1428-1444.

Hooper SL, O'Neil MB, Wagner R, Ewer J, Golowasch J, Marder E (1986) The innervation of the pyloric region of the crab, *Cancer borealis*: homologous muscles in decapod species are differently innervated. J Comp Physiol 159:227-240.

Hooper SL, Weaver AL (2000) Motor neuron activity is often insufficient to predict motor response. Curr Opin Neurobiol 10:676-682.

Kiehn O (2010) Development and functional organization of spinal locomotor circuits. Current Opin Neurobiol 21:1-10.

Kristan WB Jr, Calabrese RL, Friesen WO (2005) Neuronal control of leech behavior. Prog Neurobiol 76:279-327.

Marder E, Bucher D (2001) Central pattern generators and the control of rhythmic movements. Curr Biol 11: R986-R996.

Marder E, Bucher D (2007) Understanding circuit dynamics using the stomatogastric nervous system of lobsters and crabs. Annu Rev Physiol 69:291-316.

Marder E, Calabrese RL (1996) Principles of rhythmic motor pattern generation. Physiol Rev 76:687-717.

Marder E, Bucher D, Schulz DJ, Taylor AL (2005) Invertebrate central pattern generation moves along. Curr Biol 15:R685-R699.

Morris LG, Hooper SL (1997) Muscle response to changing neuronal input in the lobster (*Panulirus interruptus*) stomatogastric system: spike number- versus spike frequency-dependent domains. J Neurosci 17:5956-5971.

Morris LG, Hooper SL (1998) Muscle response to changing neuronal input in the lobster (*Panulirus interruptus*) stomatogastric system: slow muscle properties can transform rhythmic input into tonic output. J Neurosci 18:3433-3442.

Morris LG, Thuma JB, Hooper SL (2000) Muscles express motor pattern of non-innervating neural networks by filtering broad-band input. Nat Neurosci 3:245-250.

Neustadter DM, Herman RL, Drushel RF, Chestek DW, Chiel HJ (2007) The kinematics of multifunctionality: comparisons of biting and swallowing in *Aplysia californica*. J Exp Biol 210:238-260.

Rosenbaum P, Wosnitza A, Büschges A, Gruhn M (2010) Activity patterns and timing of muscle activity in the forward walking and backward walking stick insect *Carausius morosus*. J Neurophysiol 104:1681-1695.

Sakurai A, Katz PS (2009) State-, timing-, and pattern-dependent neuromodulation of synaptic strength by a serotonergic interneuron.J Neurosci 29:268-279.

Selverston AI (2010) Invertebrate central pattern generator circuits. Philos Trans R Soc Lond B 365:2329-2345.

Stein W, Smarandache CR, Nickmann M, Hedrich UBS (2006) Functional consequences of activity-dependent synaptic enhancement at a crustacean neuromuscular junction. J Exp Biol 209:1285-1300.

Thuma JB, Morris LG, Weaver AL, Hooper SL (2003) Lobster (*Panulirus interruptus*) pyloric muscles express the motor patterns of three neural networks, only one of which innervates the muscles. J Neurosci 23:8911-8920.

Turrigiano GG, Heinzel H.-G. (1992) Behavioral correlates of stomatogastric network function. In: Dynamic Biological Networks, The Stomatogastric Nervous System (Harris-Warrick RM, Marder E, Selverston AI, Moulins M, eds), pp. 197-220, MIT Press: Cambridge, MA.

Weimann JM, Meyrand P, Marder E (1991) Neurons that form multiple pattern generators: identification and multiple activity patterns of gastric/pyloric neurons in the crab stomatogastric system. J Neurophysiol 65:111-122.

Wenning A, Cymbalyuk GS, Calabrese RL (2004) Heartbeat control in leeches. I. Constriction pattern and neural modulation of blood pressure in intact animals. J Neurophysiol 91:382-396.

Weaver AL, Roffman RC, Norris BJ, Calabrese RL (2010) A role for compromise: synaptic inhibition and electrical coupling interact to control phasing in the leech heartbeat CPG. Front Behav Neurosci 4:38.

White RS, Nusbaum MP (2011) The same core rhythm generator underlies different motor patterns. Submitted.

Wood DE, Manor Y, Nadim F, Nusbaum MP (2004) Intercircuit control via rhythmic regulation of projection neuron activity. J Neurosci 24:7455-7463.

Wood DE, Stein W, Nusbaum MP (2000) Projection neurons with shared cotransmitters elicit different motor patterns from the same neural circuit. J Neurosci 20:8943-8953.

Zhurov Y, Brezina V (2006) Variability of motor neuron spike timing maintains and shapes contractions of the accessory radula closer muscle of *Aplysia*. J Neurosci 26:7056-7070.

Zhurov Y, Proekt A, Weiss KR, Brezina V (2005) Changes of internal state are expressed in coherent shifts of neuromuscular activity in *Aplysia* feeding behavior. J Neurosci 25:1268-1280.

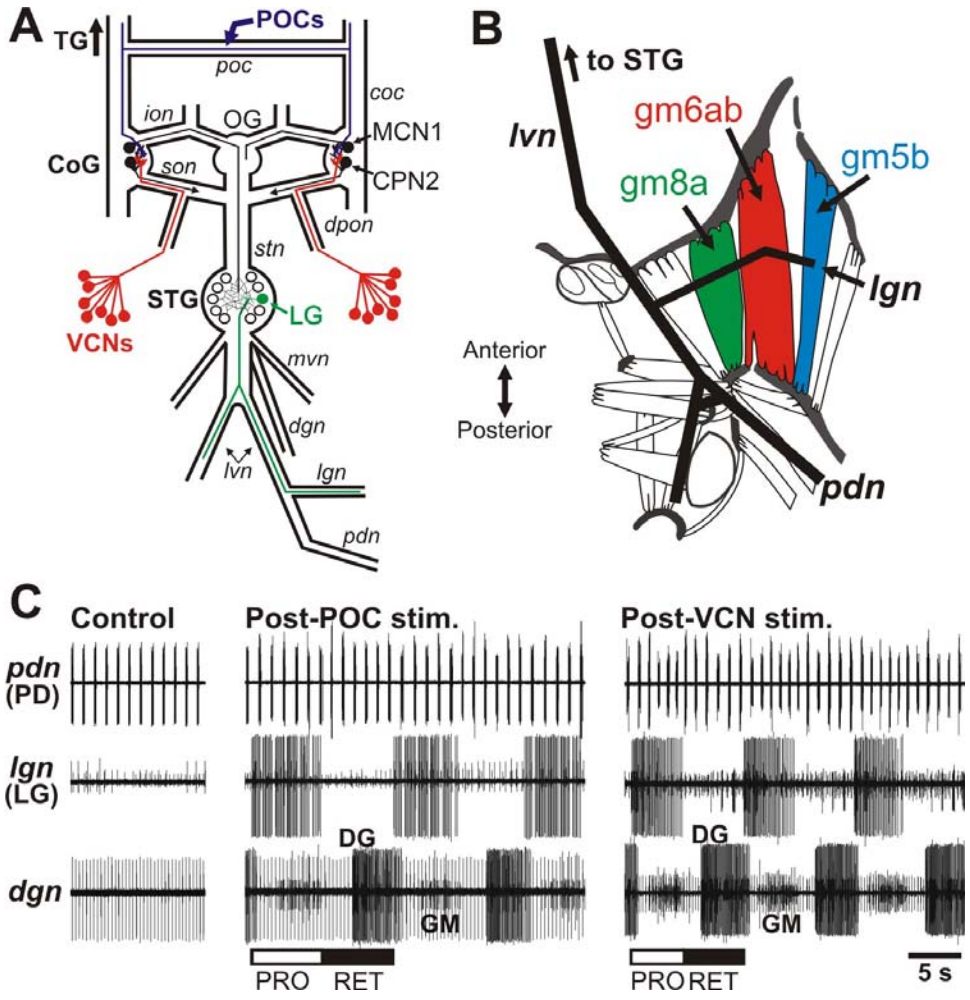

Figure 1. The protraction phase LG neuron generates different activity patterns during the POC- and VCN-triggered gastric mill rhythm. A. Schematic of the isolated STNS, including its four ganglia plus the connecting and peripheral nerves. The VCNs project into the CoGs from the cardiac sac stomach compartment via the *dpon* and *son* nerves. The POC neurons project into the CoGs via the *coc* and *poc* nerves. Abbreviations: Ganglia- CoG, commissural ganglion; OG, oesophageal ganglion; STG, stomatogastric ganglion; TG, thoracic ganglion. Neuron- LG, lateral gastric. Nerves- *coc*, circumoesophageal connective; *dgn*, dorsal gastric nerve; *dpon*, dorsal posterior oesophageal nerve; *lgn*, lateral gastric nerve; *lvn*, lateral ventricular nerve; *ion*, inferior oesophageal nerve; *mvn*, medial ventricular nerve; *pdn*, pyloric dilator nerve; *poc*, post-

oesophageal commissure; *son*, superior oesophageal nerve; *stn*, stomatogastric nerve. **B.** Schematic dorsal view (right half) of the posterior region of a dissected *C. borealis* foregut (modified from Weimann et al., 1991). LG innervates several protractor muscles, including gm8a, gm6ab and gm5b, via the *lvn* and *lgn* nerves. **C.** Gastric mill motor patterns triggered by brief stimulation of the POC- and VCN pathways and recorded extracellularly from nerves shown schematically in Panel *A*. No gastric mill rhythm was in progress before either pathway was stimulated, but the pyloric rhythm was ongoing (*pdn*: Control). Note that the LG neuron burst pattern was pyloric rhythm-timed (see *pdn*) during the POC-gastric mill rhythm but was tonic during the VCN-gastric mill rhythm. The POC- and VCN-gastric mill rhythms were recorded in separate preparations. The control recording shown was from the POC preparation. PRO, protraction phase; RET, retraction phase.

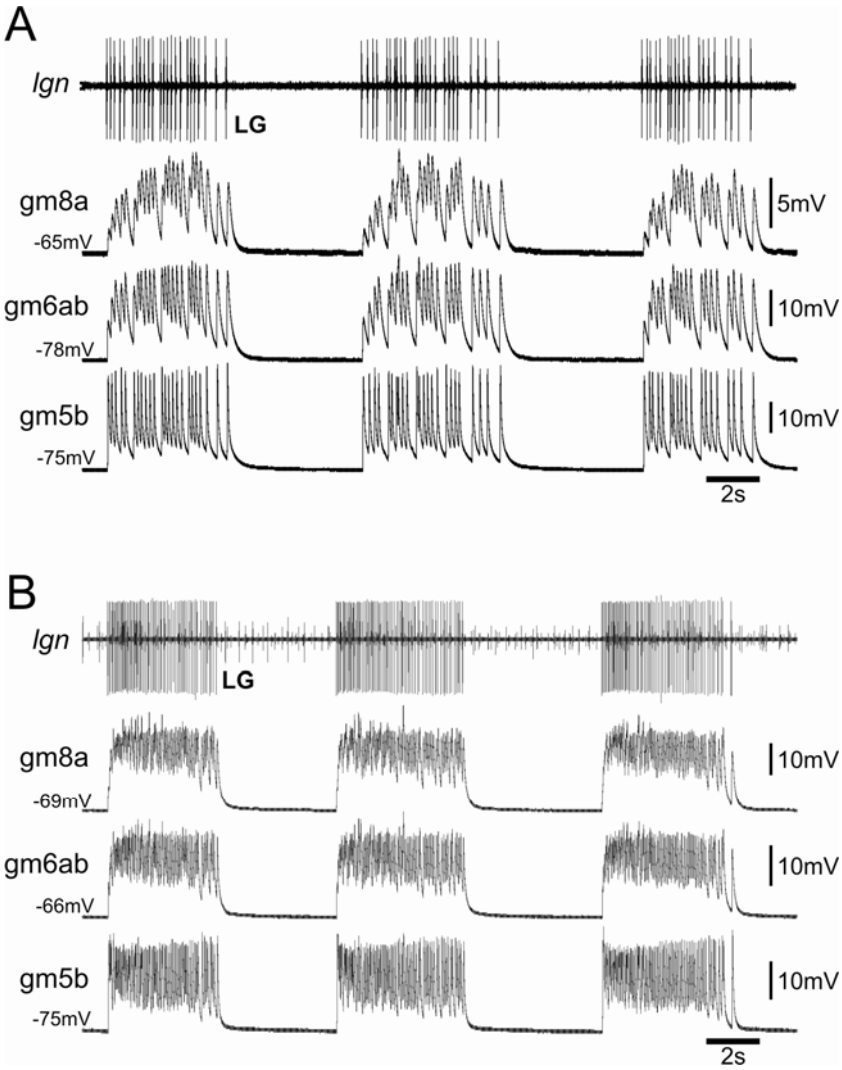

Figure 2. LG innervated muscles replicate the distinct LG patterns during the POC- and VCN-gastric mill rhythms. A. Intracellular muscle fiber recordings from three LG-innervated muscles (gm8a, gm6ab, gm5b) show that these fibers exhibit the same pyloric-timed burst pattern as their innervating motor neuron during the POC-triggered gastric mill rhythm. Note that the EJP decay immediately preceding each pyloric interruption is larger than the others within the same burstlet. LG activity is recorded extracellularly (*lgn*). **B.** Fibers from the same LG-innervated muscles also mimic the activity pattern during a VCN-triggered gastric mill rhythm. Panels A and B are from different preparations.

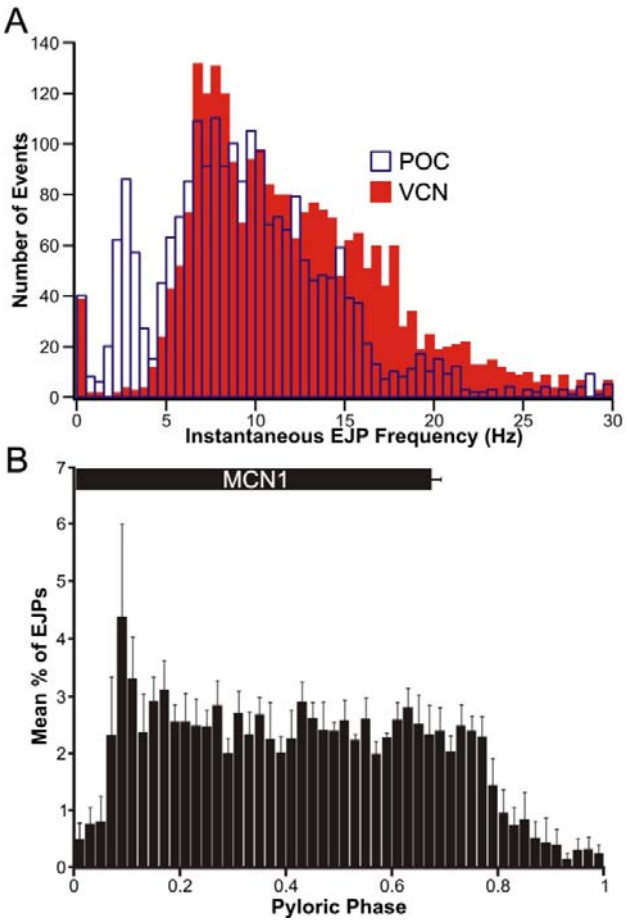

Figure 3. Quantitative analysis of the gm6ab EJP burst structure during the POC- and VCN-gastric mill rhythms. A. Distribution of instantaneous EJP frequencies during the POC- (2,225 events, n=6) and VCN-gastric mill rhythms (2,427 events, n=6). These distributions are highly likely to derive from separate populations (K-S Test: $p=1.7 \times 10^{-29}$). Note the distinct EJP distributions between 2-5 Hz (POC: 273 events; VCN: 25 events). This region represents the pyloric-timed interruptions in LG activity. The bin width is 0.5 Hz. **B.** Mean fraction of LG-mediated EJPs per bin during the normalized pyloric cycle across POC-gastric mill rhythms (n=6). The pyloric phase is normalized to the start of the MCN1 burst. The bin width is 2%.

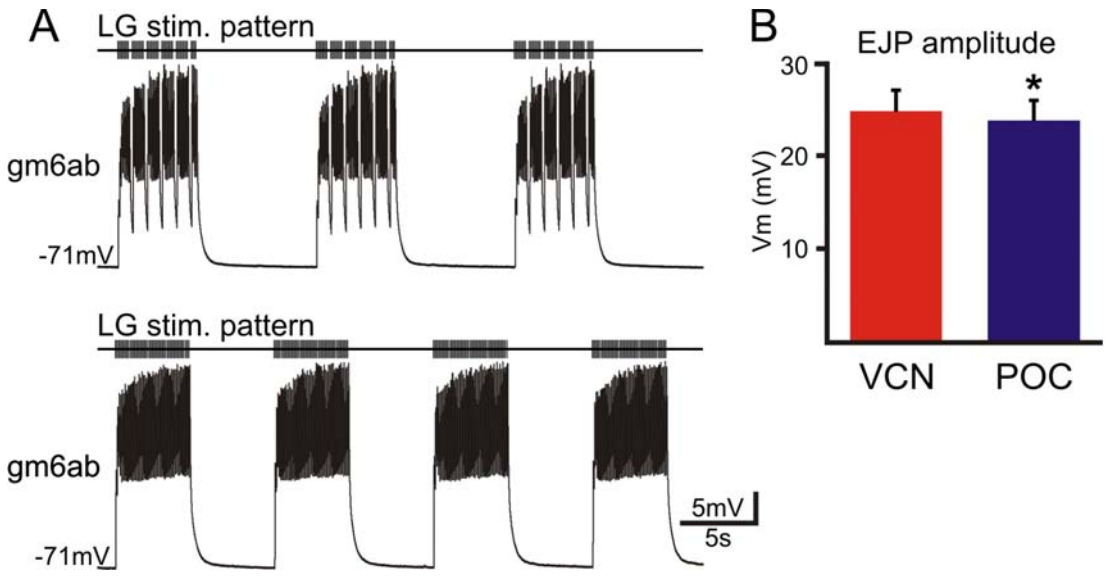

Figure 4. Distribution of the EJP decay amplitudes in the LG-innervated gm6ab muscle during the POC- and VCN-gastric mill rhythms. A, B: Expanded timescale of one EJP burst in gm6ab during a (A) POC- and (B) VCN-triggered gastric mill rhythm. Highlighted under each burst is an approximation of the underlying summation. **C**. The normalized EJP decay amplitude distribution in gm6ab muscle fibers during the POC- and VCN-gastric mill rhythms was likely to be derived from distinct populations (K-S Test, $p=2.9 \times 10^{-36}$; POC: 3,185 events; VCN: 3,597 events). Note in particular the large number of large amplitude EJP decays (0.6-1.0) during the POC-rhythm (761 events) relative to the VCN-rhythm (328 events). The bin width was 0.02. EJP decays in each burst were normalized to the distance between the largest EJP and the baseline resting potential.

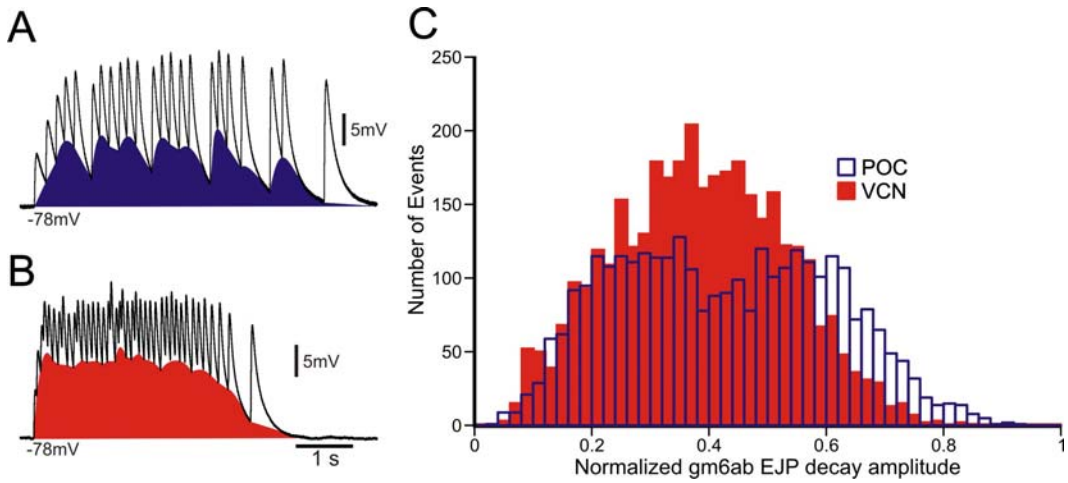

Figure 5. EJP activity pattern of gm6ab reflects its neuronal input pattern in isolated nerve-muscle preparations. A. This LG-innervated muscle fiber (gm6ab) exhibited (top) POC-like and (bottom) VCN-like EJP patterns in response to extracellular LG (*lvn*) stimulation in an isolated nerve-muscle preparation (see Methods for stimulation pattern details). **B.** The maximal EJP amplitude in gm6ab was larger during the VCN-rhythm (*$p<0.05$, $n=5$). The statistical analysis was performed on the actual mean values, not on the normalized version presented in the bar graph.

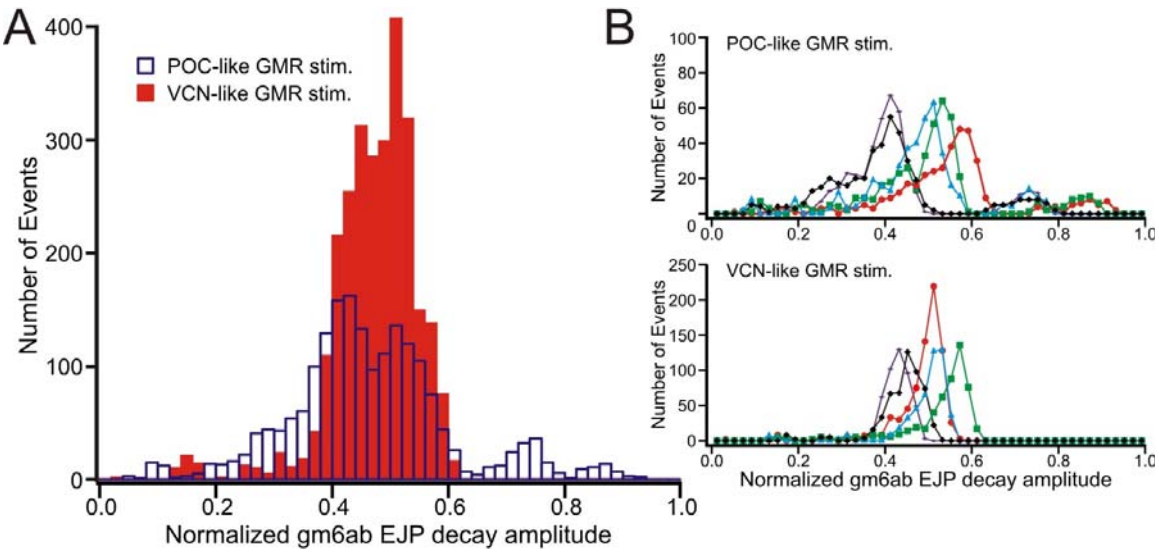

Figure 6. The distribution of gm6ab EJP decay amplitudes is distinct during POC-like and VCN-like LG stimulation patterns in nerve-muscle preparations. A. The distribution of normalized EJP decays during the POC-like and VCN-like gastric mill patterns from experiments such as the one in Figure 5A. These distributions were likely to derive from separate populations (K-S Test: 6.8 X 10^{-42}, n=5). The relatively narrow distributions relative to the comparable data during the actual rhythms (Fig. 4) results from using a fixed inter-stimulus interval during these standardized stimulations. Note the larger number of large amplitude (≥0.6) EJP decays during the POC-like stimulations (POC: 284 events; VCN: 17 events). Each EJP decay was normalized as in Figure 4. The bin width is 0.02. **B.** The distribution of each individual experiment from Panel A is plotted separately for the POC-like (top) and VCN-like (bottom) stimulation patterns. Note that the y-axis scale is larger in the top plot, to make evident the presence of large amplitude events (≥0.6) during these patterns. The bin width is 0.02.

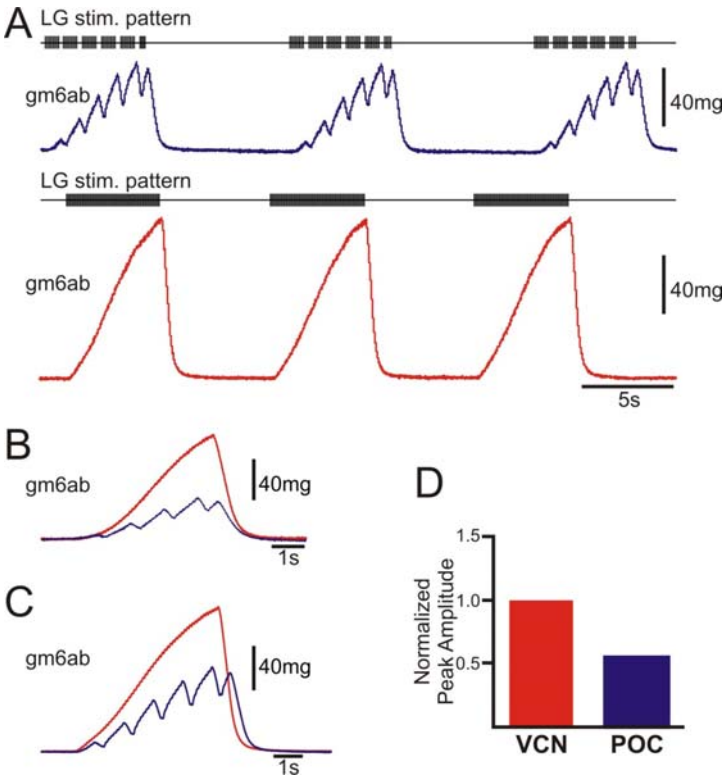

Figure 7. The LG-innervated gm6ab muscle tension pattern mimics its motor neuronal input pattern during POC- and VCN-like stimulations. A. During extracellular LG (*lvn*) stimulation in isolated nerve-muscle preparations, the LG-innervated gm6ab muscle generated rhythmic, increased tension patterns that reflected the POC-like (blue) or VCN-like (red) stimulation pattern of the LG neuron. Note also the larger amplitude peak tension generated in each burst during the VCN-pattern. Both recordings are from the same experiment. **B.** The first stimulated burst is shown from the same experiment as Panel A (blue: POC-like pattern; red: VCN-like pattern). Note that the pattern and peak amplitude differences are already present. **C.** The average of 10 successive bursts is shown from the same experiment as Panel A. **D.** The normalized peak tension amplitude was larger during the VCN-like stimulation pattern (n=2).

CHAPTER 5

State-dependent Proprioceptor Feedback During Different Gastric Mill Rhythms

Rachel S. White

Michael P. Nusbaum

Dept. of Neuroscience, University of Pennsylvania School of Medicine, 215 Stemmler Hall, Philadelphia, PA 19104.

ABSTRACT

Sensorimotor integration occurs at the level of the motor circuit and/or its projection neuron inputs. However, whether the same sensory feedback has the same or distinct action on different motor patterns generated by the same motor circuit remains to be determined in most systems. Here we are studying how an identified proprioceptor, the gastro-pyloric receptor (GPR) neuron, influences two separate versions of the gastric mill (chewing) rhythm in the isolated crab stomatogastric nervous system (STNS). These distinct rhythms are triggered by stimulating either the POC or VCN pathway. Each pathway triggers a long-lasting but distinct gastric mill rhythm by activating thesame projection neurons, MCN1 and CPN2, in the commissural ganglion (CoG). In the absence of the gastric mill rhythm, GPR stimulation excites MCN1 and CPN2 in the CoGs. These actions, however, are gated-out during the VCN-triggered gastric mill rhythm. To determine if sensory feedback to projection neurons is gated-out in a state-dependent manner, we examined the GPR influence on the POC-gastric mill rhythm. During the POC-gastric mill rhythm, GPR stimulation prolonged the retractor phase of the rhythm as it does during the VCN-gastric mill rhythm. Additionally, however, GPR prolonged the protractor phase and changed the burst structure of the gastric mill neuron LG. Lastly, based largely on indirect monitors of projection neuron activity, it appears that GPR stimulation does excite MCN1 and CPN2 during the POC-gastric mill rhythm. These data support the hypothesis that proprioceptor feedback is regulated in a state-dependent manner.

INTRODUCTION

Rhythmically active motor circuits (central pattern generators, CPGs) can generate stereotyped versions of their in vivo activity patterns in the isolated CNS (Marder and Calabrese, 1996; Marder and Bucher, 2001). In vivo, however, these circuits are continually regulated by sensory feedback (Rossignol et al., 2006; Blitz and Nusbaum, 2007**,** 2011). Additionally, the influence of an individual sensory feedback pathway can change under different behavior conditions (Rossignol et al., 2006; Blitz and Nusbaum, 2007, 2011). Thus far, most such studies of state-dependent sensory feedback have focused on sensory feedback to CPG neurons and motor neurons. Less information is available regarding state-dependent sensory feedback to the projection neurons that regulate CPG activity (Barriere et al., 2008).

We are determining if there is state-dependent sensory feedback to identified projection neurons in the biphasic (protraction, retraction) gastric mill (chewing) motor system within the crab stomatogastric nervous system (STNS). The gastric mill CPG, located in the stomatogastric ganglion (STG), is driven by activity in the commissural ganglion (CoG) projection neurons modulatory commissural neuron 1 (MCN1) and commissural projection neuron 2 (CPN2) (Beenhakker and Nusbaum, 2004; Blitz et al., 2004, 2008). This system is regulated by feedback from the gastropyloric receptor (GPR) neuron, a muscle stretch-sensitive proprioceptor (Katz and Harris-Warrick, 1991; Beenhakker et al., 2005, 2007; DeLong et al., 2009).

GPR has synaptic actions on the gastric mill CPG neurons in the STG and the projection neurons MCN1 and CPN2 in the CoG. It also inhibits the axon terminals of MCN1 in the STG ($MCN1_{STG}$). When there is no ongoing gastric mill rhythm, GPR stimulation can drive this rhythm by activating MCN1 and CPN2 (Blitz et al., 2004). During the ventral cardiac neuron (VCN)-triggered gastric mill rhythm, GPR stimulation

slows the rhythm by selectively prolonging the retractor phase (Beenhakker et al., 2005, 2007; DeLong et al., 2009). This latter action results from the GPR actions in the CoG being gated-out by recent VCN stimulation, while its actions in the STG persist (Beenhakker et al., 2007). Under these conditions, the selective prolongation of the retractor phase results from the GPR inhibition of $MCN1_{STG}$.

In this study, we assessed the influence of GPR on the gastric mill rhythm triggered by stimulating the post-oesophageal commissure (POC) pathway. The POC-triggered gastric mill rhythm is distinct from the VCN-rhythm (White and Nusbaum, 2011). During this rhythm, GPR stimulation prolonged both phases of the gastric mill rhythm, and it altered the POC-specific burst pattern of the lateral gastric (LG) motor neuron to a VCN-like burst pattern. Based largely on changes in the activity of post-synaptic targets of MCN1 and CPN2, GPR stimulation during the POC-rhythm appeared to excite these projection neurons, in contrast to its ineffectiveness during the VCN-gastric mill rhythm. Thus, proprioceptor feedback onto projection neurons likely can be regulated in a state-dependent manner.

MATERIALS AND METHODS

Animals. Male Jonah crabs (*Cancer borealis*) were obtained from commercial suppliers (Yankee Lobster; Marine Biological Laboratory) and maintained in aerated, filtered artificial seawater at 10 – 12°C. Animals were cold anesthetized by packing in ice for at least 30 min before dissection. The foregut was removed from the animal, and the dissection of the STNS from the foregut was performed in physiological saline at ~4°C.

Solutions. C. borealis physiological saline contained the following (in mM): 440 NaCl, 26 $MgCl_2$, 13 $CaCl_2$, 11 KCl, 10 Trisma base, 5 maleic acid, 5 glucose, pH 7.4 – 7.6. All preparations were superfused continuously with *C. borealis* saline (8-12°C).

Electrophysiology. Electrophysiology experiments were performed by using standard techniques for this system (Beenhakker and Nusbaum, 2004). The isolated STNS (Fig. 1*A*) was pinned down in a silicone elastomer-lined (Sylgard 184, KR Anderson) Petri dish. Each extracellular nerve recording was made using a pair of stainless steel wire electrodes (reference and recording) whose ends were pressed into the Sylgard-coated dish. A differential AC amplifier (Model 1700: AM Systems) amplified the voltage difference between the reference wire, placed in the bath, and the recording wire, placed near an individual nerve and isolated from the bath by petroleum jelly (Vaseline, Lab Safety Supply). This signal was then further amplified and filtered (Model 410 Amplifier: Brownlee Precision). ,Extracellular nerve stimulation was accomplished by placing the pair of wires used to record nerve activity into a stimulus isolation unit (SIU 5: Astromed/Grass Instruments) that was connected to a stimulator (Model S88: Astromed/Grass Instruments).

Stimulation of the POC neurons was performed by extracellular stimulation of the post-

oesophageal commissure (*poc*) (Fig. 1), using a tonic stimulation pattern (duration: 15 – 30 s, intraburst frequency: 15 – 30 Hz) (Blitz et al. 2008). In all experiments, the *poc* was bisected and each half was surrounded by a petroleum jelly well to stimulate them separately. However, the left and right *pocs* were stimulated simultaneously in all experiments. Because GPR is activated when protraction muscles are stretched by contraction of the retraction muscles with which they share an attachment point, during the gastric mill rhythm we stimulated GPR rhythmically and manually during the retraction phase DG burst. The effect of the stimulation was determined by analyzing the burst duration and firing frequency of the protraction phase neurons LG and GM, as well as the cycle period, before, during and after GPR stimulation. In each experiment, GPR was stimulated during 5 successive cycles.

Data acquisition and analysis. Data were acquired in parallel onto a chart recorder (MT-95000; Astromed) and by digitizing (~5 KHz) and storing the data on computer with data acquisition software (Spike2:Cambridge Electronic Design). Digitized data were analyzed using a custom-written Spike2 program called "The Crab Analyzer" (freely available at http://www.uni-ulm.de/~wstein/spike2/index.html).

The burst duration of a neuron was defined as the duration between the first and last action potential in a burst wherein no single interspike interval was larger than 2 sec. This duration is twice the average duration of the pyloric rhythm, which regulates the burst pattern of some gastric mill neurons, and shorter than the average gastric mill interburst duration (Blitz et al., 2008). The gastric mill cycle period was defined as extending from the onset of two consecutive LG bursts. Firing frequency was determined by dividing the total number of spikes in a burst minus one by the burst duration. Statistical analyses were performed with Microsoft Excel (Microsoft) and

SigmaStat 3.0 (SPSS). Comparisons were made to determine statistical significance using the paired Student's *t*-test and the repeated measures analysis of variance (RM-ANOVA). Data are presented as the mean ± standard error (SE).

RESULTS

GPR stimulation alters the POC-triggered gastric mill rhythm

There are two, bilaterally symmetric GPRs, which arborize on the gastric mill protractor muscles gm8b and gm9a (Katz et al., 1989). The gastric mill protractor motor neurons LG and MG innervate these muscles (Weimann et al., 1991). Each GPR can be selectively stimulated via an extracellular electrode associated with the appropriate motor nerve (gm8b: *lgn* or *mgn*; gm9a, *gpn*). The GPRs project centrally to influence CPG neurons in the STG and projection neurons in each CoG (Fig. 1A).

The GPRs are activated by stretch of the protractor muscles on which their dendrites arborize (Katz et al., 1989). During the gastric mill rhythm, the protractor muscles are stretched during the retractor phase (Heinzel et al., 1993). Hence, during gastric mill rhythms in the isolated STNS, we stimulated GPR during each retraction phase (Beenhakker et al., 2005, 2007). However, stimulating GPR during the protractor phase has no effect on the gastric mill rhythm and as a result, tonic GPR stimulation is equivalent to retraction phase stimulation of GPR (DeLong et al., 2009).

Within the STG, GPR excites the gastric mill CPG neuron interneuron 1 (Int1), inhibits the CPG neuron LG and presynaptically inhibits $MCN1_{STG}$ (Fig. 1B) (Beenhakker et al., 2005; DeLong et al., 2009). In each CoG, GPR causes a lasting activation of MCN1 and CPN2 (Fig. 1B) (Blitz et al., 2004). During the VCN-triggered gastric mill rhythm, the only effective GPR synapse is its presynaptic inhibition of $MCN1_{STG}$ (Fig. 1C) (Beenhakker et al. 2007). The functional consequence is that GPR stimulation during VCN-rhythm selectively prolongs the retraction phase.

The POC neurons also activate MCN1 and CPN2 (Fig. 2) (Blitz et al., 2008). However, they trigger a distinct gastric mill rhythm in which the LG neuron burst is rhythmically interrupted by the pyloric rhythm (Fig. 3) (White and Nusbaum 2011). To

determine the GPR influence on the POC-triggered gastric mill rhythm, we stimulated GPR during a succession of POC-retractor phases (Fig. 3).

GPR stimulation prolonged the POC-gastric mill cycle period (pre-GPR, 12.3 ± 1 s; during GPR, 17 ± 2.5 s; RM-ANOVA, $p<0.001$; n=16) (Fig 3). This prolongation resulted from an increase in the duration of both the retraction phase (pre-GPR, 7.6 ± 0.7 s; during GPR, 11.7 ± 1.7 s; RM-ANOVA, $p<0.001$; n=16) and protraction phase (pre-GPR, 4.7 ± 0.5 s; during GPR, 5.3 ± 0.5 s; RM-ANOVA, $p<0.01$; n=16) (Figs. 3,4). In contrast, as indicated above, the comparable GPR stimulation during the VCN-gastric mill rhythm only prolonged the protractor phase (Fig. 4) (Beenhakker et al., 2007). These GPR stimulations during the POC-rhythm also frequently and reversibly changed the LG burst pattern from being pyloric rhythm-timed to tonic (Fig. 3). The MCN1 firing pattern, monitored extracellularly, also appeared to change during GPR stimulation. Specifically, the pyloric-timed MCN1 burst commonly increased in duration during GPR stimulation, and often these bursts merged into a tonic pattern (n=12/16) (Fig. 4).

In addition to increasing POC-protraction duration, GPR stimulation increased the intraburst firing rate of the protractor neurons LG and GM (Fig. 5). The LG firing rate increased from 8.6 ± 0.7 Hz, before GPR stimulation, to 10.7 ± 0.8 Hz during GPR stimulation (RM-ANOVA, $p<0.01$; n=16) (Fig. 5). The GM firing rate increased from 2.6 ± 0.3 Hz before GPR stimulation to 3.4 ± 0.4 Hz during stimulation (RM-ANOVA, $p<0.01$; n=8) (Fig. 5).

DISCUSSION

Our results indicate that the proprioceptor GPR prolongs both phases of the POC-triggered gastric mill rhythm, and increases the firing rate of at least two protractor motor neurons (LG, GM) (Fig. 6). The fact that these two motor neurons exhibit increased activity suggests that GPR stimulation is exciting the projection neurons MCN1 and CPN2, because these projection neurons are primarily responsible for driving LG and GM activity, respectively, during the gastric mill rhythm (Fig. 5) (Beenhakker and Nusbaum, 2004). Additional support for this conclusion derives from the qualitative determination that the MCN1 burst duration appears to consistently increase when GPR is stimulated during the POC-rhythm, and the activity patterns in both LG and MCN1 change from being pyloric-timed to tonic during the GPR stimulation. These data therefore support the hypothesis that the GPR actions on the projection neurons are not gated-out during the POC-gastric mill rhythm, in contrast to the VCN-gastric mill rhythm (Beenhakker et al., 2007). This change in the effectiveness of the GPR actions in the CoGs under these two conditions (VCN- vs. POC stimulation) could result from the POC pathway affecting different cellular properties in the projection neurons than the VCN pathway. For example, VCN stimulation could activate the same ionic current(s) in MCN1/CPN2 as GPR, thereby occluding the effectiveness of GPR stimulation after VCN stimulation. In contrast, POC stimulation might influence a different current. Alternatively POC stimulation could be affecting different interneurons in the CoG than VCN, causing a difference in the strength of the AB synapse on MCN1 and CPN2 which is responsible for the pyloric timing in the projection neurons. A more direct, quantitative evaluation of MCN1 and CPN2 activity will be necessary before a firm conclusion is appropriate.

As summarized in Figures 6 and 7, in addition to the apparently distinct gating of

GPR excitation of MCN1 and CPN2 in the CoG, GPR stimulation had several different influences on the VCN- and POC-gastric mill rhythms. For example, GPR only prolongs retraction during the VCN-rhythm but it prolongs both phases during the POC-rhythm. Additionally, the protractor motor neuron firing rates were only increased during the POC-rhythm (Fig. 6). It remains to be determined to what extent these differences result from a differential action of the GPR synapses on the projection neurons and gastric mill circuit neurons during these two versions of the gastric mill rhythm. However, it seems likely that these distinctions result primarily from GPR access to the projection neurons during the POC-rhythm, given the known excitatory actions of MCN1 and CPN2 on protractor neurons (Coleman and Nusbaum, 1994; Beenhakker and Nusbaum, 2004; Stein et al., 2007), and the fact that GPR directly inhibits the LG neuron (DeLong et al., 2009) (Fig. 8).

Previous studies have focused primarily on the state-dependent actions of sensory feedback at the level of the CPG (Rossignol et al., 2006; Blitz and Nusbaum, 2007, 2011). If further experiments confirm the state-dependent nature of GPR influence on MCN1 and CPN2, it will provide a novel locus for state-dependent sensory feedback.

REFERENCES

Barrière G, Simmers J, Combes D (2008) Multiple mechanisms for integrating proprioceptive inputs that converge on the same motor pattern-generating network. J Neurosci. 28:8810-8820.

Beenhakker MP, Nusbaum MP (2004) Mechanosensory activation of a motor circuit by coactivation of two projection neurons. J Neurosci 24: 6741-6750.

Beenhakker MP, Blitz DM, Nusbaum MP (2004) Long-lasting activation of rhythmic neuronal activity by a novel mechanosensory system in the crustacean stomatogastric nervous system. J Neurophysiol 91:78-91.

Beenhakker MP, DeLong ND, Saideman SR, Farzan N, Nusbaum MP (2005) Proprioceptor regulation of motor circuit activity by presynaptic inhibition of a modulatory projection neuron. J Neurosci 25:8794-8806.

Beenhakker MP, Kirby MS, Nusbaum MP (2007) Mechanosensory gating of proprioceptor input to modulatory projection neurons. J Neurosci 27:14308-14316.

Blitz DM, Nusbaum MP (2011) Sensorimotor integration in the stomatogastric nervous system. Curr Opin Neurobiol, In Press.

Blitz DM, Nusbaum MP (2007) Mechanosensory regulation of invertebrate motor systems. In: Invertebrate Neurobiology (Greenspan RJ, North G, eds). Cold Spring Harbor Laboratory Press: Cold Spring Harbor, NY.

Blitz DM, Nusbaum MP (2008) State-dependent presynaptic inhibition regulates central pattern generator feedback to descending inputs. J Neurosci 28:9564-9574.

Blitz DM, White RS, Saideman SR, Cook AP, Nadim F, Nusbaum MP (2008) A newly identified extrinsic input triggers a distinct gastric mill rhythm via activation of modulatory projection neurons. J Exp Biol 211:1000-1011.

Blitz DM, Beenhakker MP, Nusbaum MP (2004) Different sensory systems share

projection neurons but elicit distinct motor patterns. J Neurosci 24: 11381-11390.

Coleman MJ, Nusbaum MP (1994) Functional consequences of compartmentalization of synaptic input. J Neurosci 14:6544-6552.

DeLong ND, Beenhakker MP, Nusbaum MP (2009) Presynaptic inhibition selectively weakens peptidergic cotransmission in a small motor system. J Neurophysiol 102:3492-3504.

Heinzel HG, Weimann JM, Marder E (1993) The behavioral repertoire of the gastric mill in the crab, *Cancer pagurus*: an in situ endoscopic and electrophysiological examination. J Neurosci 13:1793-1803.

Katz PS, Eigg MH, Harris-Warrick RM (1989) Serotonergic/cholinergic muscle receptor cells in the crab stomatogastric nervous system. I. Identification and characterization of the gastropyloric receptor cells. J Neurophysiol 62:558-570.

Katz PS, Harris-Warrick RM (1991) Recruitment of crab gastric mill neurons into the pyloric motor pattern by mechanosensory afferent stimulation. J Neurophysiol 65:1442-1451.

Marder E, Bucher D (2001) Central pattern generators and the control of rhythmic movements. Curr Biol 11: R986-R996.

Marder E, Calabrese RL (1996) Principles of rhythmic motor pattern generation. Physiol Rev 76:687-717.

Rossignol S, Dubuc R, Gossard JP (2006) Dynamic sensorimotor interactions in locomotion. Physiol Rev 86:89-154.

Stein W, DeLong ND, Wood DE, Nusbaum MP (2007) Divergent co-transmitter actions underlie motor pattern activation by a modulatory projection neuron. Eur J Neurosci 26:1148-1165.

White RS, Nusbaum MP (2011) Distinct Input Pathways Elicit Different Motor Patterns

Driven by the Same Core Rhythm Generator. J Neurosci (submitted)

Weimann JM, Meyrand P, Marder E (1991) Neurons that form multiple pattern generators: identification and multiple activity patterns of gastric/pyloric neurons in the crab stomatogastric system. J Neurophysiol 65:111-122.

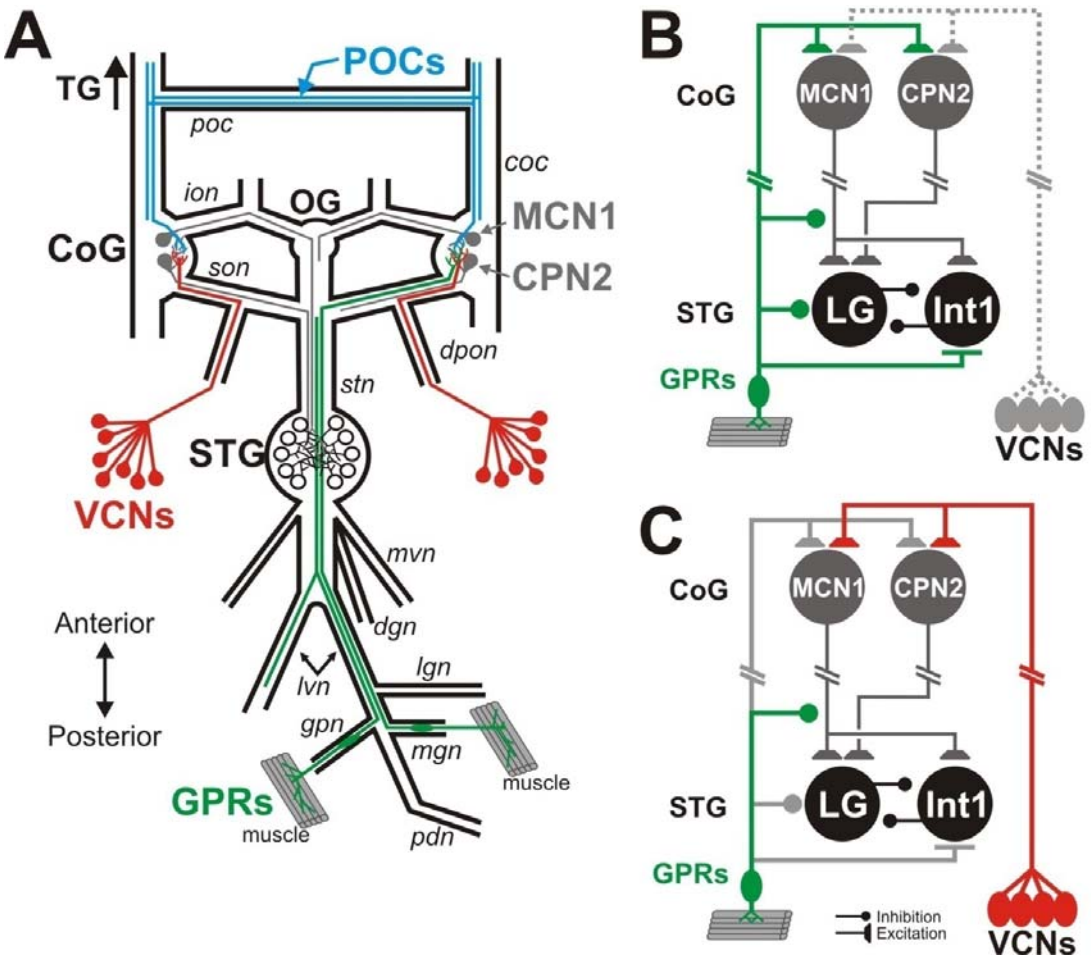

Figure 1. GPR innervates both the STG and CoGs to influence gastric mill circuit output. A. Schematic of the isolated STNS, including its four ganglia plus their connecting and peripheral nerves. The VCNs project into the CoGs from the cardiac sac stomach compartment via the *dpon* and *son* nerves. The POC neurons project into the CoGs via the *coc* and *poc* nerves. Each (of two) bilaterally symmetric GPRs arborize in a protractor muscle within the gastric mill stomach compartment. They project to the STG and CoGs to make synaptic connections. Abbreviations: Ganglia: CoG, commissural ganglion; OG, oesophageal g.; STG, stomatogastric g.; TG, thoracic g. Nerves- *coc*, circumoesophageal commissure; *dgn*, dorsal gastric nerve; *dpon*, dorsal posterior oesophageal n.; *gpn*, gastropyloric n.; *ion*, inferior oesophageal n.; *lgn*, lateral gastric n.;

lvn, lateral ventricular n.; *mgn*, medial gastric n.; *mvn*, medial ventricular n.; *pdn*, pyloric dilator n; *poc*, post-oesophageal commissure; *son*, superior oesophageal n.; *stn*, stomatogastric n. Neurons- CPN2, commissural projection neuron 2; GPRs, gastropyloric receptors; MCN1, modulatory commissural neuron 1; POCs, post-oesophageal neurons; VCNs, ventral cardiac neurons. **B.** Schematic showing how GPR influences the gastric mill system when there is no ongoing gastric mill rhythm. Green, active neuron/synapses; Grey, inactive neuron/synapses. Based on: Blitz et al. (2004); DeLong et al. (2009). **C.** Schematic showing how GPR influences the gastric mill system when there is an ongoing VCN-gastric mill rhythm. Color, active neuron/synapses; Grey, inactive neuron/synapses. Note that the only GPR synapse effective under this condition is its inhibition of the MCN1 terminals in the STG. Based on: Beenhakker et al. (2007).

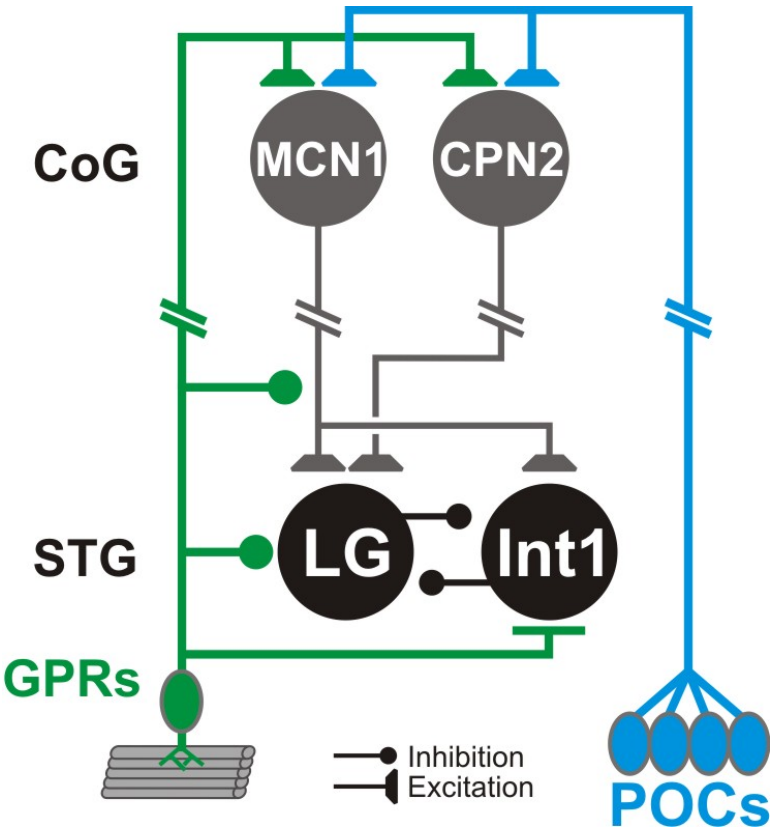

Figure 2. The POC neurons activate the same projection neurons as the GPRs. Schematic showing that the POC neuron actions converge onto the same projection neurons (MCN1, CPN2) as the GPRs. Based on: Blitz et al. (2004, 2008).

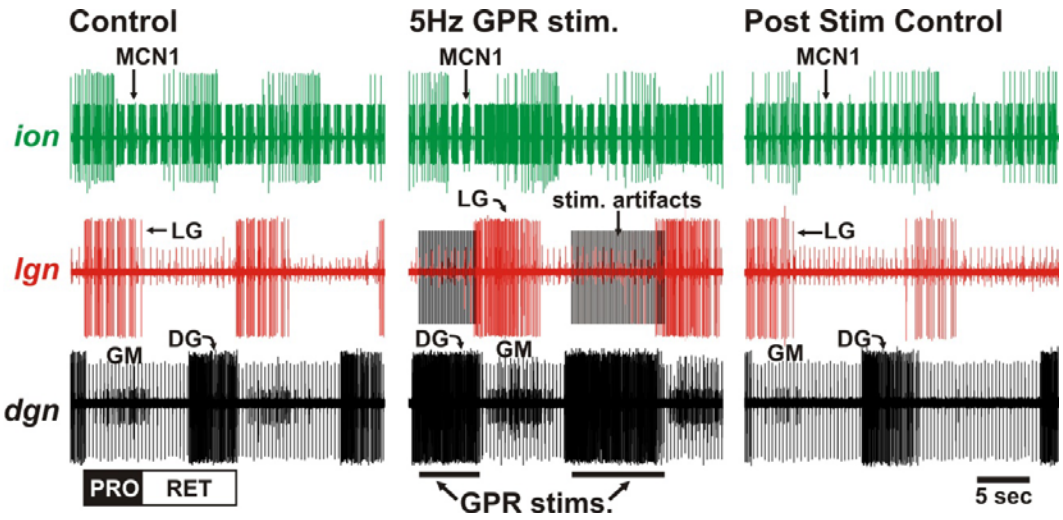

Figure 3. GPR stimulation during a POC-triggered gastric mill rhythm reversibly alters the ongoing activity pattern. (Left) During an ongoing, POC-triggered gastric mill rhythm, the projection neuron MCN1 (*ion*) fires regular pyloric rhythm-timed bursts that contribute to driving the gastric mill rhythm (*lgn*, *dgn*). Note that each LG burst is divided into pyloric-timed burstlets, as is typical of the POC-gastric mill rhythm (Blitz et al., 2008). **(Middle)** During the same gastric mill rhythm, GPR was rhythmically stimulated (intraburst freq: 5 Hz) for a succession of retractor phase cycles. GPR is activated during retraction by stretch of the protractor muscles. Note that each GPR stimulation increased MCN1 activity, prolonged the retractor phase (LG interburst), including prolonging DG neuron activity, and it both prolonged and changed the pattern (from pyloric-timed to tonic) of the LG neuron. **(Right)** Soon after GPR stimulation was terminated, the gastric mill rhythm returned to its pre-stimulation pattern.

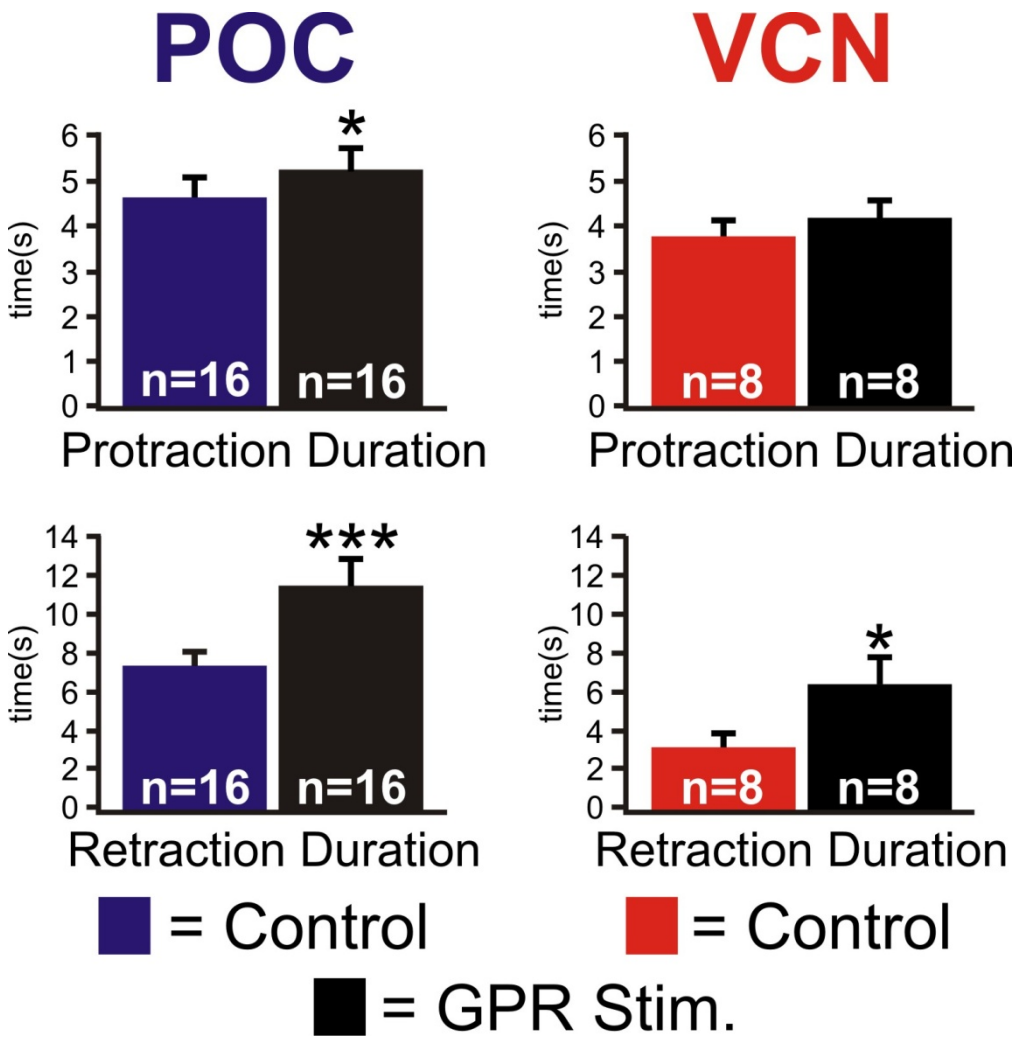

Figure 4. GPR stimulation has distinct actions on the POC- and VCN-triggered gastric mill rhythms. (Left) During the POC-gastric mill rhythm, GPR stimulation consistently prolonged both (top) protraction and (bottom) retraction. **(Right)** During the VCN-gastric mill rhythm, GPR stimulation selectively prolonged the retraction phase, as shown previously by Beenhakker et al. (2005). Symbol: *p<0.05, ***p<0.001 one way repeated measures ANOVA .

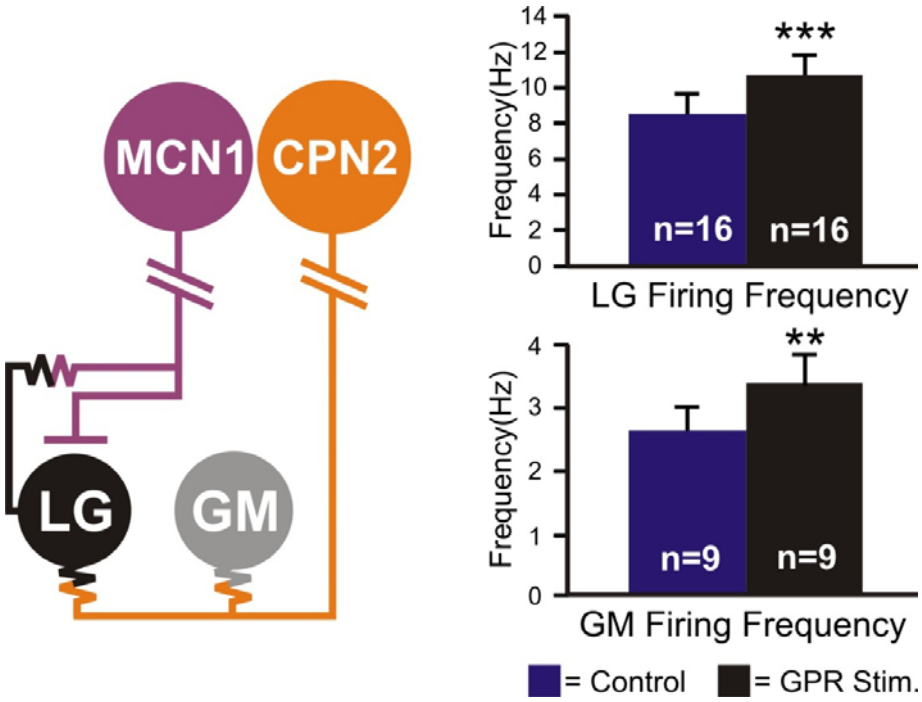

Figure 5. GPR stimulation during POC-triggered gastric mill rhythm appears to increase the firing rate in the projection neurons MCN1 and CPN2. (Left) Circuit schematic highlighting the synaptic actions of MCN1 and CPN2 on the gastric mill protractor neurons LG and GM. MCN1 provides the major excitatory drive to LG, while CPN2 provides the major excitatory drive to GM (Norris et al., 1994; Beenhakker and Nusbaum, 2004). Symbols: t-bar, synaptic excitation; resistor, electrical coupling. Broken lines in the MCN1 and CPN2 axons represent additional distance between their somata in the CoG and their arborizations in the STG. **(Right)** The LG and GM firing frequency increased when GPR was stimulated during the POC-gastric mill rhythm, suggesting that GPR stimulation increased the firing rate of MCN1 and CPN2. Symbol: **p<0.01; ***p<0.001.

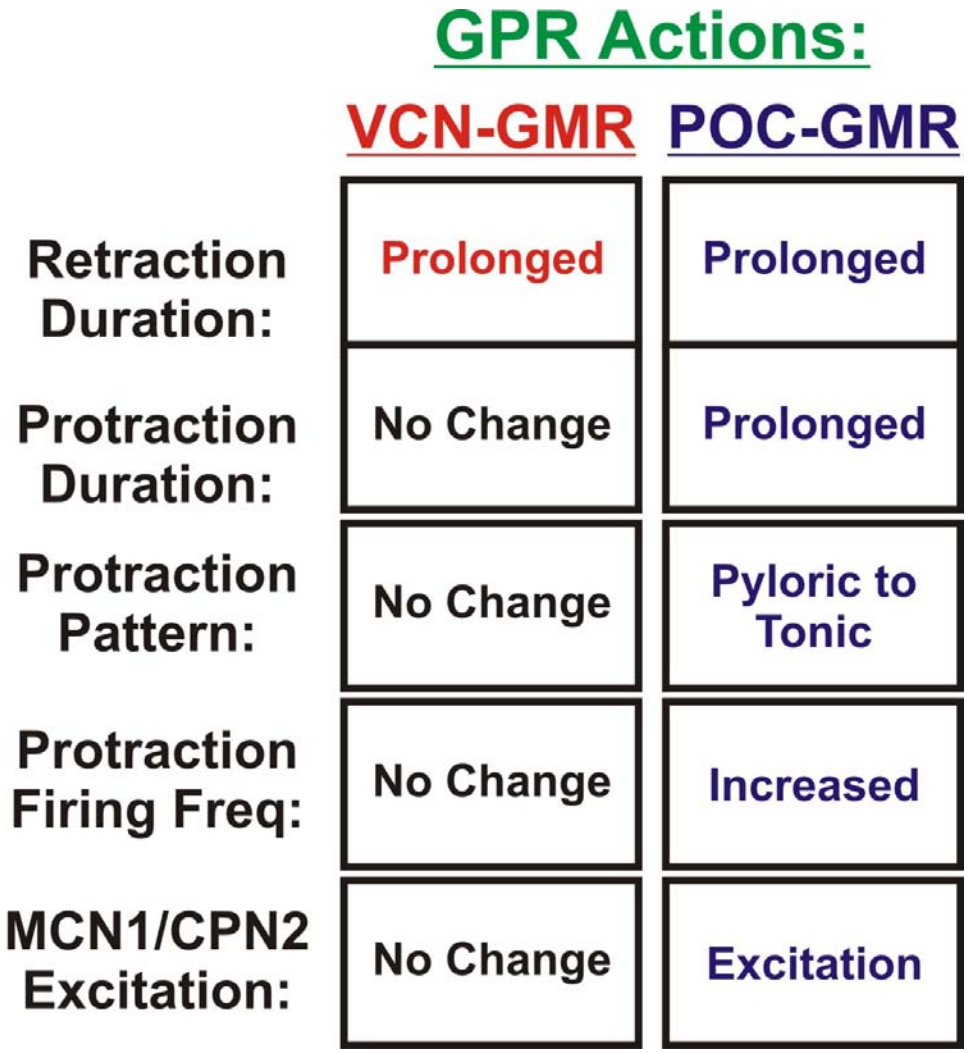

Figure 6. Summary of the distinct GPR effects on the VCN- and POC-triggered gastric mill rhythms. GPR stimulation selectively prolongs retraction and does not alter MCN1 and CPN2 activity during the VCN-triggered gastric mill rhythm, as shown previously by Beenhakker et al. (2007). In contrast, GPR stimulation alters both phases of the POC-gastric mill rhythm and it appears to enhance activity in MCN1 and CPN2. Interestingly, GPR stimulation also changes the pyloric-timed LG pattern during the POC-rhythm into the tonic pattern that occurs during the VCN-gastric mill rhythm.

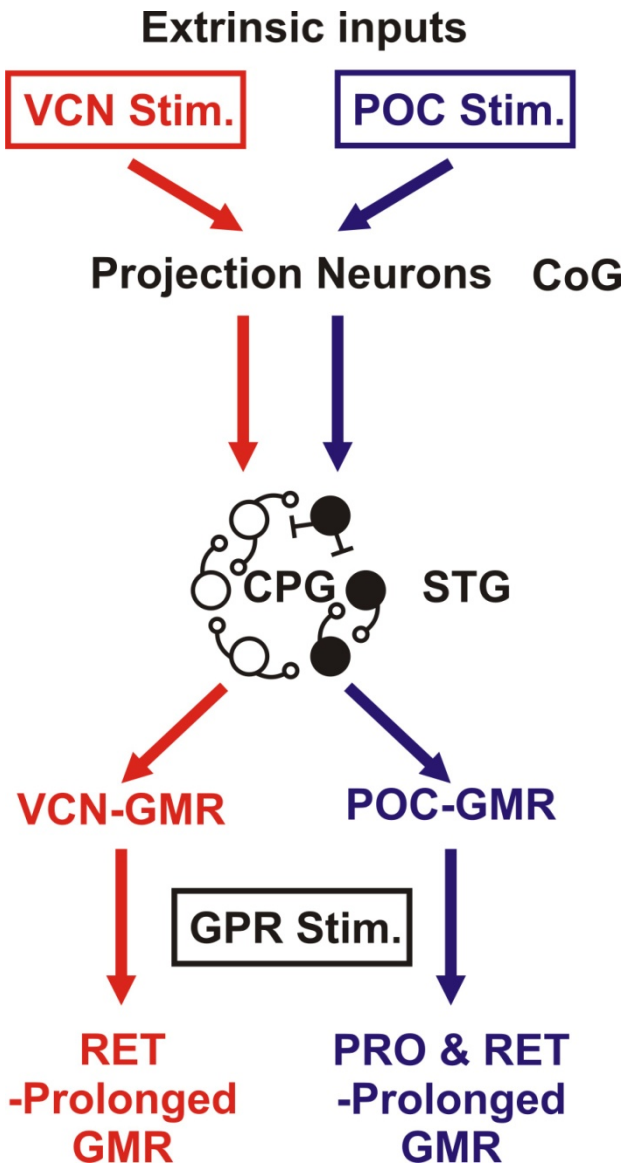

Figure 7. The GPR effect the VCN- and POC-triggered gastric mill rhythms is distinct. The VCN and POC neurons both activate the same projection neurons (MCN1, CPN2) in the CoGs, which then drive distinct gastric mill rhythm in the STG (White and Nusbaum, 2011). GPR stimulation has distinct consequences on the phase durations of each of these gastric mill rhythms.

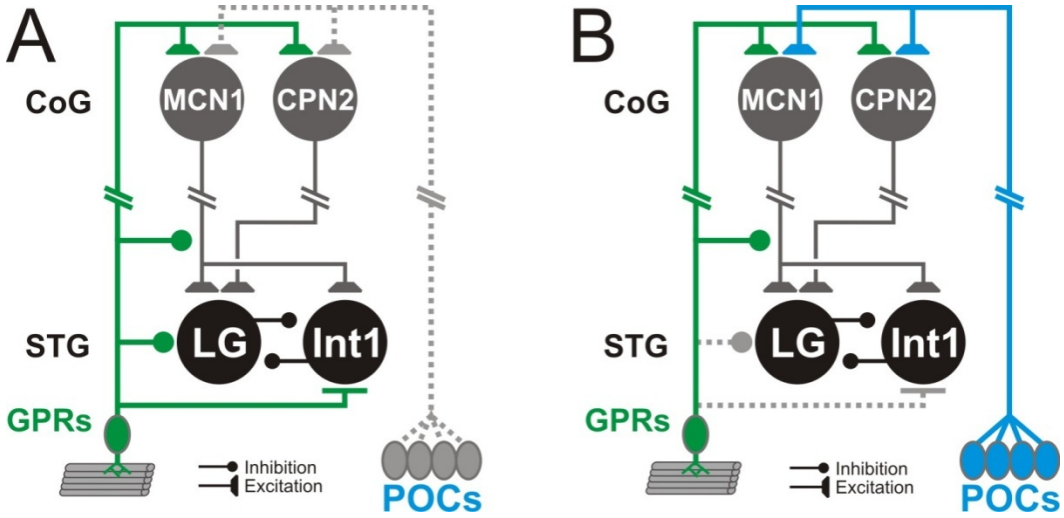

Figure 8. Proposed hypothesis for which GPR synapses influence the POC-triggered gastric mill rhythm. **(Left)** Schematic showing how GPR influences the gastric mill system when there is no ongoing gastric mill rhythm. Green, active neuron/synapses; Grey, inactive neuron/synapses. Based on: Blitz et al. (2004); DeLong et al. (2009). **(Right)** Hypothesis for which GPR synapses influence the POC-gastric mill rhythm. Based on the results of our experiments, it appears that GPR stimulation continues to excite MCN1 and CPN2 in the CoG (in contrast to the VCN-rhythm), as well as inhibiting the MCN1 terminals in the STG. It is not yet clear whether the direct GPR synapses onto LG and Int1 are effective during this motor pattern.

CHAPTER 6

SUMMARY, DISCUSSION AND FUTURE DIRECTIONS

My thesis work focused on establishing the ability of a small neuronal network to generate distinct rhythmic motor outputs in response to activation of two different neuronal input pathways, not only in the isolated CNS but also at the effector (i.e. muscle) level. Most previous studies of reconfiguration in identified circuits have relied upon either direct application of modulatory transmitters or individual stimulation of single modulatory neurons, neither of which is a "natural" means for activating these circuits.

In Chapter 2, I participated in a collaboration that identified an extrinsic input, the post-oesophageal commissure (POC) neurons, that triggers a long-lasting gastric mill motor pattern via activation of previously identified commissural ganglion (CoG) projection neurons (MCN1, CPN2). The POC axons project as a tightly associated bundle of *Cancer borealis* tachykinin-related peptide Ia (CabTRP Ia)-immunopositive axons through the medial aspect of each *coc* nerve, from the direction of the thoracic ganglion, to innervate the ipsilateral CoG. A subset of these axons also project through the *poc* nerve, enabling them to innervate the contralateral CoG. The CabTRP Ia axons arborize densely in the same CoG neuropil region as the neuropilar branches of MCN1 and CPN2, and we provide evidence that POC-released CabTRP Ia excites these two neurons. The gastric mill motor pattern activated by the POC neurons is likely identical to the spontaneous one studied previously by Wood et al. (2004: J Neurosci), and it was clearly qualitatively different from all previously identified versions of this motor pattern. This study supports the hypothesis that distinct outputs can be generated from the same CPG despite the coactivation of the same set of projection neurons, insofar as the previously characterized VCN- and GPR-gastric mill rhythms also result from a

coactivation of MCN1 and CPN2. These latter two gastric mill rhythms exhibit similar, albeit quantitatively distinct motor patterns and both are clearly distinct from the POC-pattern (as shown in Chapter 3).

In Chapter 3, I established that the gastric mill circuit in the crab stomatogastric nervous system can generate different gastric mill motor patterns, and that both motor patterns are generated by the same core rhythm generator. Specifically, I determined that the qualitatively distinct POC-gastric mill motor pattern is also quantitatively distinct from the previously studied VCN-triggered gastric mill motor pattern. The distinction results in part from the LG neuron burst pattern being pyloric rhythm-timed instead of tonic, and from additional changes in burst parameters of other gastric mill motor neurons. I also showed that the reciprocally inhibitory gastric mill neurons LG and Int1 are the only gastric mill neurons necessary for generating both of these gastric mill rhythms. In combination with previous studies, the finding that the same rhythm generator neurons underlie different versions of the gastric mill rhythm (a network-driven CPG) indicates that, unlike other shared general principles of CPG operation, there is no consistent expectation regarding the degree of preservation of the rhythm generator for different configurations of a given CPG. Additionally, given that the POC- and VCN-gastric mill rhythms share projection neurons and rhythm generator neurons, their distinct motor patterns must result from one or more differences in other variables. In contrast, most previously studied, distinct motor patterns generated from the same CPG are known or believed to result from changes in the cellular and synaptic properties of the CPG neurons.

In Chapter 4, I determined that the distinct LG protraction patterns that occur during the VCN- and POC-gastric mill rhythms in the isolated stomatogastric nervous system produce distinct muscle activity patterns at both the EJP (excitatory junction

potential) and tension levels. Specifically, I showed that despite the slow contraction dynamics that characterize stomatogastric system striated muscles, the LG-innervated muscle gm6ab can reproduce the pyloric-timed pauses in LG neuron activity during the POC-gastric mill rhythm, and hence generate a distinct pattern than does the same muscle during the VCN-gastric mill rhythm. There is extensive work done in many systems showing that CPG output can be reconfigured to produce distinct motor patterns, but most of these studies were performed in the isolated CNS. Insofar as many of the CPG systems known for their multifunctional ability are found in invertebrate systems that drive muscles with slow dynamics, it is not a foregone conclusion that centrally-generated motor patterns would remain distinct at the level of the muscles that mediate the behavior.

In Chapter 5, I investigated the state-dependence of sensory feedback in the gastric mill motor system. Specifically, I assessed whether the identified proprioceptor GPR had the same influence on the POC- and VCN-triggered gastric mill rhythms. I found that this was not the case. During the VCN-rhythm, the GPR excitation of MCN1 and CPN2 is gated out, as are its direct synapses onto LG and Int1 (Beenhakker et al., 2007: J Neurosci). As a result, GPR only influences this system via its presynaptic inhibition of the STG axon terminals of MCN1, by which action GPR selectively prolongs the retractor phase. In contrast, I showed that during the POC-rhythm GPR prolongs both protraction and retraction. Although I did not directly analyze the GPR influence on MCN1 and CPN2 during the POC-rhythm, it appeared likely that GPR does excite them during this rhythm. This presumption is based on my finding that GPR caused increased activity in the gastric mill motor neurons LG and GM during the POC-rhythm, and the two projection neurons (MCN1, CPN2) are primary sources of excitation to these motor neurons. Additional support for this presumption derives from my qualitative

assessment that the MCN1 burst duration appeared to consistently increase when GPR is stimulated during the POC-rhythm. These data therefore support the hypothesis that the GPR actions on the projection neurons are not gated-out during the POC-gastric mill rhythm, in contrast to the VCN-gastric mill rhythm. Previous studies have focused primarily on the state-dependent actions of sensory feedback at the level of the CPG (Rossignol et al., 2006: Physiol Rev; Blitz and Nusbaum, 2011: Curr Opin Neurobiol). If further experiments confirm the state-dependent nature of GPR influence on MCN1 and CPN2, it will provide a novel locus for state-dependent sensory feedback.

Future Directions

Much of the future work for this study lies in the CoGs and the muscles. One major issue is to understand exactly how the same projection neurons drive distinct gastric mill motor patterns. No comparable example yet exists in any other motor system. Some information is already available from Blitz and Nusbaum (2008: J Neurosci), who showed that after VCN-stimulation the pyloric (AB neuron) circuit feedback to the projection neurons is gated out, within the CoGs, during the protractor phase, whereas this feedback is strong and effective during POC-protraction. However, differences in the motor patterns persist when the pyloric rhythm is suppressed (Chapters 2 and 3), so there are additional, unknown distinctions in how the POC- and VCN-pathways influence MCN1 and CPN2.

With respect to the LG-innervated muscle gm6ab ability to generate different tension patterns in response to distinct, realistic input patterns, it will be interesting to determine whether the other LG-innervated muscles can also follow these different input patterns. This will not necessarily be the case, given the slow dynamics of these muscles, and the fact that there is at least one example in this system where two

muscles innervated by the same motor neuron (pyloric PD neuron) respond quite differently (phasic following vs. maintained tonic contraction) to their shared motor neuronal input. It also remains to understand the mechanisms underlying the larger tension amplitude attained by gm6ab during the VCN- than the POC-pattern. Presumably the different patterns themselves are pivotal, but there may well also be contributions from the different burst and interburst durations during each gastric mill rhythm. Finally, extending this analysis to other gastric mill muscles will help determine whether the complete gastric mill neuromuscular system does or does not simply follow its motor neuron input pattern. Particularly interesting will be determining the response of the retractor DG-innervated muscles (gm4), because gm4 attaches to the same ossicle as gm6ab and the other LG-innervated muscles. Thus, when gm4 contracts in situ it stretches gm8, gm6 and gm5, which in turn activates the GPR proprioceptor neuron. Acquiring these data will therefore provide a more realistic assessment of how GPR activity is regulated during these different gastric mill rhythms.

Finally, with respect to the GPR actions on these gastric mill rhythms, much work remains. In the short term, a quantitative determination of whether GPR excitation of MCN1 and CPN2 persists during the POC-gastric mill rhythm would enable a firm conclusion regarding the presence (or absence) of state-dependent regulation of sensory feedback onto projection neurons. Direct manipulation of these projection neurons would also enable understanding whether GPR prolongs the protractor phase during the POC-gastric mill rhythm (but not during the VCN-rhythm) due to actions in the CoGs or, perhaps, its ability to influence LG and/or Int1 in the STG.

Collectively, the more complete understanding of the gastric mill motor system activated by the distinct extrinsic inputs, POC and VCN neurons, that would come from these future studies will provide a more extended appreciation of what it means for a

CPG to be able to generate multiple versions of a basic motor pattern. I look forward to reading the results of these future studies from the work of future Nusbaum lab students.